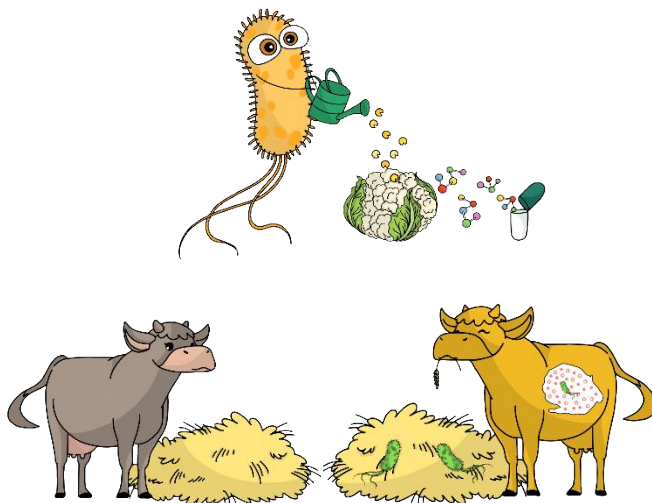




# UNIVERSITÀ DI PAVIA

Dipartimento di Biologia e Biotecnologie  
“L. Spallanzani”

***Bacillus subtilis* from soil to industry: optimization of the  
intrinsic cellulolytic abilities and biotechnological applications**



**Valeria Bontà**

Dottorato di Ricerca in  
Genetica, Biologia Molecolare e Cellulare  
Ciclo XXXV – A.A. 2019-2022

## Table of Contents

<b>Abbreviations .....</b>	<b>5</b>
<b>Chapter 1.....</b>	<b>6</b>
1.1 Introduction .....	7
1.1.1 <i>Bacillus subtilis</i> from soil to industry .....	7
1.1.2 Lignocellulosic biomass.....	8
1.1.3 Carbon-active enzymes.....	12
References .....	16
1.2 Aim of the work .....	21
<b>Chapter 2: Optimization of enzymes production in <i>Bacillus subtilis</i>.....</b>	<b>22</b>
2.1 Abstract.....	23
2.2 Introduction .....	24
2.3 Materials and Methods.....	28
2.3.1 Bacterial strains.....	28
2.3.2 Bacterial growth .....	28
2.3.3 Cellulase and endo-xylanase activities .....	29
2.3.4 Arabinofuranosidase activity.....	29
2.3.5 Xylosidase activity .....	29
2.3.6 Phytase activity .....	30
2.3.7 Statistical analyses.....	30
2.4 Results .....	31
2.4.1 Cellulase and endo-xylanase determination .....	31
2.4.2 Arabinofuranosidase determination .....	32
2.4.3 Xylosidase determination .....	33
2.4.4 Phytase detection.....	37
2.5 Discussion.....	38
References .....	41
<b>Chapter 3: Effect of supplementation of cellulolytic enzymes of <i>Bacillus subtilis</i> on the nutritional value of ruminal fodders .....</b>	<b>43</b>
3.1 Abstract.....	44
3.2 Introduction .....	45

3.3	Materials and Methods .....	47
3.3.1	Liquid fraction of rice straw preparation and characterization .....	47
3.3.2	<i>Bacillus subtilis</i> cultures .....	47
3.3.3	Cellulase and xylanase activity assays.....	48
3.3.4	<i>In vitro</i> analysis .....	48
3.3.5	<i>In vitro</i> NDF digestibility.....	49
3.3.6	<i>In vitro</i> gas production .....	49
3.3.7	Statistical analyses.....	50
3.4	Results .....	51
3.4.1	Medium characterization .....	51
3.4.2	<i>Bacillus subtilis</i> growth on WL fraction .....	51
3.4.3	Cellulase and xylanase activity assays.....	52
3.4.4	Fiber digestibility .....	52
3.4.5	Gas Production and ruminal fermentative profile .....	54
3.5	Discussion.....	56
	References .....	59
<b>Chapter 4: Extraction of phytochemicals from cauliflower waste by <i>Bacillus subtilis</i>-derived enzymes .....</b>		<b>62</b>
4.1	Abstract.....	63
4.2	Introduction .....	64
4.3	Materials and Methods .....	68
4.3.1	Bacterial strains.....	68
4.3.2	Bacterial growth .....	68
4.3.3	Cellulase and xylanase activity assays.....	68
4.3.4	Plant material .....	68
4.3.5	Extraction by methanol and acetone .....	69
4.3.6	EAE pre-treatment procedure of the cauliflower waste material .....	69
4.3.7	Extraction process.....	69
4.3.8	Total polyphenol content .....	70
4.3.9	Total flavonoids content .....	70
4.3.10	Catechins and chlorogenic acid HPLC analyses .....	70
4.3.11	Isothiocyanates HPLC analyses .....	71

4.3.12 Statistical Analysis .....	71
4.4 Results .....	72
4.4.1 Cellulase and xylanase activity assays.....	72
4.4.2 Recovery of phytochemicals: preliminary experiments.....	73
4.4.3 Recovery of phenolic compounds.....	76
4.4.4 Catechins .....	77
4.4.5 Chlorogenic Acid .....	78
4.4.6 Isothiocyanates .....	78
4.5 Discussion.....	80
References .....	83
<b>5 Conclusions.....</b>	<b>87</b>
<b>List of original manuscripts.....</b>	<b>88</b>
<b>Acknowledgements.....</b>	<b>119</b>



**Abbreviations**

WT	Wild-type
OD	Optical Density
CAZymes	Carbohydrate-Active enZymes
CBP	Consolidated Bioprocessing
CCR	Carbon Catabolite Repression
DM	Dry Matter
DMI	Dry Matter Intake
SEM	Standard Error of the Mean
WL	Washing Liquid
CFU	Colony Forming Unit
RT	Room Temperature
NDFd	Neutral Detergent Fiber degradability
GP	Gas Production
VFA	Volatile Fatty Acids
TMR	Total Mixed Ration
EAE	Enzyme Assisted Extraction
MAE	Microwave Assisted Extraction
UAE	Ultrasound Assisted Extraction
SFE	Supercritical Fluid Extraction
PEF	Pulse Electric Field
TPC	Total Phenolic Compounds
HPLC	High-Performance Liquid Chromatography
LMM	Linear Mixed Model
DF	Degrees of Freedom

# **Chapter 1**

## 1.1 Introduction

### 1.1.1 *Bacillus subtilis* from soil to industry

The Gram-positive genus *Bacillus* includes many rod-shaped, aerobic, endospore-forming bacterial species. This genus is generally non-pathogenic, with some exceptions i.e., *Bacillus anthracis*, and some opportunistic pathogen species such as *Bacillus cereus* (Messelhäußer & Schulz, 2018; Ehling-Schulz et al., 2019).

The most studied among *Bacillus* species is the non-pathogenic *Bacillus subtilis*, the model organism of Gram-positive bacteria. It is found mainly in the soil and in the plant rhizosphere, but also in water and as part of the gut microbiome of ruminants, insects and humans (Hong et al., 2009).

The wild environment had tailored the genetic evolution of *B. subtilis* so that it can handle diverse environmental changes, showing great adaptability and competitive success in those habitats (Earl et al., 2008). To tackle environmental fluctuations, the bacterium evolved different strategies such as the use of flagella for motility and chemotaxis, and the natural competence, consisting of the uptake of exogenous DNA for recombination, an unlimited source of new skills that can be acquired through horizontal gene transfer (Hamoen et al., 2003). Moreover *B. subtilis* is capable of forming spores that are metabolically inactive, dormant cells able to survive in harsh environments until favourable growth conditions are restored (Paredes-Sabja et al., 2011).

*B. subtilis*, like other species, displays two different modalities of growth: a single cell-planktonic mode and a surface-adhered biofilm mode. The biofilm is a multicellular community of bacteria encased in a hydrophobic matrix and cell are specialized for different functions. Biofilm is formed as a protection strategy against antimicrobial factors and environmental insults (Branda et al., 2001; Hamon and Lazazzera, 2001). This species is generally recognized as safe (G.R.A.S.), allowing the use of its bioproduct for many human and animal applications (Su et al., 2020). Thanks to its safety, whole cells of *B. subtilis* can also be employed as microbial additive to improve intestinal function in animals (Sella et al., 2021) and humans (Lee et al., 2019). Some studies suggest that *B. subtilis* can improve the balance of intestinal flora and food absorption efficiency as well as prevent diseases by secreting polypeptides that have an antagonistic effect against intestinal pathogens, thus acting as probiotic (Su et al., 2020). Indeed, it can secrete highly active proteases, lipases and amylases in the upper intestinal tract, which are helpful to degrade complex carbohydrates constituting plant feeds. In order to survive in dynamic environments subjected to continuous changes, *B. subtilis* is naturally endowed with an excellent protein secretion system/apparatus; indeed, it secretes massive amounts of different molecules as degradative enzymes and antibiotics (Esakkiraj et al., 2009). This characteristic is extremely attractive at the industrial level, since the endogenous products are naturally secreted in the growth media and are therefore easily separated from the cells, simplifying the downstream processes compared to intracellularly-produced molecules, and reducing the process costs (Westers et al., 2004).

Moreover, being *B. subtilis* the model organism of Gram-positive bacteria, wide

knowledge has been gathered on it and there is a broad array of genetic tools, promoters, and plasmid expression systems, which are used for metabolic engineering, protein expression studies, and synthetic biology that allow to modify this bacterium and achieve industrial scale production of biocommodities (Liu et al., 2013). Finally, *B. subtilis* has well-developed fermentation technologies, excellent physiological characteristics, highly adaptable metabolism, simple nutrient requirements and cheap carbon source demand, which makes it easy to cultivate on poor substrates such as lignocellulosic material decreasing the overall fermentation costs of its bioproducts (Liu et al., 2013).

All these features make *B. subtilis* an industrial workhorse and one of the most used “industrial bacteria”. In fact, it has been widely used as a cell factory for microbial production of several enzymes, as proteases, cellulolytic enzymes, as well as heterologous proteins, antibiotics, vitamins, amino acids, and biopolymers, such as levan and poly- $\gamma$ -glutamic acid, and biosurfactants, such as surfactin (Schallmey et al., 2004).

The compounds produced by *B. subtilis* find applications in several industrial fields, such as in detergents, food and feed, textiles, paper and pulps, cosmetics, and pharmaceuticals (Furhan & Sharma, 2015). Indeed, it has been reported that the production of enzymes by *B. subtilis* accounts for 50% - 60% of the total enzyme market (Su et al, 2020). For instance, proteases are one of the *Bacillus*-derived enzyme families most abundantly produced. Since the first isolation from *B. subtilis*, alkaline serine protease Subtilisin A (EC 3.4.21.62) occupied the largest portion of the worldwide protein production industry (Svendsen, 1976; Ikemura et al., 1987). Proteases are in fact an important ingredient of laundry detergents; they are also used to degrade fibres on leather materials and are important components of contact-lens cleaners and debriding agents (Solanki et al., 2021). In the food industry, proteases are used to improve food flavours and milk digestibility (Singh et al., 2016).

### 1.1.2 Lignocellulosic biomass

Lignocellulosic biomass, defined as plant or plant-based material, is the most abundant renewable material on earth. Lignocellulosic biomass consists of cellulose, a carbohydrate polymer wrapped by the dense structure formed by another carbohydrate polymer, hemicellulose, and an aromatic polymer, lignin (Yousuf et al., 2020), occurring in plant biomass at 35-50 %, 20-35 %, and 10-25 %, respectively, even though the composition ratio varies among different species. Other compounds that are found in the plant cell wall, kept together by covalent and non-covalent interactions, are pectin, starch, lipids, pigments and proteins, creating a three-dimensional complex matrix (Sánchez, 2009).

Cellulose is one of the most common natural biopolymers synthesized annually on several billion-ton scale (McNamara et al., 2015). It is a linear biopolymer composed of glucose units linked by  $\beta$ -1,4-glycosidic bonds establishing the disaccharide cellobiose as the repeat unit (McKendry, 2002). The formation of intermolecular hydrogen bonds among cellulose chains establishes a crystalline super molecular structure. Then, bundles of linear cellulose chains form

microfibrils oriented in the longitudinal direction of the cell wall structure (Isikgor & Becer, 2015; Rongpipi et al., 2019) (Fig. 1).

The second major chemical component in vegetable biomass is hemicellulose. In contrast to cellulose, which is a homopolymer, hemicellulose is a co-polymer of different sugars, five-carbon sugars, usually xylose and arabinose, and six-carbon sugars, such as galactose, glucose, and mannose, which are highly substituted with acetic acid (Fig. 1) (Huang et al., 2021). For its branched nature, hemicellulose is amorphous and relatively easy to hydrolyse into its monomeric sugars as compared with cellulose. The main components of hemicellulose are xylans which can be divided into homoxylans and heteroxylans, as glucuronoxylyans, (arabino)glucuronoxylyans, (glucurono)arabinoxylans, arabinoxylans, and more complex heteroxylans. Glucuronoxylyans, containing glucuronic acid and xylose as their main constituents, are the primary components of hemicellulose found in hardwood trees, while softwood is mainly composed of (arabino)glucuronoxylyan (Heinze & Liebert, 2012). In nature, xylans, interweaved and linked with the overlying sheath of lignin, create a complex structure able to coat around underlying strands of cellulose, maintaining the integrity of the plant cell wall and protecting the fibres against degradation by enzymes.

The third biomass component is lignin, a very complex aromatic heteropolymer of phenylpropanoid building units (p-coumaryl, coniferyl, and sinapyl alcohol) (Fig. 1) (Agbor et al., 2011). It is responsible for hydrophobicity and rigidity of plant material acting as a natural barrier against microbial attack and allowing water and nutrient transport through plant tissues (Zoghlami & Paës, 2019).

These biopolymers, made up of long, repeating strands of molecules, constitute the major attractiveness of plant feedstocks for the industrial substitution of petroleum-based polymers towards green production, as, once depolymerized, can release a large quantity of sugars, used as source of carbon and hydrogen, and then converted into value-added products such as bioethanol, biobutanol, itaconic acid and others (Robak & Balcerak, 2018).

However, so far, the production of bioethanol, biodiesel and other biocommodities has been mainly based on edible biomass addressed to food, called first generation feedstock, i.e., sugarcane, sweet sorghum, sugar beet, starches as corn, wheat, barley, potato. However, the first-generation feedstock competes with food and feed crops, raising criticisms on the sustainability of this type of biomass. Indeed, to keep agricultural productivity high up and preserve arable land, the use of fertilizers and the deforestation have progressively increased, making first-generation biofuels and bio-products non-sustainable (Springmann et al., 2018; Verma & Kumar, 2021).

In the last decades, a more sustainable approach to biocommodities production led to the replacement of first-generation feedstocks with lignocellulosic waste, that has become the current strategy to decrease environmental impacts. Second-generation feedstocks include agricultural wastes, crop residues, wastes from fruit and vegetable industry, and household garbage (Verma & Kumar, 2021). This huge waste biomass has crucial advantages over other biomass sources because it constitutes the non-edible portion of the plant and therefore, it does not interfere with food and feed (Nayak & Bhushan, 2019; Kargbo et al.,

2021). Furthermore, it represents an unlimited biomass, considering that plant-derived food waste represents 63% of the waste volume generated by the food supply chain, and that this scenario is predicted to worsen in conjunction with the world population growth (Jin et al., 2018). Agri-food waste triggers a cascading series of problems, starting from its disposal. Indeed, landfilling, incineration, and composting remain the most used practices for food waste removal, generating a strong environmental impact, from greenhouse gas emissions in the atmosphere (the disposal of every ton of food waste emits more than 4.2 tons of CO<sub>2</sub>), to soil and water pollution caused by the release of excessive nitrogen and phosphorus inputs on the aquatic and terrestrial environments (Xiong, et al., 2019). In addition to the environmental problem, these losses and discards also represent a waste of critical resources such as land, water, fertilizers, chemicals, energy, and a conspicuous loss of profitability, which affects all the subjects involved in the agri-food chain (Vilariño et al., 2017).

Alarming and dramatic data on the food waste issue has caught the attention of the United Nations that, in 2015, adopted the Sustainable Development Goals; goal 12.3 calls everyone to action to “By 2030, halve global food waste per capita at the retail and consumption level and to reduce food loss along the production and supply chains” (<https://www.fao.org/sustainable-development-goals/indicators/1231/en/>).

In agreement to the concept of the 4-R, comprising Reduce, Reuse, Recycle, and Recover, this huge waste biomass is considered an extremely valuable, sustainable, and free raw material source of value-added products. Indeed, despite being a waste, this biomass is still rich in cellulose, hemicellulose, lignin and sugars that can be converted into biocommodities, as well as pectin, proteins, lipids, polysaccharides, flavor compounds, and phytochemicals that, can be extracted, thus acquiring high value as food additives, nutraceuticals, pharmaceuticals, cosmetics, food preservatives, etc. (Ning et al., 2021). From this perspective, waste biomass should no longer be considered a problem, rather it represents an abundant, non-expensive, valuable resource to be exploited, and its efficient conversion into value-added products is considered crucial for an effective bioeconomic strategy and a sustainable development (Abdeshahian et al., 2021; Ning et al., 2021).

However, the literature is full of problems plaguing the production of biocommodities from biomass. One of the hindrances related to biomass exploitation is the recalcitrance of lignocellulosic matrix, which makes the release of sugars and valuable molecules of industrial interest extremely difficult (Zoghalmi & Paës, 2019). As a renewable energy source, this biomass is affected by a second critical issue, i.e., the lower efficiency in terms of energy return on energy invested in comparison to either fossil fuels or intermittent alternative sources such as wind and solar energy.

As a result of the recalcitrance, pre-treatment of the lignocellulosic feedstock is considered a *sine qua non* process which helps the deconstruction of the complex matrix and thus improves sugar release from polysaccharides. This additional step precedes the real conversion of the biomass into biocommodities that generally occurs via anaerobic digestion or fermentation depending on the desired product (Chen et al., 2010; Vasco-Correa et al., 2016).

Pre-treatment of lignocellulosic biomass has been traditionally performed by thermochemical processes that make use of chemicals (acids, bases, solvents) and strong physical conditions (elevated temperature and pressure) to disrupt the cell wall components. Although the effectiveness of some of these pre-treatments has been proved, the high energy and chemical requirements make this step among the most expensive ones in the conversion of lignocellulosic biomass. In addition, the employed chemicals produce streams with high-contamination potential and generate byproducts that can inhibit subsequent processes in the biorefinery (Robak & Balcerek, 2018). The use of high-energy demanding processes and polluting compounds for the production of green products that should reduce the negative environmental impact appears contradictory. If, indeed, the attention on the prevention of food waste has been very concrete, an equally important consideration should be put on the sustainability of the exploitation of unavoidable food wastes, preventing further side-effects.

On the way towards sustainability, biological pre-treatment, mediated by microorganisms and/or their degradative enzymes, is considered a viable and sustainable alternative to chemo-physical approaches. It is performed under milder conditions, close to ambient temperature and pressure, thus requiring lower energy and chemical inputs, and reducing the production of inhibitors and highly-contaminant byproducts (Mishra et al., 2018).

However, even biological pre-treatments reserve some critical aspects, such as the long incubation time required and the low overall efficiency (Vasco-Correa, et al., 2016), not to mention the high costs still related to enzymes provision, varying from 3.3 US\$ kg<sup>-1</sup> to 316 US\$ kg<sup>-1</sup> (Ferreira et al., 2020). This implies that improvements are still required to make biological pre-treatments a competitive alternative to thermo-chemical methods (Vasco-Correa, et al., 2016).

In this context, the biorefinery concept has been raised as a solution conceived to counterbalance the low efficiency and the high-cost processes related to biological waste biomass conversion. The biorefinery is defined as a multi-product system, where biomass is integrally processed in a closed-loop production approach that makes the most of it, releasing a series of different products (Moncada, et al., 2016; Qing et al., 2018). In biorefineries, the process revenues are maximized by drawing upon the value of co-products and the cogeneration of energy. Exemplary works based on the biorefinery concept taking advantage of co- and byproducts are represented by the research of de Castro et al., (2014). In this work, the solid material remained after solid state fermentation of babassu cake, a solid residue derived from the process of oil extraction from the babassu coconut palm fruit, still rich in carbohydrates (starch, cellulose, and hemicelluloses) and proteins, was sold as a supplement for animal feed. In another example, residues of dry spruce chips from ethanol production, still particularly rich in lignin, were addressed to energy generation in the form of steam (Barta et al., 2010).

However, despite these few examples, the development of biorefineries able to convert biomass into valuable bioproducts, exploiting all the by- and co-products generated during the production, and therefore defined as zero-waste processes

in compliance with the circular economy system, are still far from being widespread (Demichelis, et al., 2018).

Another strategy that goes hand in hand with the biorefinery system, is the development of genetically modified microorganisms to boost the enzymatic efficiency as well the creation of consolidated bioprocessing microorganisms, able to saccharify the biomass and produce biocommodities at the same time (Abdel-Rahman, et al., 2011).

Consolidated bioprocessing (CBP) is a system in which enzyme production, substrate saccharification, and fermentation are accomplished in a single process by lignocellulosytic microorganisms, thus saving the cost of investing in multi-step processes. It has been estimated that CBP has reduced production costs of ethanol by as much as 41%, characterizing this process as a less energy-intensive method and a potential low-cost route for production of industrially important products (Agbor, et al., 2014). Maleki et al., (2021) performed CBP bioethanol production by engineered *Bacillus subtilis* using renewable plant biomass and wastes.

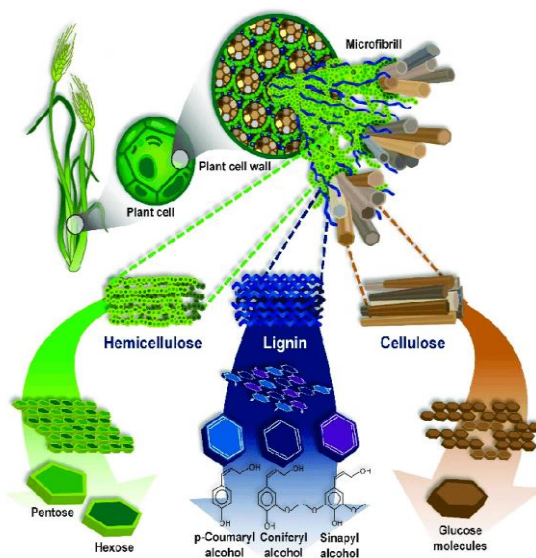


**Figure 1.** The main components and structure of lignocellulose (from Isikgor & Becer, 2015).

### 1.1.3 Carbon-active enzymes

The enzymes able to degrade complex carbohydrates and glycoconjugates in lignocellulosic biomass are called Carbohydrate-Active enZymes (CAZymes). In the Carbohydrate Active Enzymes database (CAZy; <http://www.cazy.org/>) they are classified in different families, based on the amino acid sequence of the



related catalytic module. Their action occurs in a synergistic way for the complete hydrolysis of carbohydrate polymers of biomass into sugars (Menon & Rao, 2012).

Due to its highly ordered and crystalline structure, cellulose requires the action of three enzymes acting on the  $\beta$ -1,4-glycosidic bond to be degraded: an endo- $\beta$ -glucanase (EC 3.2.1.4), a cellobiohydrolase (EC 3.2.1.91) and a  $\beta$ -glucosidase (EC 3.2.1.21) (Fig. 2) (de Souza, 2013). The synergistic action of these enzymes allows the release of monomeric fermentable glucose from cellulose. Endoglucanase acts on inner sites of the polymer; cellobiohydrolase hydrolyzes non-reducing ends of crystalline cellulose and forms cellobiose, while  $\beta$ -glucosidase acts on non-reducing ends of cellobiose and cellobiose forming glucose as the major end-product (Patel et al., 2019).

Contrarily to cellulose, hemicellulose, being a heterogeneous polymer composed of different sugars and highly substituted, needs a larger number of different enzymes for its complete hydrolysis as compared to cellulose. Fig. 3 depicts the enzymes involved in arabinoxylan degradation which include endo-1,4- $\beta$ -xylanases (EC 3.2.1.8),  $\alpha$ -L-arabinofuranosidases (EC 3.2.1.55),  $\beta$ -D-xylosidases (EC 3.2.1.37),  $\alpha$ -D-galactosidases (EC 3.2.1.22),  $\alpha$ -D-glucuronidases (EC 3.2.1.139), feruloyl esterase (EC 3.1.1.73), acetyl xylan esterase (E.C. 3.1.1.72), and arabinoxylan arabinofuranohydrolase (AXAH; EC 3.2.1.136) (Houfani et al., 2020).

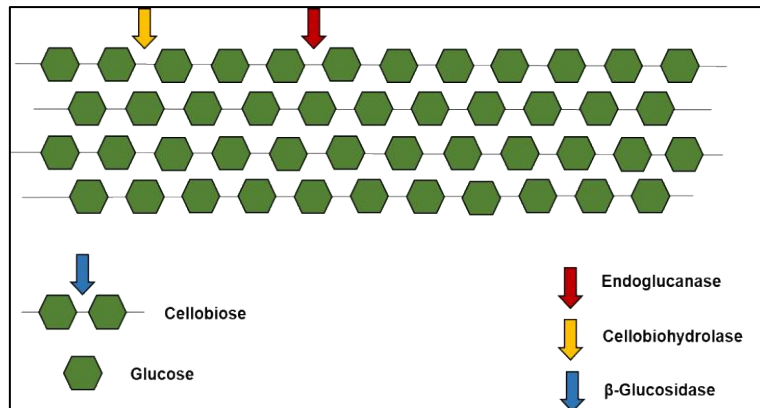


**Figure 2.** Schematic view of cellulose degradation.

Another family of CAZy enzymes is constituted by pectinases, a large group of enzymes that catalyze the degradation of pectic substances. They are categorized based on their mode of action: esterases act only on pectin, while depolymerases also act on polygalacturonic acid and rhamnogalacturonan. Pectinases classification is provided in Fig. 4 based on their target sites on pectin (Singh et al., 2019).

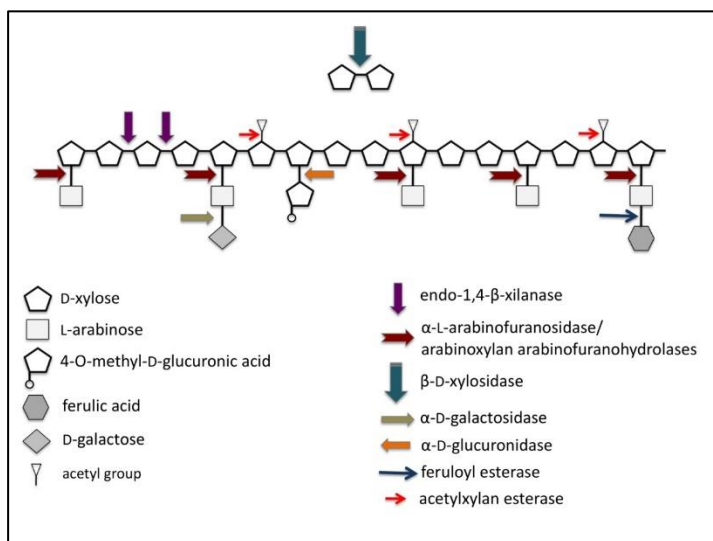


**Figure 3.** Schematic view on a hemicellulolytic system degradation, specifically, degradation of arabinoxylan is depicted. The arrows represent each enzyme active for a determined substrate (from de Souza, 2013).

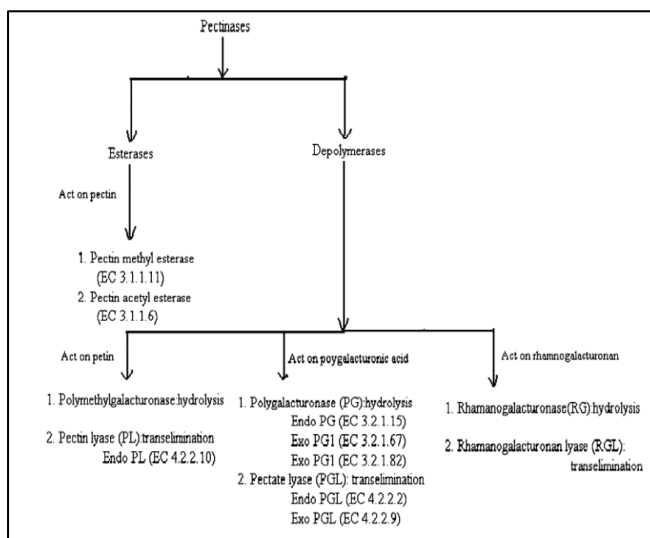


**Figure 4.** Classification of different pectinases based on their reaction with different pectin substances (from Sharma et al., 2013).

All these plant cell wall degrading enzymes are among the leading enzymes commercially produced for diversified industrial applications. A recent market report estimated the value of the industrial enzyme market in 2020 to be around USD 5.9 billion. It is further predicted that this value would increase to

approximately USD 8.7 billion by the year 2026 (<https://www.precedenceresearch.com/industrial-enzymes-market>).

This prediction is based on the assumption that environmental concerns around the use of chemicals in industrial processes will increase the demand for sustainable and environmentally friendly enzymes. Other factors considered are the increasing demand for biofuels and green products towards a truly sustainable economy.

Among the enzymes surveyed, cellulases account for a significant share of the market. Owing to the widespread applications of this biopolymer across a plethora of sectors, including food, textiles, pharmaceutical, detergent, biofuels, pulp and paper industries, and its abundance in nature, the demand for cellulases is always on the rise. The most popular and successful application of cellulases occurs in the textile industry, where these enzymes are used for jeans bio-stoning, biopolishing of fabrics and cotton and to improve appearance of fabrics. In fabrics detergents, alkaline cellulases improve the brightness of color and dirt removal (Ejaz et al., 2021; Rodrigues & Odaneth, 2021). Treatment with cellulases also improves the quality of wine, helping in clarification, color development, maceration, and reduced wort viscosity. Cellulases are also utilized for the extraction of oil from olives resulting in less wastage, lower tendency to rancidity, increase in antioxidant components, better quality and extraction yield.

The other CAZymes widely employed as green tools by industry are xylanases. In the bakery, the addition of xylanase within the dough improves its rheological properties such as softness, extensibility, and elasticity along with bread-specific volume and crumb firmness (Harbak & Tygesen 2002; Camacho & Aguilar 2003). Paper and pulp industry employs both cellulases and xylanases for bio-bleaching to produce bright and completely white finished paper and for deinking, which is a necessary process for removing printing ink from fibers of recycled paper (Ejaz, et al., 2021). The same also occurs in the feed industry, in which cellulases and xylanases can be employed as pre-treatment of grains and agricultural silage to improve the nutritional value of animal feed (Ejaz, et al., 2021).

Pectinases have been applied in various processes, such as plant fiber processing, tea and coffee fermentation, treatment of industrial wastewater, and so forth. In the food processing industry, pectinases, together with xylanases, are used for fruit juice clarification, as color and yield enhancers, as well as in the fruit mash treatment. Apart from these applications, pectinases are also used in degumming/retting fiber crops, as enzyme cocktails for the extraction of oils, and as de-sizing agents in the textile industry (Sharma et al., 2013; Singh et al., 2019).

## References

**Abdel-Rahman M.A., Tashiro Y., Sonomoto K.** 2011. Lactic acid production from lignocellulose-derived sugars using lactic acid bacteria: overview and limits. *J Biotechnol.* 156, 286-301. DOI: 10.1016/j.jbiotec.2011.06.017.

**Abdeshahian P., Ascencio J.J., Philippini R.R. et al.** 2021. Valorization of Lignocellulosic Biomass and Agri-food Processing Wastes for Production of Glucan Polymer. *Waste Biomass Valor.* 12, 2915-2931. DOI: 10.1007/s12649-020-01267-z.

**Agbor V., Carere C., Cicek N., Sparling R., Levin D.** 2014. Biomass pre-treatment for consolidated bioprocessing (CBP), Editor(s): Keith Waldron, *Advances in Biorefineries*, Woodhead Publishing, 8, 234-258, DOI: 10.1533/9780857097385.1.234.

**Barta Z., Kovacs K, Reczey K, Zacchi G.** 2010. Process Design and Economics of On-Site Cellulase Production on Various Carbon Sources in a Softwood-Based Ethanol Plant. *Enzyme Res.* 2010. DOI: 10.4061/2010/734182.

**Branda S. S., Gonzalez-Pastor J. E., Ben-Yehuda S., Losick R., Kolter R.** 2001. Fruiting body formation by *Bacillus subtilis*. *PNAS* 98, 11621-11626. DOI: 10.1073/pnas.191384198.

**Camacho N.A., Aguilar O, G.** 2003. Production, purification, and characterization of a low-molecular-mass xylanase from *Aspergillus* sp. and its application in baking. *Appl. Biochem. Biotechnol.* 104, 159-171. DOI: 0.1385/ABAB:104:3:159.

**Chen S., Zhang X., Singh D., Yu H., Yang X.** 2010. Biological pre-treatment of lignocellulosics: potential, progress and challenges. *Biofuels* 1, 177-199, DOI: 10.4155/bfs.09.13.

**de Castro A.M., López J.A., Castilho L. R., Freire D.M.G.** 2014. Techno-economic analysis of a bioprocess for the production of multienzyme solutions from the cake of babassu industrial processing: Evaluation of five different inoculum propagation strategies. *Biomass Convers. Biorefin.* 4, 237-247. DOI: 10.1007/s13399-013-0106-2.

**de Souza W. R.** 2013. Microbial Degradation of Lignocellulosic Biomass. In: Chandel, A. K., Silva, S. S. d., editors. *Sustainable Degradation of Lignocellulosic Biomass - Techniques, Applications and Commercialization*. DOI: /10.5772/54325.

**Demichelis F., Fiore S., Pleissner D., Venus J.** 2018. Technical and economic assessment of food waste valorization through a biorefinery chain. *Renew. Sust. Energ. Rev.* 94, 38-48. DOI: 10.1016/j.rser.2018.05.064.

**Earl A. M., Losick R., Kolter R.** 2008. Ecology and genomics of *Bacillus subtilis*. *Trends Microbiol.* 16, 269. DOI: 10.1016/j.tim.2008.03.004.

**Ehling-Schulz M., Lereclus D., Koehler T.M.** 2019. The *Bacillus cereus* Group: *Bacillus* Species with Pathogenic Potential. *Microbiol. Spectr.* 7, 6. DOI: 10.1128/microbiolspec.GPP3-0032-2018.

**Ejaz U., Sohail M., Ghanemi A.** Cellulases: 2021. From Bioactivity to a Variety of Industrial Applications. *Biomimetics* 6, 44. DOI: 10.3390/biomimetics6030044.

- Esakkiraj P., Immanuel G., Sowmya S. M., Iyapparaj P., Palavesam A.** 2009. Evaluation of protease-producing ability of fish gut isolate *Bacillus cereus* for aqua feed. *Food Bioproc. Tech.* 2, 383-390. DOI: 10.1007/s11947-007-0046-6 .
- Ferreira R.G., Azzoni A.R., Freitas S.** 2020. On the production cost of lignocellulose-degrading enzymes. *Biofuels, Bioprod. Bioref.* 15, 85-99. DOI: 10.1002/bbb.2142.
- Furhan J., Sharma S.** 2015. Microbial alkaline proteases: findings and applications. *Int. J. Invent. Pharm. Sci.* 2, 823-834.
- Hamoen L. W., Venema G., Kuipers O. P.** 2003. Controlling competence in *Bacillus subtilis*: shared use of regulators. *Microbiology* 149, 9-17. DOI: 10.1099/mic.0.26003-0.
- Hamon M. A., Lazazzera B. A.** 2001. The sporulation transcription factor Spo0A is required for biofilm development in *Bacillus subtilis*. *Mol. Microbiol.* 42, 1199-1209. DOI: 10.1046/j.1365-2958.2001.02709.x.
- Harbak L., Thygesen H.V.** 2002. Safety evaluation of a xylanase expressed in *Bacillus subtilis*. *Food Chem. Toxicol.* 40, 1-8. DOI: 10.1016/s0278-6915(01)00092-8
- Heinze T., Liebert T.** 2012. Celluloses and Polyoses/Hemicelluloses. Editor(s): Krzysztof Matyjaszewski, Martin Möller. *Polymer Science: A Comprehensive Reference*, Elsevier 10, 83-152. DOI: 10.1016/B978-0-444-53349-4.00255-7.
- Hong H. A., et al.** 2009. *Bacillus subtilis* isolated from the human gastrointestinal tract. *Res. Microbiol.* 160, 134-143. DOI: 10.3389/fbioe.2021.690773.
- Houfani A. A., Anders N., Spiess A. C., Baldrian P., Benallaoua S.** 2020. Insights from enzymatic degradation of cellulose and hemicellulose to fermentable sugars— a review, *Biomass Bioenerg.* 134, 105481. DOI: 10.1016/j.biombioe.2020.105481.
- Huang L. Z., Ma M. G., Ji X.X., Choi S. E., Si C.** 2021. Recent Developments and Applications of Hemicellulose From Wheat Straw: A Review. *Front Bioeng. Biotechnol.* 9, 2296-4185. DOI: 10.3389/fbioe.2021.690773.
- Ikemura H., Takagi H., Inouye M.** 1987. Requirement of pro-sequence for the production of active subtilisin E in *Escherichia coli*. *J. Biol. Chem.* 262, 7859-7864. DOI: 10.1016/S0021-9258(18)47646-6.
- Isikgor F. H., Becer C. R.** 2015. Lignocellulosic biomass: a sustainable platform for the production of bio-based chemicals and polymers. *Review Article. Polym. Chem.* 6, 4497-4559. DOI: 10.1039/C5PY00263J.
- Jin Q., Yang L., Poe N., Huang H.** 2018. Integrated processing of plant-derived waste to produce value-added products based on the biorefinery concept. *Trends Food Sci. Technol.* 74, 119-131. DOI: 10.1016/j.tifs.2018.02.014.
- Kargbo H., Harris J. S., Phan A. N.** 2021. “Drop-in” fuel production from biomass: Critical review on techno-economic feasibility and sustainability. *Renewable Sustainable Energy Rev.* 135, 110168. DOI: 10.1016/j.rser.2020.110168 .

**Lee N.K., Kim W.S., Paik H.D.** 2019. Bacillus strains as human probiotics: characterization, safety, microbiome, and probiotic carrier. *Food Sci. Biotechnol.* 28, 1297-1305. DOI: 10.1007/s10068-019-00691-9.

**Liu L., Liu Y., Shin H., Chen R. R., Wang N. S., Li J., Du G., Chen J.** 2013. Developing Bacillus spp. as a cell factory for production of microbial enzymes and industrially important biochemicals in the context of systems and synthetic biology. *Appl. Microbiol. Biotechnol.* 97, 6113-6127. DOI: 10.1007/s00253-013-4960-4.

**Maleki F., Changizian M., Zolfaghari N., Rajaei S., Noghabi K.A., Zahiri H.S.** 2021. Consolidated bioprocessing for bioethanol production by metabolically engineered Bacillus subtilis strains. *Sci Rep.* 11, 13731. DOI: 10.1038/s41598-021-92627-9.

**McKendry P.** 2002. Energy production from biomass (Part 1): Overview of biomass. *Bioresour Technol.*, 83, 37-46. DOI: 10.1146/annurev-biochem-060614-033930.

**McNamara J. T., Morgan J. L., Zimmer J.** 2015. A molecular description of cellulose biosynthesis. *Annu Rev Biochem.* 84, 895-921. DOI: 10.1146/annurev-biochem-060614-033930.

**Menon V., Rao M.** 2012. Trends in Bioconversion of Lignocelluloses: Biofuel, Platform Chemicals & Biorefinery Concept. *Prog. Energy Combust. Sci.* 38, 522-550. DOI: 10.1016/j.pecs.2012.02.002.

**Messelhäüßer U., Ehling-Schulz M.** 2018. Bacillus cereus-a Multifaceted Opportunistic Pathogen. *Curr. Clin. Micro. Rpt.* 5, 120–125. DOI: 10.1007/s40588-018-0095-9.

**Mishra S., Singh P.K., Dash S., Pattnaik R.** 2018. Microbial pre-treatment of lignocellulosic biomass for enhanced biomethanation and waste management. *3 Biotech.*, 8, 458. DOI: 10.1007/s13205-018-1480-z.

**Moncada B.J., Aristizábal M.V., Cardona A.C.A.** 2016. Design strategies for sustainable biorefineries. *Biochem. Eng. J.* 116, 122-134. DOI: 10.1016/j.bej.2016.06.009.

**Nayak A., Bhushan B.** 2019. An overview of the recent trends on the waste valorization techniques for food wastes. *J. Environ. Manag.* 233, 352–370. DOI: 10.1016/j.jenvman.2018.12.041.

**Ning P., Yang G., Hu L. Sun J., Shi L., Zhou Y., Wang Z., Yang J.** 2021. Recent advances in the valorization of plant biomass. *Biotechnol. Biofuels* 14, 102. DOI: 10.1186/s13068-021-01949-3.

**Paredes-Sabja D., Setlow P., Sarker M. R.** 2011. Germination of spores of Bacillales and Clostridiales species: mechanisms and proteins involved. *Trends Microbiol.*, 19, 85-94. DOI: 10.1016/j.tim.2010.10.004.

**Patel A.K., Singhania R.R., Sim S.J., Pandey A.** 2019. Thermostable cellulases: Current status and perspectives. *Bioresour. Technol.*, 279, 385–392. DOI: 10.1016/j.biortech.2019.01.049.

**Qing J., Yang L., Poe N., Huang H.** 2018. Integrated processing of plant-derived waste to produce value-added products based on the biorefinery concept. *Trends Food Sci. Technol.*, 74, 119-131, DOI: 10.1016/j.tifs.2018.02.014.

- Robak K., Balcerek M.** 2018. Review of Second Generation Bioethanol Production from Residual Biomass. *Food Technol Biotechnol.*, 56, 174-187. DOI: 10.17113/ftb.56.02.18.5428.
- Rodrigues V. J., Odaneth A. A.** 2021. Chapter 10 - Industrial application of cellulases. Editor(s): Deepak K.Tuli, Arindam Kuila. *Current Status and Future Scope of Microbial Cellulases*, Elsevier, 189-209. DOI: 10.1016/B978-0-12-821882-2.00007-7.
- Rongpipi S., Ye D., Gomez E.D., Gomez E.W.** 2019. Progress and Opportunities in the Characterization of Cellulose - An Important Regulator of Cell Wall Growth and Mechanics. *Front Plant Sci.* 9. DOI: 10.3389/fpls.2018.01894.
- Sánchez C.** 2009. Lignocellulosic residues: biodegradation and bioconversion by fungi. *Biotechnol. Adv.*, 27, 185-94. DOI: 10.1016/j.biotechadv.2008.11.001.
- Schallmeyer M., Singh A., Ward O. P.** 2004. Developments in the use of *Bacillus* species for industrial production. *Can. J. Microbiol.* 50, 1-17. DOI: 10.1139/w03-076.
- Sella Ruiz SRB., Bueno T., de Oliveira AAB., Karp SG., Socol CR.** 2021. *Bacillus subtilis* natto as a potential probiotic in animal nutrition. *Crit. Rev. Biotechnol.* 41, 355-369. DOI: 10.1080/07388551.2020.1858019.
- Sharma N., Rathore M., Sharma, M.** 2013. Microbial pectinase: sources, characterization and applications. *Rev. Environ. Sci. Biotechnol.* 12, 45–60. DOI: 10.1007/s11157-012-9276-9.
- Singh R. S., Singh T., Pandey A.** 2019. Chapter 1 - Microbial Enzymes—An Overview, Editor(s): Ram Sarup Singh, Reeta Rani Singhania, Ashok Pandey, Christian Larroche. In *Biomass, Biofuels, Biochemicals, Advances in Enzyme Technology*, Elsevier 1-40. DOI: 10.1016/B978-0-444-64114-4.00001-7.
- Singh R., Mittal A., Kumar M., Mehta P. K.** 2016. Microbial Proteases in Commercial Applications. *Int. j. pharm. chem. biol. sci.* 4, 365-374.
- Solanki P., Putatunda C., Kumar A., Bhatia R., Walia A.** 2021. Microbial proteases: ubiquitous enzymes with innumerable uses. *3 Biotech.* 11, 428. DOI: 10.1007/s13205-021-02928-z.
- Springmann M., Clark M., Mason-D’Croz D., et al.** 2018. Options for keeping the food system within environmental limits. *Nature* 562, 519-525. DOI: 10.1038/s41586-018-0594-0.
- Su Y., Liu C., Fang H., Zhang D.** 2020. *Bacillus subtilis*: a universal cell factory for industry, agriculture, biomaterials and medicine. *Microb. Cell Fact.* 19, 173. DOI:10.1186/s12934-020-01436-8.
- Svendsen I.** 1976. Chemical modifications of the subtilisins with special reference to the binding of large substrates. A review. *Carlsberg Res. Commun.* 41, 237. DOI: 10.1007/BF02906260.
- Vasco-Correa Ge J. X., Li Y.** 2016. Chapter 24. Biological Pre-treatment of Lignocellulosic Biomass, Editor(s): Solange I. Mussatto. *Biomass Fractionation Technologies for a Lignocellulosic Feedstock Based Biorefinery*, Elsevier 561-585. DOI: 10.1016/B978-0-12-802323-5.00024-4.

**Verma N., Kumar V.** 2021. Microbial conversion of waste biomass into bioethanol: current challenges and future prospects. *Biomass Conv. Bioref.* DOI: 10.1007/s13399-021-01824-z.

**Vilariño M. V., Carol F., Caitlin Q.** 2017. Food loss and Waste Reduction as an Integral Part of a Circular Economy. MINI REVIEW article, *Front. Environ. Sci.* 5, 21. DOI: 10.3389/fenvs.2017.00021.

**Westers L., Westers H., Quax W. J.** 2004. *Bacillus subtilis* cell factory for pharmaceutical proteins: a biotechnological approach to optimize the host organism. *Biochim. Biophys. Acta Mol. Cell Res.* 1694, 299-310. DOI: 10.1016/j.bbamcr.2004.02.011.

**Xiong X., et al.** 2019. Value-added chemicals from food supply chain wastes: state-of-the-art review and future prospects. *Chem. Eng. J.* 375, 121983. DOI: 10.1016/j.cej.2019.121983.

**Yousuf A., Pirozzi D., Sannino F.** 2020. Chapter 1 - Fundamentals of lignocellulosic biomass, Editor(s): Abu Yousuf, Domenico Pirozzi, Filomena Sannino. *Lignocellulosic Biomass to Liquid Biofuels*, Academic Press 1-15, DOI: 10.1016/B978-0-12-815936-1.00001-0.

**Zoghlami A., Paës G.** 2019. Lignocellulosic Biomass: Understanding Recalcitrance and Predicting Hydrolysis. *Front. Chem.* 7, 874. DOI: 10.3389/fchem.2019.00874.



## 1.2 Aim of the work

This thesis deals with the optimization of the degradative capabilities of *Bacillus subtilis*, taken as industrial model organism, and with the biotechnological applications of the improved strains.

The enzymes that underwent the optimization process are plant cell wall-degrading enzymes that *B. subtilis* already possesses in its genome; therefore, the strain optimization did not require the integration of any exogenous DNA. The efforts dedicated to the choice of the target and to the evaluation of the effects of the genetic improvements in terms of enzyme yield are described in Chapter 2.

The second main goal of the thesis is the implementation of the hyperproducing strains in two rather different biotechnological applications. Both of them are part of the same main objective, which is the development of viable, sustainable and cheap biotechnological processes, based on *B. subtilis* enzymatic properties, for the efficient conversion of biomasses into resources.

A large body of literature demonstrated the positive effect of *B. subtilis* spores, added to dairy cattle feed, on ruminal fermentation, lactation performance and milk composition. To identify the scientific rationale for the increase in animal productivity observed *in vivo*, in Chapter 3, several ruminant forages were treated with wild-type or optimized *B. subtilis* strains to investigate the presence of any correlation between feed quality and degradative enzymes levels.

In Chapter 4, the enzymatic activities of the optimized strain were exploited for the extraction of nutraceutical molecules encased in the vegetable matrix of cauliflower waste, thereby ensuring a truly sustainable extraction process.

**Chapter 2: Optimization of enzymes production in  
*Bacillus subtilis***

## 2.1 Abstract

The current trend towards a sustainable economy, aimed at exploiting the agri-food waste, has made research and development activities on more efficient enzymes-producing microorganisms essential, and has set a primary focus on the development of cost-effective and versatile green technologies.

One of the strategies to improve enzymatic efficiency is to enhance the production capacity of enzyme producing-microorganisms by genetic engineering, to obtain suitable enzyme yields for industrial applications.

Among the enzyme-producing microorganisms, *Bacillus subtilis*, the model organisms of gram-positive, is considered a relevant industrial workhorse due to its high secretion capacity, safety, high metabolic adaptability, and excellent fermentation properties. Being a soil bacterium, it is endowed with genes encoding enzymes able to degrade plant biomass.

In this work, its intrinsic enzyme producing aptitude has been boosted by genetic engineering without the introduction of any heterologous DNA sequence. Extensive preliminary searches were conducted in the literature on the degradative-enzymatic pathways present in *B. subtilis*. With the knowledge acquired, several target genes were identified and subjected to an optimization strategy aimed at improving their production. The genes under investigation were a cellulase-encoding gene, involved in cellulose degradation, several xylanases-encoding genes, for the degradation and utilization of xylan, and a phytase-encoding gene which role is the degradation of phytic acid, considered an anti-nutritional factor. The aim of the work was, principally, to issue a patent on the optimization procedure; therefore, the optimization system and the chosen genes will not be the object of the chapter.

The optimization procedure gave rise to several strains, each containing a specific optimized enzyme, except for a strain optimized for both cellulase and xylanase. To prove the efficacy of the genetic interventions, specific and sensitive assays protocols for the detection of the enzymatic activities were developed.

The results demonstrated the higher enzyme production efficiency of the optimized strains compared to the wild-type strain for all the strains.

The future development of these efforts will be the combination of all the optimized genes in a single strain, for the creation of a microorganism adapted to biomass waste fermentation with a view to creating a consolidated bioprocessing microorganism.

## 2.2 Introduction

Keeping in view the sustainable development, the interest has shifted from chemical products to enzymatic products for industrial processes (Liew et al., 2022). Among the others, the so-called Carbohydrate-Active enZymes (CAZymes), such as cellulase, xylanase, pectinase, laccase and others, able to hydrolyze the components of plant biomass, are the new frontier of the green economy towards a more sustainable industrial production aiming at exploiting the huge lignocellulosic biomass produced as waste every year. These enzymes have replaced the traditional chemical treatment, establishing themselves as innovative biological tools of biomass deconstruction and the release of sugars for the production of clean energy and molecules of industrial interest in a sustainable and eco-friendly way.

However, the high cost and low yield associated with enzymes production by microorganisms take a prohibitive toll on it, mining the economic viability and the efficiency of the industrial employment of enzymes. The increasing interest in CAZymes has spurred the search for new strategies to counteract the above issues; one of the strategies is the optimization of the different phases involved in enzyme production, from the enzymatic pathway (by genome mining or enzyme engineering) to strain (i.e., metabolic modeling), to fermentation process, thus increasing the overall production of enzymes by producer microorganisms (Fig. 5).

The boosting of endogenous saccharification activity may be crucial for the creation of Consolidated Bioprocessing (CBP) microorganisms able to saccharify the biomass and produce biocommodities in a single process, which can lower production costs and maintain the sustainability of the process (Abdel-Rahman, et al., 2011).

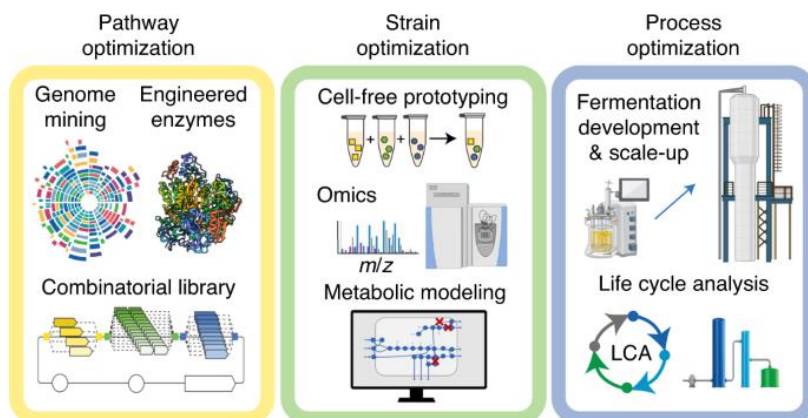


**Figure 5.** Overview of three-pronged approach for pathway, strain, and process optimization (from Liew et al., 2022).

Among the major enzyme-producers several fungi as *Trichoderma*, *Penicillium* and *Aspergillus* are ranked, while *Pseudomonas*, *Bacillus*, and *Clostridium* are the main bacterial enzyme-makers (Rodrigues & Odaneth, 2021).

The best-characterized bacterial cellulolytic enzymes, *inter alia*, are those of *Bacillus* species, particularly the ones from *B. subtilis*, being the model organism of Gram-positive bacteria (Liu et al., 2006).

The innate ability to grow on a diversity of carbohydrates, its highly amenability to genetic manipulation, together with its impressive secretion ability, make it the perfect candidate for the construction of a CBP microorganism (Agbor, et al., 2014).

According to the CAZy database (CAZy; <http://www.cazy.org/>), the genome of a common laboratory strain of *Bacillus subtilis*, as JH642, carries several genes encoding secreted enzymes involved in complex carbohydrates and lignocellulose degradation (Srivatsan et al., 2008; Smith et al., 2014). In nature, indeed, *B. subtilis*, dwelling mainly in the upper layers of the soil and in the plant rhizosphere, has evolutionary accumulated a large set of genes encoding CAZymes for the degradation of complex carbohydrates matrices of decaying plant materials.

*Bacillus subtilis* is able to degrade cellulose by secretion of an endo-1,4- $\beta$ -glucanase encoded by the gene *bg/C* (EC 3.2.1.4) which hydrolyzes the 1,4- $\beta$ -D-glycosidic linkages in cellulose (<https://www.uniprot.org/>; Liu et al., 2006).

Xylans degradation is carried out by several enzymes encoded by single or bicistronic genes. The monocistronic gene *xynA* encodes an endo-1,4- $\beta$ -xylanase (EC 3.2.1.8), which hydrolyzes xylan to  $\beta$ -xylosides, which are subsequently taken up by the  $\beta$ -xyloside transporter XynP encoded in the bicistronic *xynPB* operon. The  $\beta$ -xylosidase XynB converts  $\beta$ -xylosides to xylose, which is further converted to xylulose-5-P by the enzymes encoded in the adjacent *xylAB* operon. Finally, xylulose-5-P enters the pentose phosphate pathway. Both *xynPB* and *xylAB* operons are repressed by the binding of the XylR repressor to the operator sites in the absence of the inducer xylose. Both operons are subjected to global Carbon Catabolite Repression (CCR), which is mediated by binding of CcpA to *cre* sites downstream their respective promoters (Singh et al., 2008) (Fig. 6).

In addition to the endoxylanase XynA, *B. subtilis* secretes a second endoxylanase encoded by *xynC* gene (St John et al., 2006). In particular, the *xynC* product is an extracellular glucuronoxylanase (EC 3.2.1.136) which is involved in catalyzing the depolymerization of methylglucuronoxylan, the primary component of hemicellulose in hardwood and crop residues. *xynC* is found in a operon together with the gene *xynD*, encoding a secreted arabinoxylan arabinofuranohydrolase (EC 3.2.1.55) which cleaves arabinose units from O-2- or O-3-monosubstituted xylose residues, thereby assisting in arabinoxylan and short-chain arabinoxylo-oligosaccharide degradation (<https://www.uniprot.org/uniprotkb/Q45071/entry>).

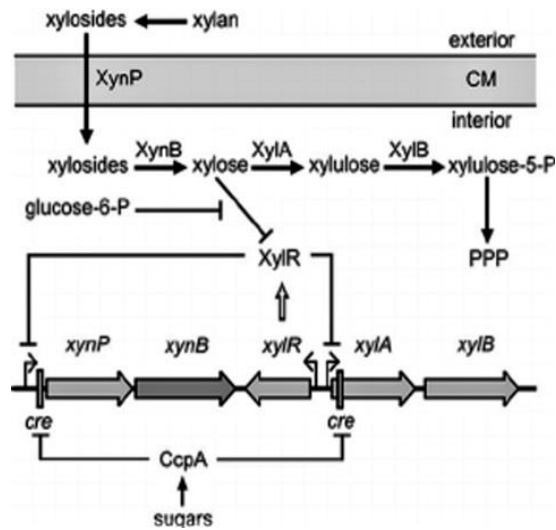


**Figure 6.** Scheme of xylan utilization in *B. subtilis* (from Singh et al., 2008).

Other enzymes involved in the degradation and utilization of xylan that are present in the genome of *Bacillus subtilis* are represented in Fig. 7 derived from the STRING Database (<https://string-db.org/network/224308.BSU18160>). Together with the previously mentioned XynC, XynA, XynB, also BglS, AbnB, XsA, AraA are involved in this task.

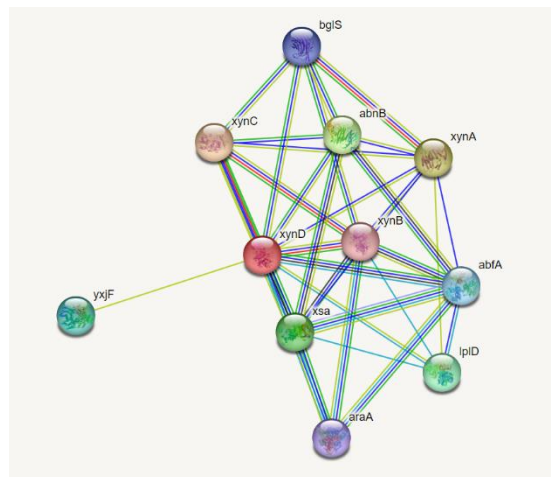


**Figure 7.** Enzymes involved in xylan degradation (from STRING Database <https://string-db.org/network/224308.BSU18160>).

According to Uniprot, *Bacillus subtilis* is capable of degrading polygalacturonic acid, the building block of pectin, by the action of the products of three genes

encoding the pectate lyases Pel, PelB and PelC (<https://www.uniprot.org/uniprotkb/P39116/entry>; <https://www.uniprot.org/uniprotkb/P94449/entry>; <https://www.uniprot.org/uniprotkb/O34310/entry>, respectively).

Another secreted enzyme of *B. subtilis* raising great interest is phytase. This enzyme is able to degrade myo-inositol hexakisphosphate known as phytic acid (phytate), the main storage form of phosphorus in plants. Besides phosphorous, phytate can also chelate essential cations such as iron, magnesium, calcium and zinc, limiting their bioavailability in food and feed, therefore acting as anti-nutrient compound. To reduce the formation of phytate and free minerals from vegetable compounds, phytase can be added to animal diets, thereby improving the nutritional value of the forages (Spier et al., 2018).

## 2.3 Materials and Methods

### 2.3.1 Bacterial strains

The optimized strains derived by genetic engineering from the common laboratory strain JH642 (GenBank accession no. CM000489.1), auxotrophic for tryptophan and phenylalanine due to the *trpC2 pheA1* mutations (Srivatsan et al., 1998). The prototrophic strain PB5700 (herein named WT) is a *swrA*<sup>+</sup> spontaneous derivative of JH642 (PB5249, Mordini et al., 2013) which was sequentially transformed with the PCR products of the *trpC* and *pheA* genes, obtained from the genomic DNA of the undomesticated NCIB 3610 strain (GenBank accession no. CP020102.1). Amplifications of the *trpC* and *pheA* genes were performed using the primer pairs *trpC*\_Up 50-AGTGAAAACACTGGTTCTGCCG-30 and *trpC*\_Dw 50-GATGGATTGCTTTACGCTGAGAAG-30 followed by *pheA*\_Up 50-AACAGCCTTTGCCAATCGTGGG-30 and *pheA*\_Dw 50-GTATACATGGATGCAGCCGCTCAG-30, respectively. For the first transformation, the selection of the *trpC*<sup>+</sup> prototroph occurred on minimal medium containing 1.5% agar, 1 mg/mL glucose and phenylalanine (50 µg/mL). Subsequently, *pheA*<sup>+</sup> transformants were selected on minimal medium without amino acids. PB5700 was chosen as mother strain to avoid the addition of amino acids to culture media. A patent application is under preparation for the optimized strains; for this reason, the details of the engineering design are undisclosed herein.

The four strains obtained from the optimization protocol will be indicated as follows: PB2OPT (cellulase and endo-xylanase optimization); PBOPT1 (arabinofuranosidase optimization); PBOPT2 (xylosidase optimization); PBOPT3 (phytase optimization).

### 2.3.2 Bacterial growth

For enzymes production, spores of either PB5700 or the optimized strains were revitalized on LB (Difco Laboratories, New York, NY, USA) 1.5% agar plates and incubated overnight at 37°C. Isolated colonies were pre-inoculated in Antibiotic Medium 3 (Difco Laboratories) containing 5 mg/mL glucose and grown 16 h at 37°C with shaking. The media used for the production of the enzymes and their detection were either LB or the synthetic medium CMD (containing, per liter: 13.67 g Na citrate; 10 g glucose; 7 g NH<sub>4</sub>Cl; 0.5 g MgSO<sub>4</sub>·7H<sub>2</sub>O; 0.5 g K<sub>2</sub>HPO<sub>4</sub>; 0.15 g CaCl<sub>2</sub>·2H<sub>2</sub>O; 0.104 g MnSO<sub>4</sub>·H<sub>2</sub>O; 0.04 g FeCl<sub>2</sub>·6H<sub>2</sub>O; pH 6.5) and, as carbon source, 1% of one of the following sugars: glucose, xylan, xylose, a combination of xylan and xylose (1:1 ratio), arabinose, and soybean flour.

The inoculum was started in the production medium at OD<sub>600</sub> 0.2 and grown for 24 h at 37°C with 150 rpm orbital shaking. Bacterial growth was followed by optical density readings at 600 nm (OD<sub>600</sub>). Culture supernatants were collected by centrifugation at room temperature at 2,268 x g for 15 minutes.

### Evaluation of enzymatic activities



### 2.3.3 Cellulase and endo-xylanase activities

Cellulase and endo-xylanase activities were assayed in an aliquot of the culture supernatants after acidification, using the specific colorimetric assays CellG3 and XylX6 Assay Kits (Megazyme®), following the protocol provided by the manufacturer.

### 2.3.4 Arabinofuranosidase activity

The assay of arabinofuranosidase derived from a process of optimization of several protocols found in the literature. It was performed as follows: 0.35 ml of culture supernatant was incubated with 0.35 ml of 5 mM of 4-Nitrophenyl- $\alpha$ -L-arabinofuranoside (O-PNPAF, Megazyme®) in 50mM sodium acetate pH 5 for 30 minutes at 50°C. The reaction was stopped by adding 0.35 ml of 1 M Na<sub>2</sub>CO<sub>3</sub>. The blank was obtained by incubating the supernatant only, without the substrate, that was added only at the end of the incubation, after the stop solution. The rate of nitrophenol liberation was measured in a spectrophotometer at 410 nm.

One unit of arabinofuranosidase is defined as the amount of enzyme which produces an increase of 0.01 optical density unit in 1 mm cuvette.

The formula applied for the conversion of absorbance into U/ml is the following:

$$((\text{Abs}_{\text{sample}} - \text{Abs}_{\text{blank}}) / t) * (V_{\text{tot}} / V_e) * (1 / 18.5)$$

where t is the reaction time (30 minutes); V<sub>tot</sub> is the total volume of the reaction mixture (1.05 ml), V<sub>e</sub> is the volume of the enzyme solution (0.35 ml); 18.5 is the molar absorbance index of p-nitrophenol.

### 2.3.5 Xylosidase activity

Contrary to the other protocols in which supernatants were used, for measuring the xylosidase activity whole cells were subjected to permeabilization protocols, based on sonication or toluene treatment.

- Cells were permeabilized using a Branson Sonicator. During the entire process the samples were kept in an ice bath and were sonicated with the following setting: amplitude 20%, with 15 seconds ON and 10 seconds OFF pulses for a total time of 10 minutes. After sonication, cells were centrifuged, and both pellet and supernatant were tested.
- Cells were permeabilized with toluene according to Roncero (1983) with the following modifications. Cultures were centrifuged (2,268 g for 15 minutes at 4°C), washed twice with 0.1 M phosphate buffer (pH 6.5) and finally suspended in one-third of the initial volume in phosphate buffer. A few drops of toluene were added to the tubes containing the cells which were mixed by vigorous vortexing. The tubes were incubated at 37°C for 30 minutes, after which the toluene was evaporated by centrifugation in speed vacuum until the pungent smell of toluene was no longer perceptible (about 30 minutes).

Both the supernatants and the pellets of permeabilized cells formed after speed vacuum centrifugation, were used for the detection of the enzyme; the cell pellet was resuspended in the same volume of buffer (1 ml per 1 ml of initial culture).

- Combination protocol: the cells were first sonicated, and then subjected to toluene-treatment according to the protocols described above.
- The assay method for the detection of  $\beta$ -1,4-xylosidase was modified from Roncero (1983) and is based on the release of colored nitrophenol from a synthetic substrate. The reaction mixture, which contained 0.35 ml of permeabilized cells/supernatant and 4 mM of p-nitrophenyl-3-D-xylopyranoside (p-NPX from Megazyme®) in 0.35 ml of 0.1 M phosphate buffer (pH 6.5), was incubated at 42°C for 30 minutes. The reaction was terminated by the addition of 0.35 ml of 1 M Na<sub>2</sub>CO<sub>3</sub>. The sample blank was represented by the incubation of the supernatant or permeabilized cells only, without substrate, that was added only at the end of the incubation after stopping the reaction. The rate of nitrophenol liberation was measured in a spectrophotometer at 410 nm.

One unit of  $\beta$ -xylosidase activity is defined as the amount of enzyme that catalyzes the formation of  $\mu$ mol of p-nitrophenol per minute under the assay conditions.

The units can be calculated using the following formula:

$$((Abs_{\text{sample}} - Abs_{\text{blank}})/t) * (V_{\text{tot}}/V_e) * (1/18.5) * D$$

where t is the reaction time (30 minutes);  $V_{\text{tot}}$  is the total volume of the reaction mixture (1.05 ml),  $V_e$  is the volume of the incubated enzyme solution (0.35 ml); 18.5 is the molar absorbance index of p-nitrophenol; D is dilution factor of the enzyme.

### 2.3.6 Phytase activity

Phytase activities were assayed in an aliquot of the culture supernatants using the K-Phytase Assay Kits (Megazyme®), a colorimetric assay, following the protocol provided by the manufacturer.

### 2.3.7 Statistical analyses

The statistical significance of the data was assessed by Standard Error of the Mean (SEM) and the Absolute error derived from Propagation of error.

## 2.4 Results

The genetic engineering procedure gave rise to several strains, each carrying the optimization of a specific enzyme, except for PB2OPT, which was optimized for both cellulase and endo-xylanase. An in-depth survey of the literature for specific and sensitive assays led to the development of optimized protocols for the detection of the enzymatic activities, which were necessary to prove the efficacy of the genetic interventions.

### 2.4.1 Cellulase and endo-xylanase determination

Cellulase and xylanase production was compared between the wild-type PB5700 strain, and the optimized PB2OPT strains (carrying both the optimized enzymes) grown in either LB medium or in the synthetic medium CMD with 1% glucose.

As shown in Fig. 8, the secretion of the enzymes was much higher for the optimized strain in both media. In LB medium, cellulase activity increased by more than 4 folds ( $88.1 \pm 2.1$  mU/ml in the engineered strain versus  $19.3 \pm 2.4$  mU/ml recorded in the supernatant of the WT strain). Xylanase activity also increased in PB2OPT albeit by only 2 folds ( $59.3 \pm 1.4$  mU/ml versus  $29.9 \pm 2.4$  mU/ml recorded in the WT) (Fig. 8a).

Notably, in CMD medium, the enzymatic units found in PB2OPT culture broth increased by over 21-folds for cellulase compared to those released by the PB5700 strain ( $82 \pm 0$  vs  $3.7 \pm 0.0$  mU/ml for the optimized and the WT, respectively) and about 2-fold for xylanase ( $64.7 \pm 0.0$  vs  $35.3 \pm 0.0$  mU/ml) (Fig. 8b).

Comparing the two experiments, it is interesting to notice that the production of the enzymes by the WT strain was influenced by the medium: LB inhibited the production of xylanase by 1.2-fold compared to CMD, while CMD had an inhibitory effect on cellulase production by about 5-fold compared to LB. In contrast, optimization resulted in stably increased enzyme production in both media. The possible reasons behind it will be discussed below.

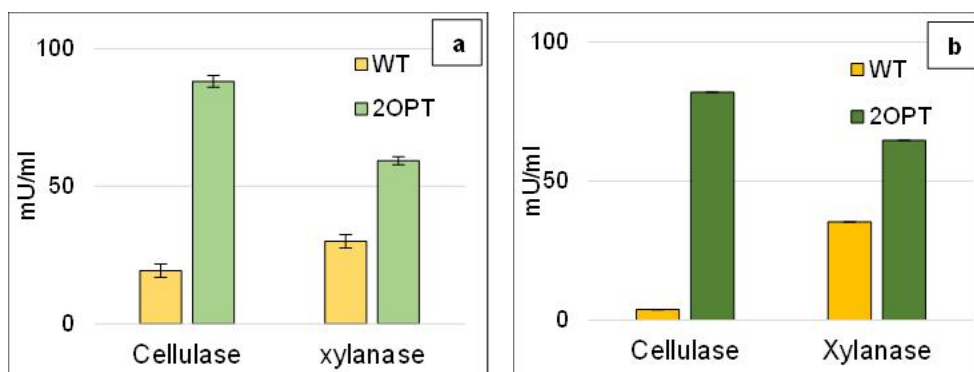


**Figure 8.** Enzymatic activity activity (in mU/mL of spent medium) of cellulase and xylanase (as indicated on the x-axis) in the WT and PB2OPT strains. Cells were grown in either LB medium (a) or 1% glucose CMD medium (b) for 24 h and assayed with a commercial kit. Values represent the average of at least three independent experiments. Error bars represent the standard error of the mean (SEM).

### 2.4.2 Arabinofuranosidase determination

The production of arabinofuranosidase, a secreted enzyme involved in xylan degradation, was also optimized and investigated. The optimized strain, OPT1, was compared to the wild-type in the synthetic medium CMD in the presence of either 1% glucose or 1% arabinose.

As shown in Fig. 9, secretion of the enzyme was generally improved in the optimized strain in both carbon sources and was particularly high in the presence of arabinose. Genetic optimization increased the intrinsic production of the enzyme by more than 5 folds in the presence of glucose ( $13.9 \pm 1.8$  mU/ml in the engineered strain versus  $2.75 \pm 0.07$  mU/ml recorded in the supernatant of the wild-type strain). In the presence of arabinose, the increased yield for OPT1 was 2-folds only ( $51.2 \pm 11.2$  mU/ml vs  $24.8 \pm 2.8$  mU/ml for the optimized and WT strains, respectively). It appears that the expression of arabinofuranosidase is under strong CCR repression: the production of the enzyme from the WT strain was 9-fold lower in glucose-containing medium). Repression was only partially reduced upon optimization (CCR repression was 3.7-fold only).

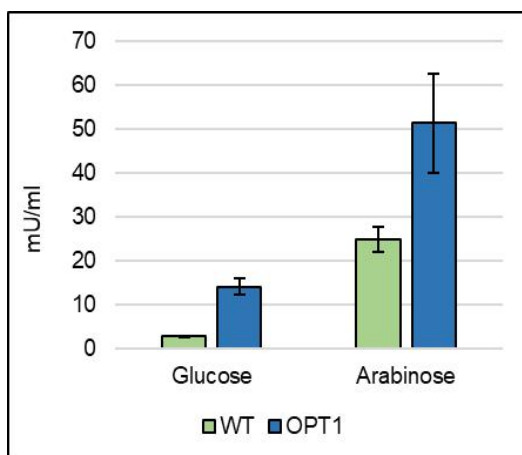


**Figure 9.** Activity (in mU/ml) of arabinofuranosidase from WT and optimized OPT1 strains. Cells were grown in CMD medium in the presence of glucose or arabinose for 24 h and assayed as described in Material and Method section. Values represent the average of four independent experiments. Error bars represent the SEM.

### 2.4.3 Xylosidase determination

Also the outcome of the xylosidase optimization was evaluated through a specific enzymatic assay. As the xylosidase is predicted to be localized in the cell membrane, and not secreted (Uniprot Database), permeabilization of the cell wall was necessary to release the enzyme prior to the enzymatic assay.

Among the cell permeabilization methods, sonication, toluene treatment, and their combination were selected for protocol optimization. Preliminary experiments were conducted on cells of the optimized strain only, grown for 24 h in LB medium. The best protocol for both sonication and toluene permeabilization, set up after several trials, is described in Material and Methods. Although the original toluene protocol considered the use of the cell pellet only, analyses were conducted on both pellets and supernatants treated by sonication or toluene, or a combination thereof, to investigate whether there was enzymatic leakage from the cells.

Figure 10 shows the enzymatic activity detected upon the different treatments in both fractions. It is evident that the sonication protocol (indicated by number one) was not effective in the release of the enzyme, which was only appreciable upon toluene treatment.

Cell permeabilization via toluene released the largest amount of enzymes, which were mainly detected in the cell pellet (2B), and, to a very limited extent, in the supernatant (2A), suggesting that during the cell wall lysis via toluene a little part

of the enzyme is released in the surrounding medium, while the main portion remains attached to the cell membrane.

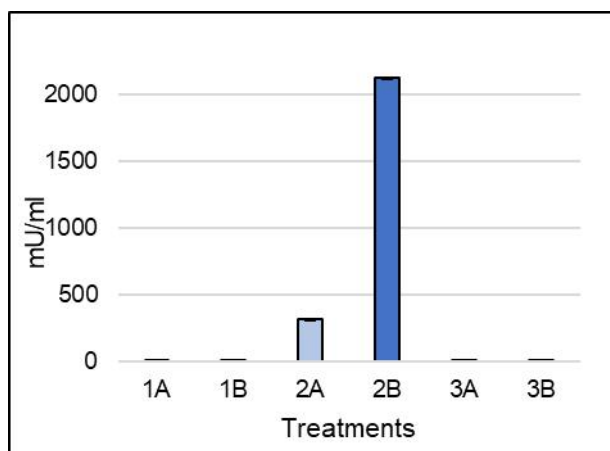


**Figure 10.** Enzymatic activity of  $\beta$ -1,4-xylosidase expressed as mU/ml derived from 1) sonication, 2) toluene treatment and 3) their combination. The letters stand for supernatants a), and pellets b). Cells were grown in LB medium for 24 h and assayed as described. Enzymatic activity is reported on the y-axis. Values represent the average of two independent experiments. Error bars represent the SEM.

Once the best permeabilization treatment was established, it was applied to the comparison of xylosidase production between the WT and the optimized PBOPT2 strains, grown on the complex CMD medium supplemented with 1% glucose.

Xylosidase activity was detected in both pellet and supernatant derived from the permeabilized cells. Since the treated pellet and supernatant derived from the same aliquot, the enzymatic units were combined in a single value showing the total amount of enzyme produced by each of the two strains. Figure 11 shows the sum of the enzymes detected in the pellet and in the supernatant produced by the WT or OPT2.

Fig. 11 shows that the optimization present in PBOPT2 led to a dramatic 128-fold increase in xylosidase production compared to PB5700.

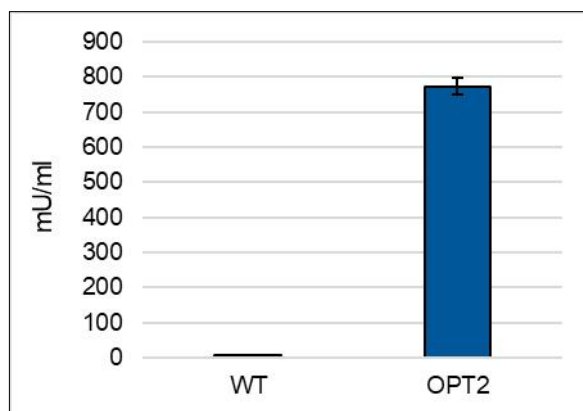


**Figure 11.** Enzymatic activity expressed as mU/ml of  $\beta$ -1,4-xylosidase activity detected in both pellet and supernatant of WT or OPT2 permeabilized cells. Cells were grown in CMD with 1% glucose for 24 h. Error bars derive from the Propagation of Error.

To evaluate the optimal carbon source for the production of xylosidase, xylan, xylose, arabinose, and soybean flour (1% each) were used as alternative sugars in CMD. Xylan and xylose were also tested together, 1% each, to study their combined effect on the optimized strain.

Fig. 12 shows the enzymatic activity detected either in the pellets or in the supernatants of permeabilized cells after 24 h-growth, and normalized on the  $OD_{600}$ , since, in the presence of glucose, the growth was higher with respect to the other carbon sources (Fig. 13) (a possible explanation will be discussed below).

In the WT strain, glucose, as expected, was highly inhibitory for xylosidase production; the same effect was exerted by arabinose and soybean flour. Xylan and xylose acted as xylosidase inducers, but the combination of the two sugars did not increase the enzyme production.

It is interesting to note that CCR repression was mitigated, although not completely removed, by the optimization operated in OPT2 strain in all conditions. Arabinose and soybean flour had a less pronounced repressive effect, while the inducer effect exerted by xylan and xylose was preserved. Surprisingly, the presence of both xylan and xylose had an additive effect on OPT2 (indeed this medium contained 1% of both carbon sources). In all substrates, the engineered strain gave a higher production of the enzyme compared to the WT, confirming once again the efficacy of the genetic engineering.

The optimization resulted in 3.4-fold, 4.5-fold, 5.4-fold, 48.4-fold and 64.8-fold higher production compared to wild-type strain in the presence of xylose, xylan, xylan-xylose, arabinose and soybean flour, respectively.

However, growth was also highly dependent on the carbon source used, and this characteristic was not modified by the genetic modification (Fig. 13).

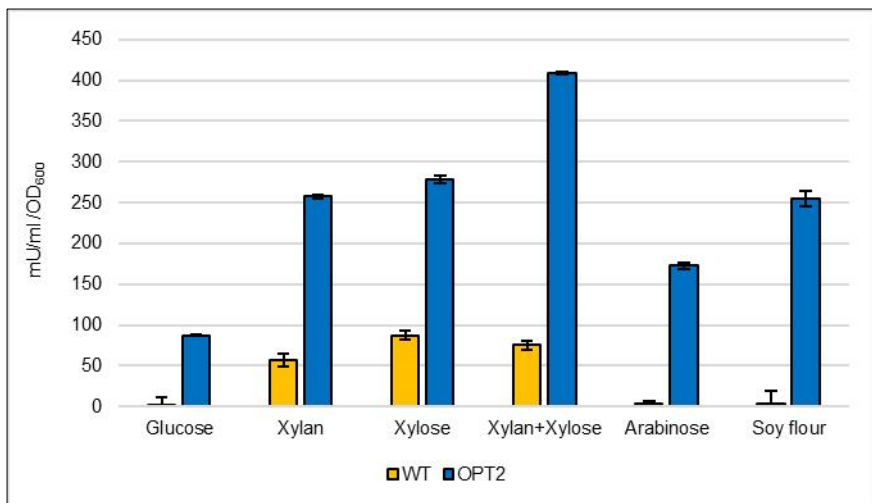


**Figure 12.** Enzymatic activity of  $\beta$ -1,4-xylosidase from WT and OPT2 expressed as ratio between mU/ml and OD<sub>600</sub> detected in CMD medium supplemented with glucose, xylan, xylose, xylan-xylose combination, arabinose, or soybeanflour (1% each). The shown data resulted from the sum of the enzymatic activity detected in the pellet and in the supernatant of the permeabilized cells representing the total amount of enzyme in the sample. Error bars derive from the Propagation of Error.

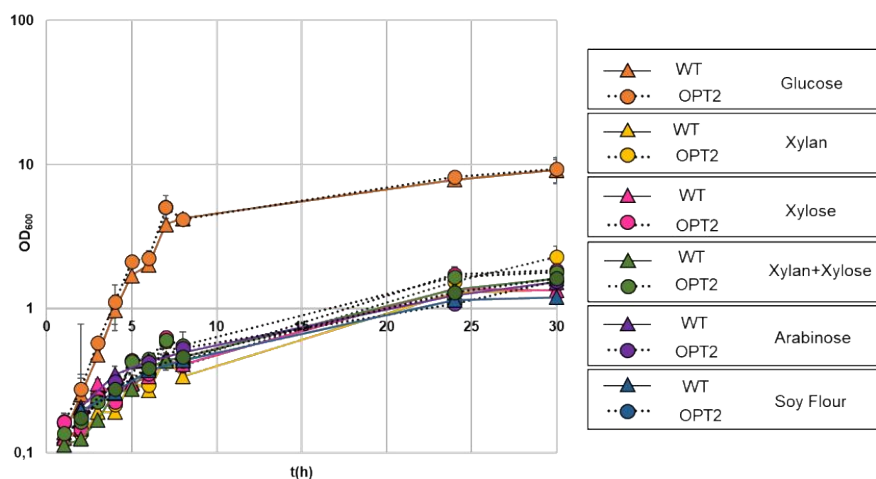


**Figure 13.** Growth curve of WT or OPT2 strains in CMD medium supplemented with 1% of glucose (in orange), xylan (in yellow), xylose (in dark pink), xylan plus xylose (in green), arabinose (in purple), soybeanflour (in blue). The triangles represent the WT strain; the circles are the optimized OPT2 strain. Values represent the average of three independent experiments. Error bars represent the SEM.



#### 2.4.4 Phytase detection

Genetic engineering also addressed the synthesis of phytase. To evaluate the efficacy of the intervention, the enzymatic activity was compared between the WT and the optimized strain OPT3 in the synthetic medium CMD supplemented with 1% glucose. As shown in Fig. 14, the optimization led to 21-fold improvement in phytase activity ( $226.3 \pm 1.9$  mU/ml versus  $10.4 \pm 15.8$  mU/ml for the WT strain).

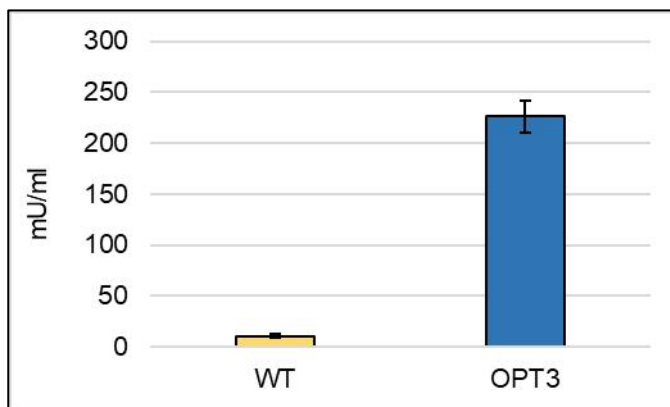


**Figure 14.** Enzymatic activity expressed in mU/ml of phytase produced by WT and OPT3 strains growth in the synthetic medium CMD with the supplementation of 1 % glucose for 24 h and assayed as described in Material and Method section. Enzymatic activity is reported on the y-axis. Values represent the average of two independent experiments. Error bars represent the SEM.

## 2.5 Discussion

In Chapter 2, the effect of the genetic optimization of the intrinsic degradative propensity of *Bacillus subtilis* was verified, comparing the engineered strains to the wild-type one.

The first enzymes that underwent genetic engineering were cellulases, responsible for cellulose degradation by randomly hydrolyzing  $\beta$ -(1,4)-glucan substrates (Rongpipi et al., 2019), and endo-xylanases, mainly responsible for the hydrolysis of  $\beta$ -1,4 bonds in plant xylan, the main component of hemicellulose (Huang et al., 2021). The two optimizations were combined in a single strain, PB2OPT. PB2OPT has been truly characterized since it has been extensively used in the biotechnological application discussed in chapters 3 and 4.

Both enzymatic activities were hyper-produced by PB2OPT, in both LB and CMD media, compared to the wild-type strain (Fig. 8). Interestingly, the optimization, besides increasing enzyme production, flattened their distinction present in the WT strain (cellulase production was inhibited in CMD, while growth in LB inhibited xylanase expression). This could be explained by the fact that these genes are normally subjected to CCR and/or other repression systems that lead to variable production depending on the growth medium. Optimization partly abolished these repressive mechanisms, thus allowing a high and steady enzymatic production regardless of the medium.

For the evaluation of the strain optimized for the production of arabinofuranosidase, another secreted enzyme involved in the degradation of arabinose-substituted xylans, enzyme production was compared between the engineered and the parental strains. Productivity was evaluated in the presence of glucose and also in the presence of arabinose, which is known to trigger a lower CCR compared to glucose (Singh et al., 2008). The results confirmed the successful improvement of enzyme accumulation, which further increased in the presence of arabinose; in the latter condition, a higher productivity was also observed for the WT strain, in line with data in the literature (Singh 2008).

The work was then focused on other *B. subtilis* genes encoding enzymes involved in the metabolism of xylan. One of them encodes for a membrane-bound xylosidase, acting upstream in the xylan degradation pathway. For its detection, a permeabilization protocol based on toluene-treatment was developed, followed by the measurement of the enzymatic activity in the permeabilized cell pellets. The enzymatic activity of the optimized strain was much higher compared with the one of PB5700 in the presence of several carbon sources. Xylan and its constitutive xylose monomers, known to stimulate xylosidase production, were employed singly or in combination (Singh et al., 2008). Indeed, they acted as inducers of xylosidase production in both strains; compared to the enzyme level in a glucose-based medium, enzyme production in the optimized strain further increased by 2.9-fold and 3.2-fold in the presence of xylan and xylose, respectively; despite, in the latter condition, enzyme production rose by 78.5-folds and 119.5-fold in the WT strain, the performance of the engineered strain was roughly 5 folds higher and reached a 48-fold increase in the presence of both xylan and xylose. This result is consistent with the fact that genes encoding

degrading enzymes are generally not constitutively expressed, but are inducible by their substrates; the combination of the two sugars displayed an additive effect in the optimized strain, which was not observed in the WT.

Soybean flour, a cost-effective feed frequently used in media for the industrial production of degradative enzymes (Matsumoto et al., 2000) did not induce (or did not repress) xylosidase expression in the optimized strain, while unexpectedly it maintained the CCR in the WT genetic background. In contrast to the expectations, in the WT strain arabinose did not remove the CCR on enzyme production, which remained low as observed when glucose was used; conversely, it had a positive effect on the optimized strain.

In summary, despite a slight substrate-dependency in enzyme expression was still observable in the engineered strain, the optimization dramatically increased enzyme yield under all the conditions examined.

It was assumed that the optimized production of an enzyme involved in xylan utilization would lead to increased growth. However, no correlation was observed between xylosidase production and strain growth (Fig. 13); contrary to expectations, glucose gave the highest growth rate compared to the other substrates. This result can be explained by the fact that the optimization only improved the upstream steps of the xylan utilization pathway (Fig. 15), while enzymes acting downstream were not modified. In other words, the hyperproduction of intermediates, that cannot be further processed, cannot reach the Pentose Phosphate Pathway, the metabolic pathway parallel to glycolysis.

Downstream enzymes of this pathway have also been optimized (data not shown); in future, these genetic optimizations will be unified to produce a super strain able to efficiently grow on xylan-based media, such as biomass waste, in view of constructing an ideal CBP organism. Indeed, the ability of *B. subtilis* to be fed on plant biomass is supported by a wide range of literature, but biomasses were mostly pre-treated with commercial enzymes or chemical compounds (Sharma et al., 2016; Akhtar et al., 2017; Sharma et al., 2018). However, this bacterium possesses the capability to directly saccharify plant biomass feedstocks relying on its cellulolytic properties only, even if only few studies directly addressed this feature (Wu et al., 2021).

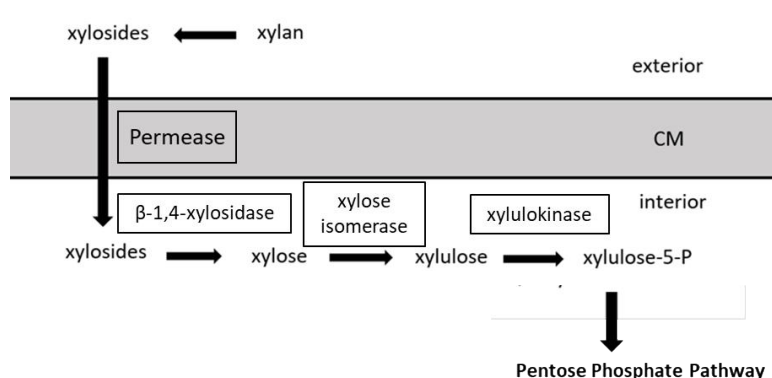


**Figure 15.** General overview of xylan utilization pathway. Several enzymes are involved until xylulose-5-P is formed to enter Pentose Phosphate Pathway.

Considering that the role of phytases is steadily increasing in the sustainable economy, also the endogenous *B. subtilis* phytase gene has been targeted for optimization. The optimization strategy was successful also in this case, with a considerable increase in phytase production by the optimized strain compared to the wild type.

## References

**Ermoli F., Bontà V., Vitali G., Calvio C. 2021.** SwrA as global modulator of the two-component system DegSU in *Bacillus subtilis*. Res. Microbiol. 172, 103877. DOI: 10.1016/j.resmic.2021.103877.

**Huang L. Z., Ma M. G., Ji X.X., Choi S. E., Si C. 2021.** Recent Developments and Applications of Hemicellulose From Wheat Straw: A Review. Front Bioeng. Biotechnol. 22, 690773. DOI: 10.3389/fbioe.2021.690773.

**Liew F.E., et al. 2022.** Carbon-negative production of acetone and isopropanol by gas fermentation at industrial pilot scale. Nat. Biotechnol. 40, 335–344. DOI: 10.1038/s41587-021-01195-w.

**Liu M., Wang J., Liu, J. Yao J, Yu Z. 2006.** Expression of *Bacillus subtilis* JA18 endo- $\beta$ -1,4-glucanase gene in *Escherichia coli* and characterization of the recombinant enzyme. Ann. Microbiol. 56, 41. DOI: 10.1007/BF03174968.

**Matsumoto T., Sugiura Y., Kondo A., Fukuda H. 2000.** Efficient production of protopectinases by *Bacillus subtilis* using medium based on soybean flour. Biochem. Eng. J. 6, 81-86. DOI: 10.1016/s1369-703x(00)00079-6.

**Mordini S., Osera C., Marini S., Scavone F., Bellazzi R., Galizzi A., Calvio C. 2013.** The role of SwrA, DegU and PD3 in fla/che expression in *B. subtilis*. PLoS ONE 8. DOI: 10.1371/journal.pone.0085065.

**Roncero M. I. 1983.** Genes controlling xylan utilization by *Bacillus subtilis*. J. Bacteriol. Res. 156, 257-263. DOI: 10.1128/jb.156.1.257-263.1983.

**Rongpipi S., Ye D., Gomez E.D., Gomez E.W. 2019.** Progress and Opportunities in the Characterization of Cellulose - An Important Regulator of Cell Wall Growth and Mechanics. Front. Plant Sci. 9. DOI: 10.3389/fpls.2018.01894.

**Sharma R., Lamsal B. P., Mba-Wright M. 2018.** Performance of *Bacillus subtilis* on fibrous biomass sugar hydrolysates in producing biosurfactants and techno-economic comparison. Bioprocess Biosyst. Eng. 41, 1817-1826. DOI: 10.1007/s00449-018-2004-2.

**Sharma R., Lamsal B.P., Colonna W.J. 2016.** Pretreatment of fibrous biomass and growth of biosurfactant-producing *Bacillus subtilis* on biomass-derived fermentable sugars. Bioprocess Biosyst. Eng. 39, 105-113. DOI: 10.1007/s00449-015-1494-4.

**Singh K.D., Schmalisch M.H., Stülke J., Görke B. 2008.** Carbon catabolite repression in *Bacillus subtilis*: quantitative analysis of repression exerted by different carbon sources. J. Bacteriol. 190, 7275-84. DOI: 10.1128/JB.00848-08.

**Smith J. L., Goldberg J. M., Grossman A. D. 2014.** Complete Genome Sequences of *Bacillus subtilis* subsp. *Subtilis* Laboratory Strains JH642 (AG174) and AG1839. Genome Announc. 2. DOI: 10.1128/genomeA.00663-14.

**Spier M. R., Rodrigues M., Paludo L., Cerutti L.M.N. 2018.** Chapter 5 - Perspectives of phytases in nutrition, biocatalysis, and soil stabilization. Editor(s):

**Srivatsan A., et al.** 2008. High-Precision, Whole-Genome Sequencing of Laboratory Strains Facilitates Genetic Studies. *PLoS Genet.* 4. DOI: 10.1371/journal.pgen.1000139.

**St John F.J., Rice J.D., Preston J.F.** 2006. Characterization of XynC from *Bacillus subtilis* subsp. *subtilis* strain 168 and analysis of its role in depolymerization of glucuronoxylan. *J Bacteriol.* 188, 8617-26. DOI: 10.1128/JB.01283-06.

**Wu Y., Guo H., Rahman M.S., Chen X., Zhang J., Liu Y., Qin W.** 2021. Biological pretreatment of corn stover for enhancing enzymatic hydrolysis using *Bacillus* sp. P3. *Bioresour. Bioprocess.* 8, 92. DOI: 10.1186/s40643-021-00445-8.

**Chapter 3: Effect of supplementation of cellulolytic enzymes of *Bacillus subtilis* on the nutritional value of ruminal fodders**

### 3.1 Abstract

The increased pressure on animal production systems, prompted by the world population growth, is raising significant environmental issues.

A promising strategy to boost animal productivity without impacting on the environment is the improvement of the nutritional value of forages, thereby increasing animal performance per unit of feed. This objective can be obtained by increasing feed digestibility.

Among sustainable strategies for increasing fiber digestibility in common dairy cows' feeds, this work investigated the supplementation of the safe soil bacterium *B. subtilis*, naturally endowed with a large array of enzymes able to degrade complex vegetable polymers.

To evaluate whether a link exists between the enzymatic degradation of biomass and the quality of forages, raw cultures of wild-type or engineered *B. subtilis* strains, releasing cellulase and xylanase at higher levels, were applied to several types of common forages.

Results indicated that the enzymes released by the optimized strain increased both the gas produced by ruminal microorganisms and the fiber digestibility of the feeds, two parameters positively correlated to digestibility of the organic matter. Thus, the cellulolytic properties of *B. subtilis* might account for part of the beneficial effects observed upon administration of this bacterium as probiotic in animal diets.



### 3.2 Introduction

The ever-growing world population and the consequent increase in the demand for meat and animal products, have broadened animal production systems, thus raising enormous pressure on natural resources and serious environmental problems (Adesogan et al., 2019). An increase in animal productivity entails a greater demand for cereals, grains and other forages, partly in competition with human nutrition, requiring a high consumption of natural resources, water, and lands. Moreover, the ruminant livestock sector causes direct methane (CH<sub>4</sub>) emissions via enteric fermentation, while nitrogen losses from manure cause eutrophication of the soil (Nasiru et al., 2014). Sustainable technologies able to boost animal performances, leading to a reduction in the negative environmental repercussions per animal product unit, is therefore the current challenge for the livestock sector (Capper and Bauman, 2013; Adesogan et al., 2019).

A viable strategy to boost animal performances without negative externalities on the environment is to improve the nutritional properties of the available forages, avoiding the expansion of lands for pasture. In ruminants, forage fibers are mainly constituted by cellulose and hemicellulose, whose digestibility by the rumen microorganisms is described by the Neutral Detergent Fiber digestibility (NDFd) parameter. NDFd has been positively correlated to animal productivity (Oba and Allen, 1999; Kendall, 2009; McGrath, 2018), and a direct correlation between animals fed with high NDFd forages and both dry matter intake (DMI) and milk yield was identified in several studies (Oliver et al., 2004; Mertens et al., 2005). Indeed, it has been calculated that 1 unit rise in NDFd in the diet results in a 0.17 kg/day increase in DMI and 0.25 kg increase in 4% fat-corrected milk (OBA and Allen, 1999; Kendall, 2009). Another parameter known to be positively correlated with the digestibility of the organic matter is the amount of gas produced during the fermentation process in the ruminal environment (Matthews et al., 2019).

An additional non-negligible advantage of incrementing fiber digestibility is the possibility of using less nutritious forages that, differently from grains, are not in competition with human nutrition (Adesogan et al., 2019).

Several forage treatments ranging from physicochemical approaches, e.g., treatments with strong alkalis, ammonium, urea, or steam, have been investigated, all aiming to increase the fiber surface area accessible to rumen microbial activity (Donnelly et al., 2018; Mor et al., 2018; Adesogan et al., 2019). However, these approaches might increase the negative environmental burden of farming, by raising energy consumption or pollution. Alternatively, environmentally friendly strategies, based on the application of exogenous hydrolytic enzymes to deconstruct the lignocellulosic biomass have also been evaluated (Adesogan et al., 2019). Such sustainable strategies still entail issues linked to the high costs associated with the use of expensive commercial enzymes (Ferreira et al., 2021), or the premature loss of enzymatic activity within the rumen environment (Adesogan et al., 2019). A viable alternative is the direct supplementation into forages of degradative enzyme-producer microorganisms, which continuously secrete hydrolytic enzymes and ferment the biomass contributing to its deconstruction.

Many microorganisms are known to secrete large amounts of hydrolytic enzymes that attack the lignocellulosic matrix of vegetable material (Himmel et al., 2010). The main enzyme-producer organisms responsible for lignocellulose degradation are fungi and soil bacteria. *Aspergillus* spp. and *Trichoderma* spp. are the most common fungi, while bacteria belonging to the *Bacillus* genus are the most frequently utilized (Danilova and Sharipova, 2020). Among this genus, the best characterized species is *Bacillus subtilis* that, in addition to the attractive characteristics widely discussed in Chapter 1, has been certified with the Presumed Safety Quantification status by the European Food Safety Authority, since its supplementation to cereals-based feed has showed no hazardous effects in animal nutrition (EFSA FEEDAP Panel, 2015).

Besides, *B. subtilis* was shown to colonize rumen and gastrointestinal tract of mammals and poultry, in the form of vegetative cells (spores) or biofilms, acting as probiotic (Bernardeau et al., 2017; Lee et al. 2019; Mun et al., 2021).

Several studies have proposed feed supplementation with different *Bacillus* strains which can provide numerous benefits including increasing milk and protein yield, growth performances, and rumen development both in calves and early lactation dairy cows without any adverse effects (Sun et al., 2011; Sun et al., 2013; Sun et al., 2016; de Souza et al., 2017; Choonkham et al., 2020; Wang et al., 2022; Jia et al., 2022); among the *Bacillus*-based probiotics already available in the market, BioPlus® 2B, a mixture of *B. licheniformis* and *B. subtilis*, has demonstrated to confer a lower mortality, as well as a lower incidence of diarrhea in pigs (Bampidis et al., 2019).

In the context of the development of a sustainable livestock sector, the improved ability of *B. subtilis* to self-saccharify biomasses may be helpful to enhance the deconstruction of animal forages, thereby increasing fiber digestibility and, consequently, incrementing animal performances.

### 3.3 Materials and Methods

*Bacillus subtilis* strains used in this study are PB5700 (WT) and its engineered version PB2OPT. The description of the characteristics of these strains is given in Chapter 2. A patent application is under preparation for the engineered strain; for this reason, the details of the engineering design are undisclosed herein.

#### 3.3.1 Liquid fraction of rice straw preparation and characterization

Open-air dried rice straw (*Oryza sativa L.*) was collected from two local farmers in the Pavia area (northwestern part of Italy) and stored in burlap sacks. Upon use, straw was minced using a kitchen blender (Moulinex AY45 Easy Power Blender) and dried to constant weight in a 60°C oven. One liter tap water was added to 25 grams of straw and the suspension was vigorously stirred at room temperature for 2 hours with a magnetic stirrer. Straw was removed through a 1 mm mesh-strainer covered with two sheets of gauze. The washing liquid (WL) was collected and subjected to low-pressure sterilization (5 psi/~0.35 bar) for 20 minutes, to avoid sugar caramelization, and then stored at -20°C.

To quantify the sugars extracted, 300 µL of WL were brought to a final volume of 500 µL with 50 mM Na-Acetate buffer pH 5 and incubated at 50°C for 64 h with shaking, either alone or in the presence of 22 µL- enzymes cocktail constituted by 1U Cellulase (product n° 22178, Millipore-Sigma), 1U β-glucosidase (product n° 49290, Millipore-Sigma), 1U Xylanase (product n° X2629, Millipore-Sigma) and 0.013 U Cellobiohydrolase I (product n° E6412, Millipore-Sigma). A mock reaction was carried out with the enzymatic cocktail in the absence of substrate. After incubation, samples were centrifuged at 16,873 × g at room temperature for 5 min, filtered through sterile 0.2 µm polyethersulfone (PES) filters and stored at -20°C until HPLC analysis (see below). Twenty-five microliter samples were injected through an automatic injector and analyzed in an LC-2000 HPLC system (Jasco) equipped with a Supelco C-610H 30 cm x 7.8 mm column (59320-U, Sigma Aldrich) and a RID 10A detector (Shimadzu). For chromatography, 0.1% H<sub>3</sub>PO<sub>4</sub> was used as mobile phase with 0,5 mL/min flow rate. Column temperature was kept at 30°C. Chromatograms were analyzed by the ChromNAV 2.0 software (Jasco). The column was previously calibrated with standard solutions of glucose, xylose, galactose, mannose, arabinose and cellobiose, serially diluted in mobile phase to prepare calibration curves based on at least three replicates for each sugar. The lower limit of quantification for all sugars was 0.3 g/liter. Background sugars present in the enzymatic cocktail were subtracted from each sample. For control samples with values below the limit of quantification (LOQ) of the calibration curve (0.3 mg/mL), the LOQ/2 value (i.e., 0.15 mg/mL) was used as background (Bergstrand and Karlsson, 2018). Sugar quantification values are the mean of two independent experiments.

#### 3.3.2 *Bacillus subtilis* cultures

The growth medium was prepared by adding to WL the following components: 7 g/L K<sub>2</sub>HPO<sub>4</sub>; 2 g/L KH<sub>2</sub>PO<sub>4</sub>; 0.5 g/L Na citrate; 0.1 g/L MgSO<sub>4</sub>; 1g/L (NH<sub>4</sub>)<sub>2</sub>SO<sub>4</sub>;

1 g/L asparagine. PB5700 and PB2OPT spores were revitalized over-night on LB plates. Few single colonies were inoculated in 3 mL of Antibiotic Medium 3 (BD-Difco, New Jersey, U.S) and grown at 37 °C with orbital shaking till culture density was appreciable. Each pre-inoculum was grown at 37 °C over-night in 20 mL of fresh Antibiotic Medium 3 containing with 5 mg/mL glucose. Bacterial growth was carried out for 24 hours in the WL-based medium at 37 °C with 150 rpm agitation, starting at OD<sub>600</sub> 0.2. Each culture was independently repeated at least three times.

### 3.3.3 Cellulase and xylanase activity assays

At the end of the incubation, cellulase and endo-xylanase activities were assayed in the culture supernatants, after acidification, using the CellG5 and XylX6 kits (Megazyme, Wicklow, Ireland) as previously described (Ermoli et al., 2021).

### 3.3.4 *In vitro* analysis

The effect of the enzymes produced by PB5700 and PB2OPT on the degradability of feeds was analyzed using two different *in vitro* incubation methods aimed to evaluate ruminal fiber NDF digestibility (NDFd) and gas production (GP). For both methods, ruminal fluid was collected (Fig. 16) from three rumen-cannulated cows (non-lactating Holstein–Friesian).

The donor animals were handled as outlined by the Directive 2010/63/EU on animal welfare for experimental animals and all animal procedures were conducted under the approval of the University of Milan Ethics Committee for animal use and care and with the authorization of the Italian Ministry of Health (authorization n. 904/2016-PR).

Cows were fed a total mixed ratio (TMR) composed by 66% hay and 34% concentrate, twice a day to achieve a Dry Matter Intake (DMI) of 8 kg/d. Rumen liquor was collected two hours after the morning feeding, immediately strained



**Figure 16.** Collection of rumen fluid from fistulated cow.

through four layers of cheesecloth into a pre-warmed (39°C) flask, flushed with CO<sub>2</sub> and used within one h from sampling.

For both NDFd and GP experiments, three different treatments were analyzed: i) the control treatment, constituted by the medium in the absence of bacteria; ii) the treatment, constituted by the medium fermented by strain PB5700; iii) the treatment, constituted by the medium fermented by strain PB2OPT.

The incubations were conducted on different types of feed ingredients (2 different meadow hays, 2 different alfalfa hays, 2 types of corn silages, and 2 types of TMR for dairy cows). All feeds were dried at 60°C for 48 h in a forced-air oven and ground to pass a 1-mm Fritsch mill (Fritsch Pulverisette, Idar-Oberstein, Germany). The NDF content of feed ingredients was determined using the Ankom200 Fiber Analyzer (Ankom Technology, Macedon, NY, USA) following the procedure reported by Mertens (2002). The experiments were independently repeated three times (three incubation runs for each method).

### 3.3.5 In vitro NDF digestibility

The NDF digestibility was determined at 48 h using the Ankom Daisy II incubator (Fig. 17a) as reported by Spanghero et al. (2019) modified as follows: each jar (Fig. 17b) was inoculated with fresh bacterial culture from one of the three experimental treatments (control, PB5700, PB2OPT, 665 mL each), a 10X salt solution (133 mL) composed by 90 g/L KH<sub>2</sub>PO<sub>4</sub>; 5 g/L NaCl; 5 g/L Urea; 4.5 g/L MgSO<sub>4</sub>·7H<sub>2</sub>O; 1 g/L CaCl<sub>2</sub>·2H<sub>2</sub>O, 532 mL of distilled water, 266 mL of reducing solution (Na<sub>2</sub>CO<sub>3</sub> 15 g/L; Na<sub>2</sub>S·9H<sub>2</sub>O 1 g/L), and 400 mL of rumen fluid. For the control experiment, the negative control was constituted by the WL medium.

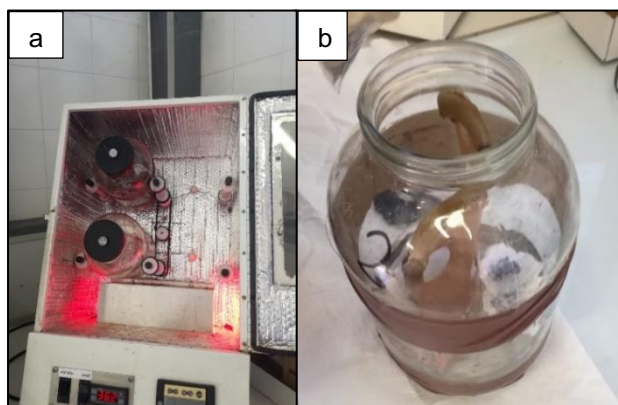


Figure 17. a) Ankom Daisy incubator b) Empty jar

### 3.3.6 In vitro gas production

Gas production was analyzed through 48-hour *in vitro* runs using 120 mL serum bottles according to Pirondini et al. (2014) for each of the three treatments

(control, PB5700, PB2OPT). Each bottle was inoculated with 30 mL final solution composed by fresh bacterial culture (8.33 mL), 10X salt solution (1,67 mL), distilled water (6.7 mL), reducing solution (3.33 mL) and rumen fluid (10 mL); for the control experiment, deionized water substituted the WL fraction as, alone, the sugars contained in the WL, and not consumed by the absence of bacteria, could be fermented by the rumen bacteria developing a high level of gas. Gas production was determined by measuring the headspace pressure in the incubation vials (Theodorou et al., 1994). The pressure was recorded after 24 and 48 hours of incubation using a digital manometer (model 840082, Sper Scientific, Scottsdale, AZ, USA). At the end of the incubation, fermentation was stopped by putting all vials into an ice bath and the pH was recorded. The content of each vial was individually transferred into 50 mL Falcon tubes and centrifuged at 10,000 g for 15 min. After centrifugation, 5 mL and 30 mL of supernatant were sampled for subsequent VFA analysis as reported in Colombini et al. (2021). The  $\text{NH}_3$  concentration was determined with a Raypa NP-1500-MP Kjeldahl distiller (Raypa, Terrassa, Spain).

### 3.3.7 Statistical analyses

Data were statistically analyzed by the proc mixed procedure of SAS 9.4 (SAS Institute Inc., Cary, NC USA), with the following model:

$$Y_{ijk} = \mu + T_i + F_j + R_k + T \times F_{ij} + E_{ijk}$$

where  $Y_{ijk}$  = dependent variable,  $\mu$  = overall mean,  $T_i$  = fixed effect of the treatment ( $i = 1$  to 3),  $F_j$  = fixed effect of the feed ( $j = 1$  to 8),  $R_k$  = random effect of the fermentation run ( $k = 1$  to 3),  $T \times F_{ij}$  = interaction treatment x feed, and  $\varepsilon_{ijk}$  is the random error. The least-square means were reported. For all statistical analyses, significance was declared at  $P \leq 0.05$  and trends at  $P \leq 0.10$ .

### 3.4 Results

According to a large body of literature, administration of *Bacillus subtilis* to forage exerts a positive effect on animal performances. To evaluate whether the positive effect on cow productivity could be related to its ability to degrade biomass, raw cultures of wild-type or engineered *B. subtilis* strains, hyperproducing cellulases and xylanases, considered pivotal enzymes for the degradation of vegetable carbohydrates, were applied to several types of common forages.

#### 3.4.1 Medium characterization

In order to reduce *B. subtilis* fermentation costs, the washing liquid (WL) of rice straw was considered as viable carbon source for bacterial growth. To characterize the WL fraction, the sugars therein contained were quantified by HPLC analyses before and after incubation with a cocktail of commercial hydrolytic enzymes (cellulase,  $\beta$ -glucosidase, xylanase and cellobiohydrolase). Xylose, galactose, and mannose showed the same retention time and the same concentration-peak area calibration lines, thereby enabling the precise quantification of their sum. However, since the rice straw content in galactose and mannose is negligible compared with the one of xylose (Belal, 2013; Krishania et al., 2018), it was assumed that the concentration of the co-eluting peak was only due to xylose. Arabinose and cellobiose could not be detected. HPLC analyses revealed not only the presence of monomeric sugars in WL, but also of complex sugars, as the amount of the formers increased substantially after hydrolysis by industrial enzymes. In particular, glucose concentration increased 4-fold upon digestion, while xylose increased by 1.4-fold (Table 1).

**Table 1.** Monomeric sugars contained in WL before and after enzymatic hydrolysis.

Carbon source	Before hydrolysis		After hydrolysis	
	Glucose <sup>a</sup>	Xylose <sup>a</sup>	Glucose <sup>a</sup>	Xylose <sup>a</sup>
WL (mg/ml)	0.54 ± 0.01	0.5 ± 0.0	2.18 ± 0.05	0.70 ± 0.05

<sup>a</sup> mg of glucose and xylose per mL of WL, as quantified by HPLC. Only monomeric sugars identified in the samples are given. Values are the average of two independent experiments with standard deviations.

#### 3.4.2 *Bacillus subtilis* growth on WL fraction

The WL fraction was thus used as carbon source for the fermentation of the wild-type and optimized strains of *Bacillus subtilis*, PB5700 and PB2OPT. Indeed, both *Bacillus subtilis* strains were able to grow on the WL fraction without any preliminary pre-treatments reaching a final OD<sub>600</sub> of 2.85 ± 0.14 for the WT and of 3.83 ± 0.14 for PB2OPT at 24h.

### 3.4.3 Cellulase and xylanase activity assays

To evaluate the contribution of cellulase and xylanase enzymes as pre-treatment of cow forages, the culture supernatants were assayed, and their enzymatic activity compared between the two strains as described in Chapter 2.

As shown in Fig. 19, secretion of both enzymes was much higher for the optimized strain. Cellulase activity in the medium supernatant increased by more than 163 folds in PB2OPT compared to the wild-type strain ( $88.8 \pm 3.8$  mU/mL versus  $0.5 \pm 0.2$  mU/mL). Xylanase activity was also significantly higher in PB2OPT, albeit by only 6.3 folds ( $18.6 \pm 1.8$  mU/mL versus  $2.9 \pm 0.6$  mU/mL recorded in the wild-type strain).

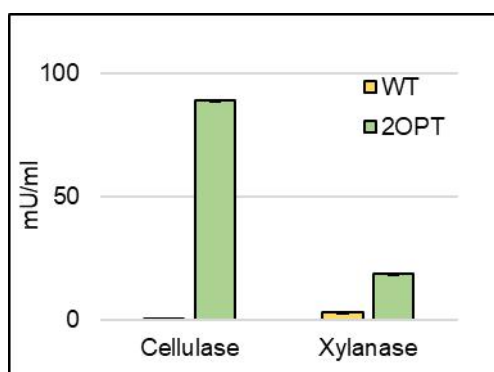


**Figure 19.** Enzymatic activity of cellulase and xylanase (as indicated on the x-axis) in the WT and PB2OPT strains detected in WL medium after 24 h and assayed with a commercial kit. Enzymatic activity (in mU/mL of spent medium) is reported on the y-axis. Values represent the average of six independent experiments. Error bars represent the standard error of the mean (SEM).

### Feeds treatments

Whole cultures of *Bacillus subtilis*, including bacteria and the fermentation medium in which degradative enzymes were secreted, were used to treat two independent samples of four different feed ingredients for dairy cows, meadow and alfalfa hays, corn silages and TMR (Total Mixed Ration), in a simulated *in vitro* rumen environment. The effect of the treatment of feeds with the enzymatic mixture was evaluated by measuring two parameters, positively correlated to feed quality, Neutral Detergent Fiber digestibility (NDFd) of the treated feeds and Gas Production (GP) derived from fermentation of organic matter by ruminal microorganisms.

#### 3.4.4 Fiber digestibility

Neutral Detergent Fiber digestibility (NDFd) was assessed from *in vitro* ruminal fermentation of the experimental feeds in the presence of *Bacillus subtilis*



cultures of either wild type or the optimized PB2OPT strains and compared to the one produced in the absence of *B. subtilis*.

The results of the treatments on NDFd are shown in Table 2. A statistically significant increment in NDFd was observed in the presence of both *Bacillus subtilis* strains, with a higher effect in the presence of the optimized strain.

As expected, a significant interaction between Treatment x Feed was also observed ( $P=0.028$ ). Particularly, the NDF fiber of maize silages was significantly more degradable by *B. subtilis* enzymes, and the degradation efficiency was higher in the presence of the engineered strain (32.5%, 38.5%, 41.9%, for Control, PB5700 and PB2OPT, respectively); on the other hand, alfalfa hay showed a significant increment in NDFd only in the presence of the optimized strain (37.9%, 39.3%, 41.8%, respectively) (Fig. 20). For meadow hay, a significant difference was found between the control and the bacterial treatment,

**Table 2.** NDF digestibility, gas production and fermentative profile from analyses of forages treated with Control, wild-type PB5700 and optimized PB2OPT strains).

	Treatment (T)			SE	p-value		
	Control	PB5700	PB2OPT		T	Feed	T x Feed
NDFd <sup>1</sup>	43.4 <sup>c</sup>	45.6 <sup>b</sup>	47.8 <sup>a</sup>	1.30	<0.001	<0.001	0.028
GP <sup>2</sup> 0-24 h (mL g DM)	83.3 <sup>b</sup>	89.6 <sup>a</sup>	91.1 <sup>a</sup>	5.07	0.019	<0.001	0.099
GP 24-48 h (mL/g DM)	29.3 <sup>b</sup>	32.2 <sup>a</sup>	32.8 <sup>a</sup>	1.56	0.016	<0.001	0.757
GP 0-48 h (mL/g DM)	113 <sup>b</sup>	122 <sup>a</sup>	124 <sup>a</sup>	5.25	0.010	<0.001	0.217
pH	6.26	6.29	6.28	0.161	0.239	<0.001	0.392
N-NH <sub>3</sub> (mg/dL)	49.1	47.9	47.6	7.59	0.556	0.005	0.938
Total VFA <sup>3</sup> (mmol/L)	92.4	97.4	94.4	13.1	0.455	0.255	0.342
VFA (% of total VFA)							
Acetic acid (%)	56.7	57.3	57.9	0.839	0.151	<0.001	0.922
Propionic acid (%)	21.4	20.2	20.1	2.74	0.063	0.051	0.528
Butyric acid (%)	17.0	17.5	16.7	1.48	0.490	<0.001	0.459
Valeric acid (%)	4.86	5.05	5.20	0.570	0.551	0.301	0.545

<sup>1</sup> NDFd: Neutral Detergent Fiber digestibility

<sup>2</sup> GP: Gas Production

<sup>3</sup> VFA: volatile fatty acids

<sup>abc</sup> Mean values in the same row with different lettering are statistically different.

independently from the strain used (on average 48% upon bacterial treatment as compared to 45.6% NDFd in the control).

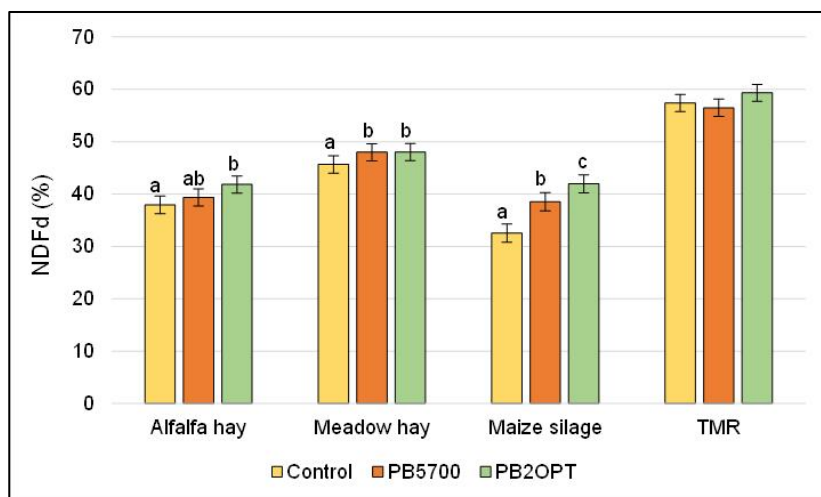


**Figure 20.** Fiber digestibility expressed as NDFd (%) of feed ingredients upon treatments: yellow bars represent the negative control without bacteria; orange bars represent treatments with the WT strain PB5700; green bars represent treatments with the optimized strain PB2OPT. Mean values in the same graph with different lettering are statistically different. Bars represents SEM.

### 3.4.5 Gas Production and ruminal fermentative profile

The other parameter evaluated to assess the effect of the bacterial treatment on the nutritional value of forages was the detection of the gas produced by ruminal fermentation. Data (Table 2) showed that both *B. subtilis* cultures were able to improve gas production compared to the control, regardless of the strain. Despite the absence of statistical significance among the two strains, the treatment with the PB2OPT strain consistently showed a trend towards a highest gas volume both at 24 and 48 h of incubation.

The analyses of the gas released by single feed ingredient showed that PB2OPT was more effective than the PB5700 strain in improving meadow hays fermentation at 48 h (95.3, 113- and 125-mL GP per g of dry matter (DM) for control, PB5700 and PB2OPT, respectively) (Fig. 21).

Regarding the rumen fermentative profile, N-NH<sub>3</sub> (mg/dL) and acetic acid production was only affected by the feed ( $P=0.001$ ) and not by the treatment (T x feed has a p-value of 0.938 and 0.922, respectively).

Propionic acid content in the total VFA released by the samples treated with either PB5700 or PB2OPT (on average 20.2%) was lower as compared to the untreated control (21.4%) ( $P=0.063$ ).

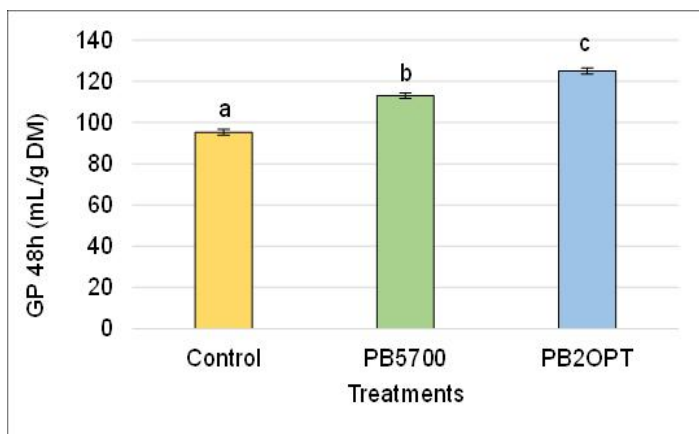


**Figure 21.** Gas (mL) produced by g of DM of meadow hays treated with control (no bacterial inoculum), PB5700 and the optimized strain PB2OPT, respectively. Mean values in the same graph with different lettering are statistically different. Bars refers to SEM.

### 3.5 Discussion

This part of my work was the result of a collaboration with the University of Milan. This work aimed to provide an appropriate sustainable application of one of the optimized strains discussed in Chapter 2. The strain PB2OPT was optimized in both cellulase and xylanase, considered key enzymes for plant carbohydrate degradation.

The project concerned the evaluation of the effect of *in vitro* supplementation of wild-type and optimized *Bacillus subtilis* strains on typical cow forages. This part of the work was performed in collaboration with the laboratory of Prof. Stefania Colombini (Department of Agricultural and Environmental Sciences, University of Milan).

Besides environmental sustainability, economic viability was also taken into account; to meet both objectives, a low-cost medium based on the waste rice straw was devised for *B. subtilis* growth. As rice straw was reported to contain water-soluble carbohydrates in significant amounts (Park et al., 2009; McIntosh et al., 2011), dried raw straw was washed with tap water in order to partially recover those nutrients. The characterization of the sugar content in the obtained liquid (WL) was performed by the laboratory of Prof. Lorenzo Pasotti (Department of Electrical, Computer and Biomedical Engineering, University of Pavia). The WL was found to contain not only monomeric sugars but also complex sugars, as the amount of the formers increased substantially after hydrolysis by industrial enzymes. The sugars detected were glucose and xylose; the presence of the latter was unexpected since it represents the degradation product of hemicellulose, which is generally released upon chemical treatments (Lu et al., 2021; Wang et al., 2022). However, the data indicated that it was possible to extract a portion of hemicellulose in the form of xylose with a simple water-washing, suggesting the possibility to bypass high-energy demanding and polluting pre-treatments generally performed to release sugars from the lignocellulosic matrix. In fact, the WL fraction, without any preliminary saccharification, supplemented with few minerals, was able to provide an adequate carbon source for *Bacillus subtilis* growth.

Cellulase and xylanase production increased by more than 163 folds and 6.3 folds in the optimized stain compared to the WT, confirming the efficiency of the optimization already demonstrated in richer media (LB and CMD, tested in Chapter 2).

The effect of the supplementation of the enzymes produced by *B. subtilis* on the nutritional quality of several feed ingredients for dairy cows showed that fiber digestibility could increase in the presence of *Bacillus subtilis* strains, and this effect was correlated to the amount of degradative enzymes secreted by the strains. Particularly, a correlation was found for maize silages, and alfalfa hays. For meadow hay, a significant difference was evident between the control and the bacterial treatment, independently from the strains. Notably, no effect of the bacterial treatment was observed in TMR forage, intrinsically characterized by a high value of NDFd, and therefore already very digestible.

Although the increment given by bacterial treatments is apparently not dramatic, it is worth to recall that one-unit percentage of increase in forage NDFd is associated with an increase of 0.17 kg of DMI per day and 0.23 kg/d of milk produced (Oba and Allen, 1999; Kendall et al., 2009). Thus, the higher degradation of the fiber content obtained through the supplementation of *B. subtilis* may lead to increased intake of feeds, improving ruminant performances. The different efficacy of the treatments might be justified by the different chemical composition of the forage substrates. Maize silage samples are characterized by a lower content of lignin than alfalfa and meadow hays; the presence of lignin is usually associated to a lower NDFd, since the lignin-polysaccharide complex stiffens the cell walls, thereby preventing degradation (Selvendran, 1984). Therefore, in low-lignin forages, the higher enzymatic activities produced by the optimized strain outperformed those produced by the PB5700 strain; in those cases, the lignocellulosic matrix could have been partially deconstructed by *B. subtilis* cellulolytic enzymes, thus increasing the substrate fermentability by ruminal microorganisms.

To have the complete degradation of high-lignin forages, lignin-degradative enzymes such as laccases are necessary. However, laccases are not generally produced by bacteria, but by fungi. Anyway, the potential biotechnological application of the engineered strains can be maximized, for instance, by using them in a consortium of microorganisms with complementary catabolic skills.

The other key parameter analyzed was the gas produced from *in vitro* ruminal fermentation of the experimental feed. Although no statistical significance was observed, gas production was generally higher for PB2OPT treatments both at 24 and 48 hours of incubation. As expected, the effectiveness of the enzymes was linked to the different chemical composition of the individual substrates, as shown by the interaction between Treatment \* Feed. The data also showed that gas production was higher during the first 24 hours of incubation rather than in the following 24 hours; this effect was most likely due to the fact that the rapidly degradable fiber fraction, simple sugars, and non-structural carbohydrates are readily fermented during the first hours of incubation. Remarkably, the positive effect of *Bacillus* enzymes is immediately appreciable and is maintained till the end of the incubation.

Regarding the rumen fermentative profile, no relationship between the treatments and the production of N-NH<sub>3</sub> and acetic acid was observed, which were affected only by the feed. Contrarily, there was a trend towards a lower propionic acid content in the samples treated with either PB5700 or PB2OPT as compared to the untreated control. The volatile fatty acids produced depend on the substrate metabolized; in this regard fiber fermentation usually promotes a higher acetic production and lower propionate formation. Therefore, the slightly lower propionic acid release in those samples, although not significant, can be related to a higher fiber digestibility.

The literature relating to the role of *Bacillus subtilis* as food additive has recently expanded, providing encouraging data on the efficiency of this bacterium in improving the nutritional properties of animal forages. In this work, a correlation was identified between the effect of forage nutritional values and amount of enzymes produced by the strains, suggesting that the ability to hydrolyze

complex biomass components might lay at the basis of the positive effect of *B. subtilis* as animal probiotic. Conveniently, the experimental setup envisaged the use of raw culture of *Bacillus subtilis*, grown on low-cost waste-based medium; this type of approach was chosen with the specific intent of designing an environmentally sustainable, easy approach, which can provide a low-cost beneficial effect on animal productivity and well-being. To our knowledge, there are no previous reports on such types of experiments. Furthermore, this technology can be further applied to monogastric animal feeds, in which *B. subtilis* is widely known to play a role of probiotic (Rhayat et al., 2019).

Last but not least, this biotechnological application might be extended to additional recalcitrant substrates, possibly waste biomasses not currently in use as animal feedstock because of their low digestibility, expanding the types of forages usable for dairy production.

Indeed, an additional goal of the project included the valorization of rice straw, the major byproduct of rice production collected after harvesting of rice grains and currently considered a poor-quality forage, as feed for ruminants by increasing its digestibility and its nutritional value throughout *Bacillus subtilis* treatment. Technical problems prevented the continuation of those experiments; however, the first replicate gave promising results, indicating an increased digestibility of rice straw upon *Bacillus subtilis* supplementation, especially with the optimized strain. Further experiments along this line are necessary to assess the potential valorization of such agricultural waste, paving the way towards a more sustainable livestock sector.

## References

- Adesogan A.T., et al.** 2019. Symposium review: Technologies for improving fiber utilization. *J Dairy Sci.* 102, 5726-5755. DOI: 10.3168/jds.2018-15334.
- Arsène M.M.J., et al.** 2012. The use of probiotics in animal feeding for safe production and as potential alternatives to antibiotics. *Vet World.* 14, 319-328. DOI: 10.14202/vetworld.2021.319-328.
- Bampidis V. et al.** 2019. EFSA Panel on Additives and Products or Substances used in Animal Feed (FEEDAP). Modification of the conditions of the authorisation of BioPlus® 2B (*Bacillus licheniformis* DSM 5749 and *Bacillus subtilis* DSM 5750) for turkeys for fattening. *EFSA J.* 17. DOI: 10.2903/j.efsa.2019.5726.
- Belal E.B.** 2013. Bioethanol production from rice straw residues. *Braz. J. Microbiol.* 44, 225-34. DOI: 10.1590/S1517-83822013000100033
- Bernardeau M., Lehtinen M. J., Forssten S. D., Nurminen P.** 2017. Importance of the gastrointestinal life cycle of *Bacillus* for probiotic functionality. *J. Food Sci. Technol.* 54, 2570–2584. DOI: 10.1007/s13197-017-2688-3.
- Capper J. L., Bauman D. E.** 2013. The role of productivity in improving the environmental sustainability of ruminant production systems. *Annu. Rev. Anim. Biosci.* 1, 469-489. DOI: 10.1146/annurev-animal-031412-103727.
- Choonkham W., Schonewille J. T., Bernard J. K., Suriyasathaporn W.** 2020. Effects of on-farm supplemental feeding of probiotic *Bacillus subtilis* on milk production in lactating dairy cows under tropical conditions. *J. Anim. Feed Sci.* 29, 199-205. DOI: <https://doi.org/10.22358/jafs/127692/2020>.
- Danilova I., Sharipova M.** 2020. The practical potential of bacilli and their enzymes for industrial production. *Front. Microbiol.* 11, 1782. DOI: 10.3389/fmicb.2020.01782.
- Diatta A., Doohong Min, S.V. Krishna Jagadish.** 2021. Chapter 2 - Drought stress responses in non-transgenic and transgenic alfalfa—Current status and future research directions, Editor(s): Donald L. Sparks, *Adv. Agron.*, Academic Press, 170, 35-100. DOI: 10.1016/bs.agron.2021.06.002.
- Donnelly D.M., de Resende L.C., Cook D.E., Atalla R.H., Combs D.K.** 2018. Technical note: A comparison of alkali treatment methods to improve neutral detergent fiber digestibility of corn stover. *J. Dairy Sci.*, 101. DOI: 10.3168/jds.2017-14317
- EFSA FEEDAP Panel** (EFSA Panel on Additives and Products or Substances used in Animal Feed), 2015. Scientific Opinion on the safety and efficacy of *Bacillus subtilis* PB6 (*Bacillus subtilis*) as a feed additive for laying hens and minor poultry species for laying. *EFSA J.* 13, 3970. DOI: 10.2903/j.efsa.2015.3970.
- Ferreira R. G., Azzoni A. R., Freitas S.** 2021. On the production cost of lignocellulose-degrading enzymes. *Biofuels Bioprod. Biorefining* 15, 85-99. DOI: 10.1002/bbb.2142.

- Himmel M. E., Xu Q., Luo Y, Ding S. Y., Lamed R., Bayer E. A.** 2010. Microbial enzyme systems for biomass conversion: emerging paradigms. *Biofuels* 1, 323-341. DOI: 10.4155/bfs.09.25.
- Jia P., et al.** 2022. Diets supplementation with *Bacillus subtilis* and *Macleaya cordata* extract improve production performance and the metabolism of energy and nitrogen, while reduce enteric methane emissions in dairy cows. *Anim. Feed Sci. Technol.* 294, 115481. DOI: 10.1016/j.anifeedsci.2022.115481.
- Kawauchi D., Anghong W., Keakliang O., Ishida T., Takahashi T., Kawashima T.** 2021. Effect of feeding *Bacillus subtilis* on rumen fermentation, blood metabolites, nutrient digestibility, and energy and nitrogen balances in non-lactating crossbred cows. *Anim. Sci. J.* 92. DOI: 10.1111/asj.13531.
- Kendall C., Leonardi C., Hoffman P. C., Combs D. K.** 2009. Intake and milk production of cows fed diets that differed in dietary neutral detergent fiber and neutral detergent fiber digestibility. *J. Dairy Sci.* 92, 313-323. DOI: 10.3168/jds.2008-1482.
- Krishania M., Kumar V., Sangwan R. S.** 2018. Integrated approach for extraction of xylose, cellulose, lignin and silica from rice straw. *Bioresour. Technol.* 1, 89-93. DOI: 10.1016/j.biteb.2018.01.001.
- Lee N.K., Kim W.S. Paik H.D.** 2019. *Bacillus* strains as human probiotics: characterization, safety, microbiome, and probiotic carrier. *Food Sci. Biotechnol.* 28, 1297-1305. DOI: 10.1007/s10068-019-00691-9.
- Matthews C., Crispie F., Lewis E., Reid M., O'Toole P.W., Cotter P.D.** 2019. The rumen microbiome: a crucial consideration when optimising milk and meat production and nitrogen utilisation efficiency. *Gut Microbes.* 10, 115-132. DOI: 10.1080/19490976.2018.1505176.
- McGrath J., et al.** 2018. Nutritional strategies in ruminants: A lifetime approach. *Res. Vet. Sci.* 116, 28-39, DOI: 10.1016/j.rvsc.2017.09.011.
- McIntosh S., Vancov T.** 2011. Optimization of dilute alkaline pretreatment for enzymatic saccharification of wheat straw. *Biomass Bioenerg.* 35, 3094-3103. DOI: 0.1016/j.biombioe.2011.04.018.
- Mertens D.R.** 2002. Gravimetric determination of amylase-treated neutral detergent fiber in feeds with refluxing in beakers or crucibles: collaborative study. *J. AOAC Int.* 85, 1217-1240.
- Mor P., et al.** 2018. Effect of ammonia fiber expansion on the available energy content of wheat straw fed to lactating cattle and buffalo in India. *J. Dairy Sci.* 101, 7990-8003. DOI: 10.3168/jds.2018-14584.
- Mun D., et al.** 2021. Effects of *Bacillus*-based probiotics on growth performance, nutrient digestibility, and intestinal health of weaned pigs. *J Anim Sci Technol.* 63, 1314-1327. DOI: 10.5187/jast. 2021.e109.
- Nasiru A., Ibrahim M.H., Ismail N.** 2014. Nitrogen losses in ruminant manure management and use of cattle manure vermicast to improve forage quality. *Int J Recycl. Org. Waste Agricult.* 3, 57. DOI: 10.1007/s40093-014-0057-z.
- Oba M., Allen M.S.** 1999. Evaluation of the Importance of the Digestibility of Neutral Detergent Fiber from Forage: Effects on Dry Matter Intake and Milk



Yield of Dairy Cows. *J. Dairy Sci.* 82, 589-596. DOI: 10.3168/jds.S0022-0302(99)75271-9.

**Oliver A.L., Grant R.J., Pedersen J.F., O'Rear J.** 2004. Comparison of Brown Midrib-6 and -18 Forage Sorghum with Conventional Sorghum and Corn Silage in Diets of Lactating Dairy Cows, *J. Dairy Sci.* 87, 637-644. DOI: 10.3168/jds.S0022-0302(04)73206-3.

**Palangi V., Taghizadeh A., Abachi S., Lackner M.** 2022. Strategies to Mitigate Enteric Methane Emissions in Ruminants: A Review. *Sustainability* 14, 13229. DOI: 10.3390/su142013229.

**Pan L., Li W., Gu X.M., Zhu W.Y.** 2022. Comparative ileal digestibility of gross energy and amino acids in low and high tannin sorghum fed to growing pigs. *Anim. Feed Sci.*, 292, 115419. DOI: 0.1016/j.anifeedsci.2022.115419.

**Park J., et al.** 2009. Efficient Recovery of Glucose and Fructose via Enzymatic Saccharification of Rice Straw with Soft Carbohydrates, *Biosci. Biotechnol. Biochem.* 73, 1072–1077. DOI: 10.1271/bbb.80840.

**Souza V.L., et al.** 2017. Lactation performance and diet digestibility of dairy cows in response to the supplementation of *Bacillus subtilis* spores. *Livest. Sci.*, 200, 35-39, DOI: 10.1016/j.livsci.2017.03.023

**Spanghero M., et al.** 2019. Rumen Inoculum Collected from Cows at Slaughter or from a Continuous Fermenter and Preserved in Warm, Refrigerated, Chilled or Freeze-Dried Environments for In Vitro Tests. *Animals (Basel)*, 9, 815. DOI: 10.3390/ani9100815.

**Sun P., Wang J.Q., Zhang H.T.** 2011. Effects of supplementation of *Bacillus subtilis* natto Na and N1 strains on rumen development in dairy calves *Anim. Feed. Sci. Tech.* 164, 154-160, DOI: 10.1016/j.anifeedsci.2011.01.003.

**Sun P., Wang J. Q., Deng L. F.** 2013. Effects of *Bacillus subtilis* natto on milk production, rumen fermentation and ruminal microbiome of dairy cows. *Animal* 7, 216–222. DOI: 10.1017/S1751731112001188.

**Sun P., Li J.A., Bu D.P., Nan X.M., Du H.** 2016. Effects of *Bacillus subtilis* natto and different components in culture on rumen fermentation and rumen functional bacteria in vitro. *Curr. Microbiol.*, 72, 589-595. DOI: 10.1007/s00284-016-0986-z.

**Wang X., et al.** 2022. High-Efficiency and High-Quality Extraction of Hemicellulose of Bamboo by Freeze-Thaw Assisted Two-Step Alkali Treatment. *Int. J. Mol. Sci.* 23, 8612. DOI:10.3390/ijms23158612.

**Yuchan L., Qiao H., Guozhi F., Qunpeng C., Guangsen S.** 2021. Extraction and modification of hemicellulose from lignocellulosic biomass: A review. *Green Process. Synth.* 10, 779-804. DOI: 10.1515/gps-2021-0065.

**Chapter 4: Extraction of phytochemicals from  
cauliflower waste by *Bacillus subtilis*-derived  
enzymes**

#### 4.1 Abstract

The market for nutraceutical molecules is growing at an extraordinary pace all over the world. A suitable source of bioactive compounds is found in vegetable waste products, and their re-use for the recovery of healthy biomolecules would improve the sustainability of the food production system. For the recovery of these beneficial molecules, safe, cheap, and sustainable technologies should be applied, avoiding the use of toxic organic solvents or high-energy demanding expensive equipment.

This work proposes a sustainable and economical procedure for bioactives extraction from food-waste replacing polluting and high-energy demanding processes. To this end, raw bacterial culture supernatants of wild-type or optimized *Bacillus subtilis* strains characterized by the hyper-production of cellulase and xylanase, were employed to assist in the extraction of bioactives from cauliflower discarded from a food processing industry.

This method, known as Enzyme Assisted Extraction (EAE), is based on the enzymatic action of bacterial enzymes to weaken or deconstruct the plant cell wall in which most bioactives are entrapped, making encased compounds more available for extraction. To increase the extraction yield and, at the same time, maintain the green connotation, EAE has been coupled with solid-liquid extraction at high pressure in an aqueous environment, avoiding the use of any polluting solvent.

The economic feasibility of the procedure relied on the use of crude *B. subtilis* culture supernatants without any expensive purification steps. The substrate, cauliflower (*Brassica oleracea* L. *conv. botrytis* (L.) *Alef. var. botrytis* L.), endowed with a large amount of phytochemicals with beneficial biological activities, derived from the ration of raw products that did not meet the qualitative standards for commercialization and were discarded by an industrial agri-food processing plant.

Many efforts have been made to reduce the intrinsic variability of the experiment through optimization and standardization trials to reach a more feasible and efficient procedure.

Results show that the recovery of compounds correlates with the amount of cellulolytic enzymes applied.

## 4.2 Introduction

The byproducts generated from the processing of fruits and vegetables are largely underutilized or discarded as organic waste. These wastes, including seeds, pulp, peels, leaves, stems, etc., contain a pool of bioactive compounds that might have health imparting benefits (Pattnaik et al., 2021).

Bioactive compounds, constituents other than nutrients generally occurring in small quantities within foods, have been associated with protective effects against adverse health or physiological disorders, and with antioxidant action. These bioactives have a diverse range of chemical structures and include many different classes of compounds (Marathe et al., 2017).

Phenolic compounds are one of the important classes of bioactive phytochemicals that are ubiquitously distributed throughout the plant kingdom. Over 8000 phenolic compounds have been identified from different natural sources. All of them possess a common structural moiety, an aromatic ring having at least one hydroxyl group called phenol (Ferreira et al., 2010). Phenolic compounds can be broadly classified into two major groups based on the chemical structure: simple phenols and polyphenols. Polyphenols are further subdivided into two groups: flavonoids (flavones, isoflavones, anthocyanins, flavonol, flavanones, etc.) and tannins (polymers of phenolic acids, catechins, or epicatechins). Simple phenols on the other hand can be broadly grouped into two subgroups: hydroxy cinnamic and hydroxy benzoic acids derivatives (Fig. 22) (Ferreira et al., 2010).

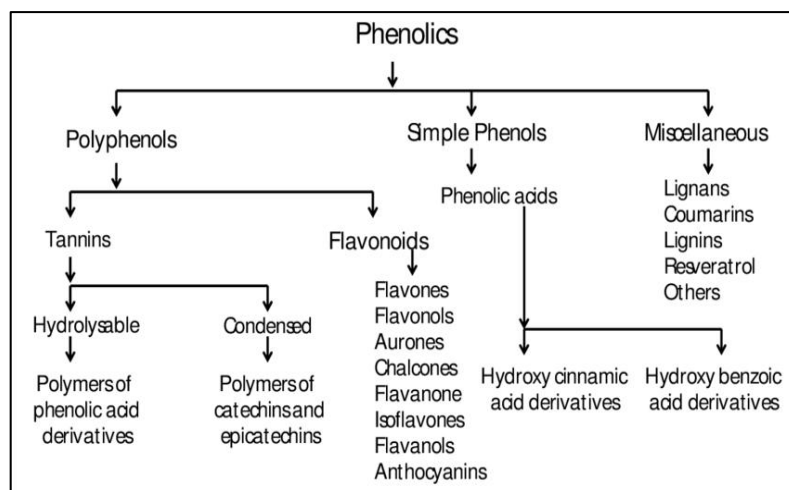


**Figure 22.** General classification of plant phenolics (from Ferreira et al., 2010).

Another class of bioactives are terpenoids, among which carotenoids are found, raising great interest due to their renowned photoprotective and antioxidant

properties (Fig. 23). Carotenoids are a large group of yellow-orange pigments that consist of eight isoprenoid units joined to form a conjugated double bond system. The conjugated polyene structure is responsible for the color of each carotenoid. The carotenoids that contain only isoprene units are called carotenes, e.g., as  $\alpha$ -,  $\beta$ -, and  $\gamma$ -carotene and lycopene, while those having oxygen in addition to the hydrocarbon chain are known as xanthophylls or oxygenated carotenoids, e.g., lutein and zeaxanthin. They play significant roles in promoting human health and reducing the risk of chronic diseases. Lutein, the main carotenoid in durum wheat, is associated with reduced incidence of cataracts, age-related macular degeneration, cancer, and cardiovascular disease (Abdel-Aal & Young, 2009). Apocarotenoids are the products of the oxidative cleavage of carotenoids; one of them is crocin, responsible for the golden bright yellow-red color of saffron (Pandita, 2021). In line with the circular economy concept, fruit and vegetable waste might be turned into a natural and unlimited resource of these biologically active

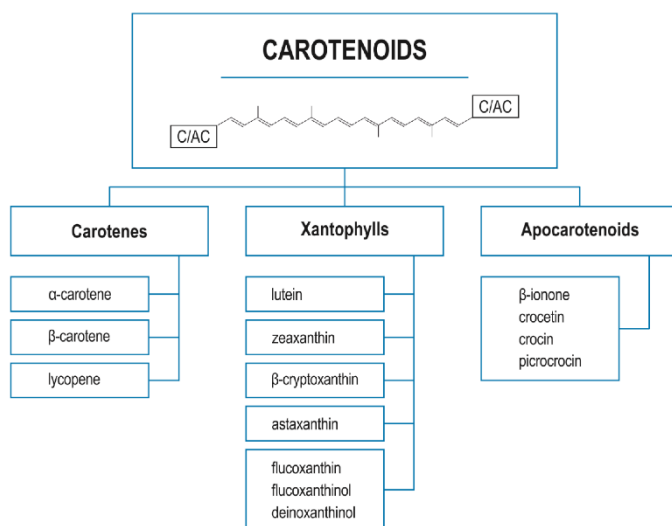


**Figure 23.** Classification of carotenoids (from Starska-Kowarska, 2022).

compounds, with enormous economic potential as nutraceutical, pharmaceutical, cosmetic, and pharmaceutical ingredients (Kumar et al, 2017; Wadhwa & Bakshi, 2022). Furthermore, the valorization of food-waste for the recovery of all these bioactive compounds can mitigate the problem of their disposal providing environmental and economic benefits.

Several techniques have been developed for the extraction of the myriads of phytochemicals. Their variety and heterogeneity make the development of a single optimal extraction process difficult. Each method should be tailored to the desired compounds and the type of vegetable matrix (Pattnaik et al., 2021). Conventional extraction methods often require the use of harsh conditions, i.e., hazardous chemicals, and high energy consuming procedures, making these

methods unsustainable and non-environmentally friendly (Rodríguez De Luna et al., 2020). Even new technologies relying on a greener approach, such as microwave assisted extraction (MAE), ultrasound assisted extraction (UAE), and supercritical fluid extraction (SFE), often take advantage of solvents for the recovery of encased compounds from the vegetable biomass. For example, UAE was used to extract 81  $\mu\text{g}$  polyphenols/mL from lettuce leaves treated with 50-75% ethanol (Plazzotta & Manzocco, 2018); combined alkaline hydrolysis and UAE were used for extraction of bioactives from cauliflower waste affording 7.3 mg/g of Total Phenolic Compounds (TPC) (Gonzales et al., 2014). MAE with 43% ethanol and temperature of 80°C allowed to obtain 22 mg of TPC/g from apricot kernel skin (Han et al., 2013).

Alternative promising sustainable methodologies are based on the use of Naviglio extractor®, pulse electric fields (PEF) and steam explosion.

Naviglio extractor®, is a solid-liquid extractor that applies the principle that a forced extraction from a solid matrix suspended in a solvent is produced by generating a negative pressure gradient and allowing it to attain an equilibrium between outside and inside of the solid material (Naviglio et al., 2014) (Fig. 24). This solid-liquid dynamic technology possesses several advantages: it allows to carry out the extraction at room temperature, thus avoiding thermal stress on thermolabile substances; moreover, the employment of high pressure allows a reduction in the extraction time and a concomitant improvement of the extraction efficacy (Panzella et al., 2020). Naviglio Extractor® was also combined with the use of solvents; for instance, Posadino et al., (2018) used the Naviglio Extractor for the recovery of phenolic antioxidants from the *Cagnulari* grape pomace by performing 21 extractive cycles in water/ethanol (60:40 v/v) environment.

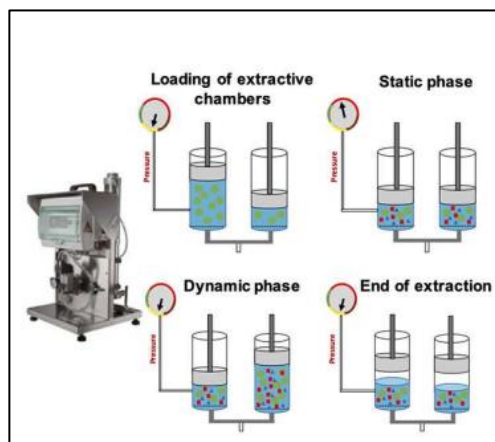


**Figure 24.** Schematic representation of the extraction of bioactive compounds with Naviglio Extractor® (from Panzella et al., 2020).

Beyond the abovementioned chemo-physical methodologies, biological methods emerged in the nutraceutical market in an effort towards a real sustainability that could completely remove chemical compounds. Indeed, to maintain the green

connotation, the methods for the recovery of natural bioactive compounds from discarded agri-food materials must guarantee that the polluting waste generated in the extraction process should not exceed the negative impact caused by the disposal of the raw biomass itself and should use non-energy-intensive procedures (Galanakis, 2015).

Enzyme-assisted extraction (EAE) offers a safe, green, and novel approach for the extraction of bioactives and can be used either as a stand-alone technique, or as a pre-treatment that increases the efficiency of a coupled extraction system (Nadar et al., 2018). EAE is based on the action of enzymes helping to weaken or deconstruct the plant cell wall in which most bioactives are entrapped, making encased compounds more accessible for extraction. The most used enzymes for this purpose are CAZymes such as cellulases (endoglucanases, cellobiohydrolases,  $\beta$ -glucosidases), hemicellulases (endoxyylanases and  $\beta$ -xylosidases), and pectinases (polygalacturonases, and pectinesterases). Other hydrolyzing enzymes (proteases, amylases, pullulanases, pectate lyases, etc.) might further support the release of precious and low-abundant secondary metabolites from cellular components (Puri et al., 2012; Nadar et al., 2018).

However, this method is still limited by the elevated cost of commercial enzymes which take a prohibitive toll on the entire process, mining the economic viability of the extraction (Marathe et al., 2017).

A possible solution to expand the use of enzymes in the phytochemicals' extraction process is producing the enzymes directly in integrated biorefineries rather than in a centralized location. Indeed, producing enzymes on-site, at biorefineries, would eliminate the need for concentration, storage, and shipping and production costs might be reduced by using biomass material already available at the biorefinery as substrates for microbial growth (Marathe et al., 2017; Patel & Shah, 2021).

### 4.3 Materials and Methods

#### 4.3.1 Bacterial strains

*Bacillus subtilis* strains used in this study are a PB5700 (WT) strain and its derivative, OS58. PB5700 was already described in the Material and Methods section of the Chapter 2.

OS58 was obtained from the PB5700 strain by genetic engineering. A patent application is under preparation for this strain, for this reason, the details of the engineering design are undisclosed herein.

#### 4.3.2 Bacterial growth

For cellulase and xylanase production, *B. subtilis* PB5700 and OS58 spores were revitalized on LB (Difco Laboratories, New York, NY, USA) 1.5% agar plates and incubated overnight at 37°C. Isolated colonies were inoculated in Antibiotic Medium 3 (Difco Laboratories) containing 5 mg/mL glucose and grown 16 h at 37°C with shaking. A second pre-inoculum in the same medium was set at OD<sub>600</sub> 0.2 and grown for 6 h at 37°C with shaking.

The synthetic medium CMD (see Chapter 2) was inoculated at OD<sub>600</sub> 0.2 and Bacterial growth, detected by OD<sub>600</sub> readings, was prolonged for 24 h at 37°C with 150 rpm orbital shaking.

Culture supernatant was collected after 40 minutes centrifugation at room temperature (RT) at 2,268 x g. The spent medium, 500 mL, was immediately used for the maceration of 5 kg-smashed cauliflowers.

#### 4.3.3 Cellulase and xylanase activity assays

Cellulase and endo-xylanase activities were assayed in an aliquot of the culture supernatants after acidification, using CellG3 and XylX6 Assay Kits (Megazyme®), following the protocol provided by the manufacturer.

#### 4.3.4 Plant material

Fresh cauliflowers (*Brassica oleracea* L. conv. *botrytis* (L.) Alef. var. *botrytis* L.) were obtained, during spring, summer, and autumn 2021, from a food processing plant that collects vegetables from farms located in southern and northern Italy. The fresh material was weighted, aliquoted, and stored at -45°C ± 1°C (monitored by a datalogger, Testo 184 T4, Liebherr) for over one month.

For each treatment (including controls) and for each of the four large scale experimental replicates, aliquots of 5 kg each (fresh weight before freezing) were thawed at RT for 2 days. After draining the residual water, each whole cauliflower, including flowers, leaves and stems, was cut into four parts and ground using an industrial mill (M100, Enoitalia s.r.l., Florence, Italy); the material was completely shattered into small pieces (0.5-1.0, cm in diameter) for subsequent processing. The extraction experiments with the supernatant of the WT and OS58 strains or the sterile medium used as negative control, were independently carried out four times each, on four different lots of cauliflowers.



#### 4.3.5 Extraction by methanol and acetone

Three control trials using traditional methanol and acetone-based extraction methods were performed on separate parts of cauliflowers: steams, flowers and leaves. For those experiments 71 g of inflorescences (flowers) (frozen at -40°C and thawed for 2 days at RT), cut with scissors and crescents, were incubated with 200 ml of extraction solvent made up of 80% methanol and 20% acetone for 2 h. The same procedure was applied to stems (71 g) and leaves (45 g).

#### 4.3.6 EAE pre-treatment procedure of the cauliflower waste material

Small-scale titration experiments were conducted to optimize the extraction procedure changing one parameter at time (pH, temperature, time of incubation of cauliflower biomass and bacterial enzymes) and led to the following optimal parameters: pH 5, 50°C, 16 hours of incubation.

To 5 kg of fresh material, ground as previously described, 500 mL of bacterial culture supernatant was added, and the final volume was brought to 5 L with water. The suspension was acidified to pH 5 with 85% phosphoric acid and was incubated for 16 h at 50°C with 40 rpm orbital shaking (LOM-7450 Incubator, MRC, London, UK). For each of the four replicates, the material was also incubated with 500 mL of sterile CMD, as negative control.

#### 4.3.7 Extraction process

An isothermal cyclically pressurized extraction process (rapid solid-liquid dynamic extraction) was applied to enzymatically pre-treated cauliflowers using the Naviglio mechanical extractor (Nuova Estrazione, Naples, Italy) (Fig. 25). The principle is based on cyclic compression and decompression phases that exert a suction effect on extractable compounds present in the vegetable matrix (Naviglio et al., 2014). The solid material was placed into a 50 µm-filtering membrane bag, together with the maceration liquid, into the pressure gradient cylinder that was then filled with deionized water, up to a total volume of 35 L. Each extraction cycle consisted of a 3 min static phase, followed by a 2 min dynamic phase; the number of cycles was 60, for a total time of 5 h. At the end of the extraction, the bag with the solid residue was removed and squeezed, and the aqueous liquid was recovered in a tank. One liter of the collected extract was dried using a rotary evaporator (Rotavapor System R-300, Büchi Labortechnik AG, Flawil, Switzerland); the solid residue was suspended in 50% methanol and filtered using 0.22 µm nylon filter before analyses.



**Figure 25.** Solid-liquid Naviglio® extractor based on cyclic pressurization phases.

#### **4.3.8 Total polyphenol content**

The total content of polyphenols was measured using the Total Polyphenols Colorimetric Assay Kit (Steroglass, Perugia, Italy) according to the manufacturer's instructions. Absorbance was measured at 725 nm and results were expressed in gallic acid equivalents using a gallic acid standard curve.

#### **4.3.9 Total flavonoids content**

The total flavonoids content was estimated using the Lola-Luze method as described by Lola-Luze et al., (2014) slightly modified as described below. An aliquot of 150  $\mu\text{L}$  of the extract was blended with 600  $\mu\text{L}$  of water and 45  $\mu\text{L}$  of 5%  $\text{NaNO}_2$ . After 10 minutes of incubation, 45  $\mu\text{L}$  of 10%  $\text{AlCl}_3$  in methanol was added; after 2 min incubation 300  $\mu\text{L}$  of 1 M  $\text{NaOH}$  plus the same volume of water were added. After 10 minutes, samples were spectrophotometrically assayed at 510 nm (PerkinElmer UV-VIS spectrophotometer) against a blank sample consisting of an extraction solution with 1,395 mL of methanol without  $\text{AlCl}_3$ . Total flavonoid content is expressed as mg of catechin equivalents/g of dry material.

#### **4.3.10 Catechins and chlorogenic acid HPLC analyses**

A 20- $\mu\text{L}$  aliquot of the filtered sample was injected into the HPLC pump (Kontron 420; Kontron Instruments, Munich, Germany) equipped with a C18 column (ZORBAX ODS 250 x 4.6 mm column, 5  $\mu\text{m}$  particle size, SepaChrom, Milan, Italy). For catechins and chlorogenic acid, HPLC analyses were performed with a 0.8 mL/min flow rate and setting the detector at 280 nm; the mobile phases consisted in 5% acetic acid (A) and pure methanol (B), and the chromatographic gradient conditions are summarized in Table 3:

**Table 3.** The mobile phase gradient

Time (Min)	A (%)	B (%)
1	90	10
5	90	10
7	80	20
8	80	20
10	75	25
15	70	30
20	20	80
25	50	50
28	70	30
30	90	10

#### 4.3.11 Isothiocyanates HPLC analyses

Isothiocyanates were analyzed by HPLC after cyclo-condensation, according to the protocol described by Tang et al. (2013), with modification. For each sample, an aliquot of 250  $\mu$ L of extract was mixed with 250  $\mu$ L of 100 mM potassium phosphate buffer (pH 8.5) and 500  $\mu$ L of 10 mM 1,2-benzenedithiol in methanol. The reaction mixture was incubated for 2 h at 65°C and then cooled at RT. The mixture was centrifuged at low speed and finally filtered with a 0,22  $\mu$ m nylon filter before being injected into the HPLC.

In this process, 1,2-benzenedithiol reacts with the carbon atom of the  $-N = C = S$  group of isothiocyanates to form a five-membered 1,3-benzodithiole-2-thione and the corresponding amine. Using RP-HPLC with an isocratic mobile phase of 80% methanol, a flow rate of 1 mL/min, at 40°C and a UV detector set at 365 nm, 1,3-benzodithiole-2-thione can be eluted and detected, providing an analytical measure of the total isothiocyanates present (Zhang et al., 2012). Different concentrations of allyl-isothiocyanate were used as standards for the calibration curve.

#### 4.3.12 Statistical Analysis

The variation in the amount of the compound extracted among the three experimental conditions, considered as response variable, was explored by using a series of linear mixed models (LMMS). Each model had a common fixed effect, represented by the experimental treatment adopted (factor with three levels: control, WT, OS58), and a common random effect (random intercept) represented by the different samples of organic matter (i.e., replicates).

The estimated means, related confidence intervals, and planned comparison among treatments were computed using the emmeans and contrast functions of the emmeans package (version 1.7.2) (Package “emmeans”). All model assumptions were explored by checking residuals distribution against fitted values (Tukey–Anscombe plot) and residual normality against theoretical normal distribution (quantile-quantile plot). Percentual changes with respect to the control were obtained from the raw data.

All statistical analyses were performed in R (<https://www.R-project.org/>).

## 4.4 Results

Raw bacterial culture supernatants of wild-type or optimized *Bacillus subtilis* strains characterized by the hyper-production of cellulase and xylanase, were employed to assist in the extraction of bioactives from cauliflower discarded from a food processing industry.

To increase the yield of bioactive recovery and maintain the green connotation, enzymatic recovery has been used as pre-treatment and coupled with solid-liquid extraction at high pressure in aqueous environment without any chemical addition.

Many efforts have been made to reduce the intrinsic variability of the experiment through optimization and standardization trials to reach a more feasible and efficient procedure.

### 4.4.1 Cellulase and xylanase activity assays

To evaluate the effectiveness of the low-cost enzymatic pre-treatment, two *B. subtilis* strains were used. The WT and the optimized strains namely OS58, obtained by improving the intrinsic cellulolytic and hemicellulolytic propensity of *B. subtilis* through genetic engineering of the WT strain. The cellulase and xylanase activities released in the growth medium by the two strains were determined after 24 h growth.

The optimization process led to a drastic enhancement in enzyme secretion. As shown in Figure 26, the enzymatic units found in OS58 culture broth increased by over 30-fold for cellulase and about 3-fold for xylanase compared to those released by the WT strain.

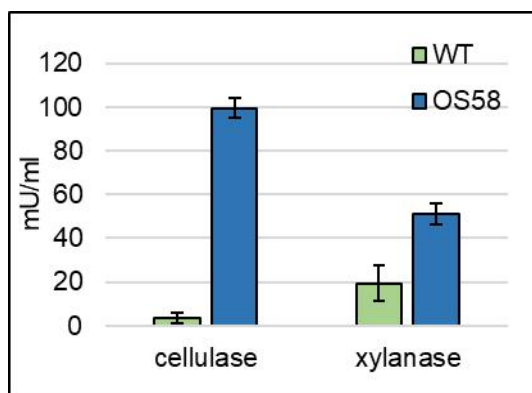


**Figure 26.** Enzymatic activity of cellulases and xylanases of the WT (in green) and PB1OPT (in blue) strains (as indicated on the x-axis). Cells were grown in CMD for 24 h and assayed with a commercial kit. Enzymatic activity (in mU/mL of spent medium) is reported on the y-axis. Values represent the average of at least five independent experiments. Error bars represent the standard error of the mean (SEM).

#### 4.4.2 Recovery of phytochemicals: preliminary experiments

To have an idea of the phytochemicals contained in the different parts of cauliflower, a traditional extraction based on methanol and acetone was performed from leaves, stems and flowers of the vegetable. Figure 27 shows the total polyphenols (27a) and flavonoids (27b) measured by two specific assays as reported in Materials and Methods. Interestingly, the higher amount of both compounds was found in the leaves which are usually discarded by food processing industries. The following experiments were performed using all the cauliflower parts without distinction.

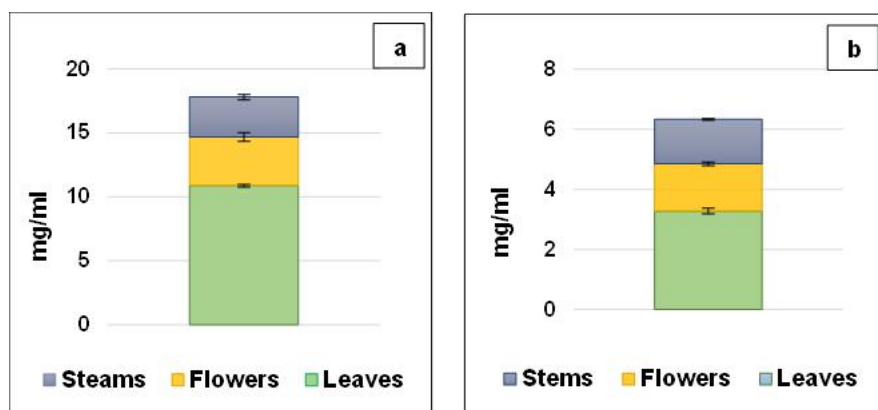


**Figure 27.** The total a) polyphenols and b) flavonoids content (calculated as mg per gram of fresh cauliflowers, before freezing) extracted by a solution of methanol and acetone from the three different parts of cauliflower: leaves (in green), flowers (in yellow), stems (in blue). Values represent the average of two independent experiments. Bars represent the SEM.

*Bacillus subtilis* enzymes-based EAE was evaluated as a stand-alone technique or coupled with the solid-liquid Naviglio® extractor.

The first procedures evaluated consisted of incubation of cauliflower biomass with crude enzymatic supernatant from *B. subtilis* PB5700 or OS58 strains for 3 hours at 50°C at pH 5, with or without the employment of the solid-liquid Naviglio® extractor. Figure 28a represents the data from HPLC analyses, carried out in the Lab. of Pharmacobiochemistry, Nutrition and Nutraceuticals, on the cauliflower extract post incubation with enzymatic supernatant from PB5700 and OS58 cultures.

The graph in Fig. 28 highlights the different extraction efficiency obtained by incubation with the two strains. With few exceptions, a better compounds recovery was observed upon treatment with OS58 supernatant compared to the treatment with the WT strain. In particular, the largest differences occur for epicatechin gallate ( $\Delta$  70.61 %) and epicatechin ( $\Delta$  50.25 %). No vitexin could be extracted from the biomass incubated with the WT-derived enzymes.

Fig. 28b shows the extraction efficiency obtained by the combination of the enzymatic pre-treatment followed by the Naviglio extraction procedure, compared to a control constituted by the Naviglio extractor only.

Chlorogenic acid showed an increased recovery by the combination of enzymatic pre-treatment and Naviglio ( $\Delta$  16.04% WT vs extractor only;  $\Delta$  47.6% OS58 vs extractor only). This is also true for epicatechin gallate ( $\Delta$  28.6% WT vs extractor only;  $\Delta$  48% OS58 vs extractor only). The significance of the results is shown in table 4.

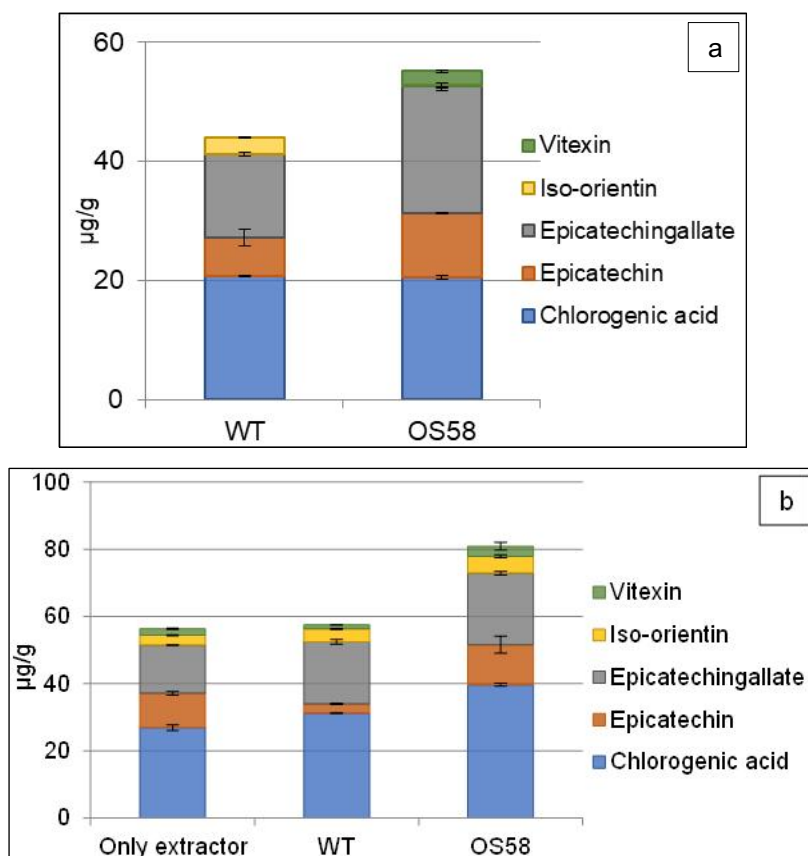


**Figure 28.** Phytochemicals (expressed as  $\mu\text{g/g}$  of cauliflower) observed a) upon incubation with either WT or OS58 for 3 hours at pH 5; b) upon incubation followed by treatment with the Naviglio extractor for 5 hours.

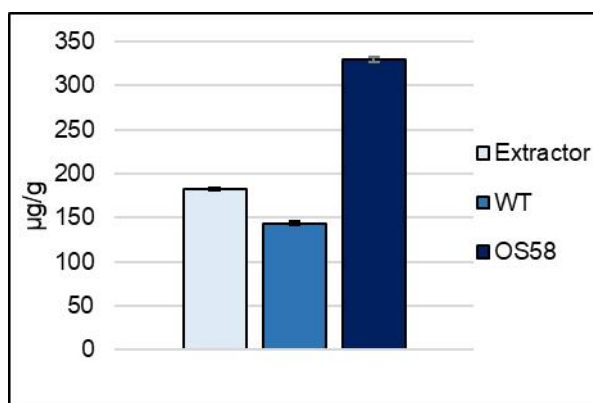
By comparing Fig. 28a and b, it was possible to conclude that the combination of enzymatic pre-treatment and high-pressure extraction increased the recovery of some compounds compared to the sole incubation with *B. subtilis* enzymes.

Figure 29 shows the polyphenols extracted by the enzymes of either *B. subtilis* PB5700 or OS58 or by Naviglio extractor only.

**Table 4.** Significancy of the above data calculated by T-Test.

	E <sup>a</sup> /WT	E <sup>a</sup> /OS58	WT/OS58
Chlorogenic acid	p<0.05	p<0.01	p<0.01
Epicatechin	p<0.01		
Epicatechin gallate	p<0.05	p<0.01	p<0.05
Iso-orientin	p<0.05	p<0.05	
Vitexin	p<0.05		

<sup>a</sup> Extraction with the Naviglio extractor only.



**Figure 29.** Polyphenols ( $\mu\text{g/g}$ ) extracted with either WT or OS58 for 3 hours at pH 5 followed by the extraction by Naviglio extractor compared to the control with the extraction step only. The dev.st. is calculated based on the technical measurements.

The positive results prompted optimization of the extraction procedure by a series of titration experiments focusing on the setting of three parameters: pH, temperature, and time of incubation with the enzymes. The parameter values tested were the following: temperature 40- vs 50- °C, pH 5 vs 7; time of incubation 3-, 6- vs 16-hours.

In this regard, the results of the titration experiments did not give dramatic differences among the tested parameters; the reason behind could lay on the fact that bacterial enzymes generally have a wide range of action, i.e., they can efficiently work in different chemo-physical conditions.

However, the optimization process led to the establishment of the following extraction parameters: 50°C, pH 5, 16 hours of incubation of the vegetable biomass together with *B. subtilis* enzymes, followed by 5 h of solid-liquid extraction.

Regarding the incubation time, since no significant differences were detected, 16 hours were found to be more practical for incubating cauliflowers with enzymes overnight to perform downstream processes the following day. However, a good extraction yield was obtained also after 3 hours of incubation.

#### 4.4.3 Recovery of phenolic compounds

The subsequent experiments were performed by an optimized protocol. The total polyphenols were recovered more efficiently upon the enzymatic treatment (Figure 30 and Table 5). In particular, the polyphenols recovered upon treatment with the WT strain increased by 1.3-fold with respect to the control ( $p < 0.1$ , weak significance); however, the recovery further increased (by 1.4-fold with respect to the control,  $p < 0.05$ ) when the treatment was performed with the optimized strain OS58, which is a better enzyme producer (Figure 30).

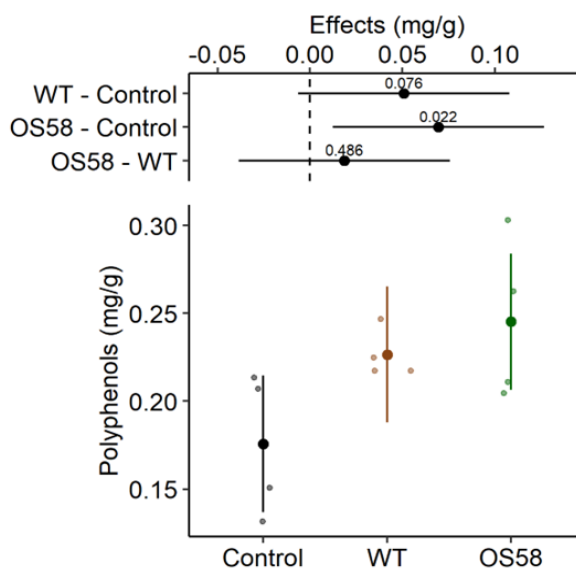


**Figure 30.** The total polyphenols content (calculated as mg per gram of fresh cauliflowers, before freezing) is reported for Control, WT, and OS58 groups as estimated means and 95% confidence intervals (larger dots and colored lines, respectively) by the linear mixed model (LMM). On the upper side of the plot, treatment effects are reported in mg/g as the estimated means and 95% confidence intervals for each comparison, as difference from the control or between enzymatic treatments, as indicated on the left (degrees of freedom-df = 10.7). The level of significance ( $p$ -value) is reported above each horizontal line; the dashed line corresponds to the “no effect” hypothesis. The values reported were obtained from the model using the emmeans package ( $n = 4$ , for each group) (Package “emmeans”).



**Table 5.** The concentration of secondary metabolite extracted (mg or  $\mu\text{g}$  per gram of fresh cauliflower) for each pre-treatment group [control = sterile medium; WT = spent medium from the WT strain; OS58 = spent medium from the optimized strain].

Bioactive compounds	Control	WT	OS58
Polyphenols (mg/ml)	$0.18 \pm 0.02$	$0.227 \pm 0.007$	$0.24 \pm 0.02^*$
Epigallocatechin gallate ( $\mu\text{g/g}$ )	$1.1 \pm 0.2$	$2.2 \pm 0.8$	$3.1 \pm 0.7^{**}$
Epicatechin ( $\mu\text{g/g}$ )	$4.7 \pm 0.8$	$8.7 \pm 1.3^*$	$11.3 \pm 2.8^{**}$
Epicatechin gallate ( $\mu\text{g/g}$ )	$3.3 \pm 0.6$	$4.4 \pm 0.6^{**}$	$4.1 \pm 0.5^*$
Chlorogenic acid ( $\mu\text{g/g}$ )	$0.9 \pm 0.6$	$1.9 \pm 0.8^{**}$	$2.7 \pm 0.9^{***}$
Isothiocyanates ( $\mu\text{g/g}$ )	$0.004 \pm 0.001$	$0.005 \pm 0.001$	$0.006 \pm 0.001$

A descriptive statistical analysis of the data- mean values  $\pm$  standard error of the mean (SEM) - was conducted to describe the difference among the treated groups vs. control. The asterisks (\*) indicate the significant differences, obtained by the Linear Mixed Models ( $p < 0.05$  \*;  $p < 0.01$  \*\*;  $p < 0.001$  \*\*\*).

#### 4.4.4 Catechins

The analysis of polyphenols was further deepened to the group of catechins. The HPLC profile for these compounds was evaluated in the treated and control groups, revealing a significant improvement in their recovery even with the WT strain (Fig. 31). With respect to the control, the WT supernatant allowed the extraction of 2-fold more epigallo-catechin gallate, 1.8-fold more epicatechin, and 1.3-fold more epicatechin gallate (Table 5). As observed for polyphenols in general, in all but the last case, the effect of the bacterial pre-treatment appeared stronger with the optimized OS58 strain, where the yield, with respect to the control, raised by 2.8-fold for epigallocatechin gallate and by 2.4-fold for epicatechin. Conversely, the recovery of epicatechin gallate upon OS58 treatment (1.2-fold increase) was slightly lower than that obtained with the WT strain (1.3-fold higher than the control) (Table 5).

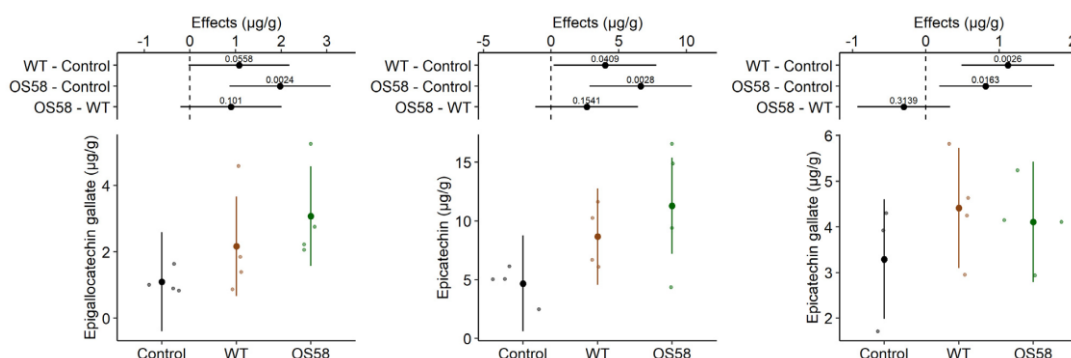


**Figure 31.** The catechins content (calculated as  $\mu\text{g}$  per gram of fresh cauliflowers) is reported for the Control, WT, and OS58 groups. A detailed description of these types of plots is provided in Fig. 30 caption.

#### 4.4.5 Chlorogenic Acid

Among the phenolic acids, chlorogenic acid was examined. As shown in Figure 32 and Table 5, the enzymatic pre-treatment appeared to be extremely efficient in releasing the compound from the matrix. The enzymes produced by the WT strain were able to release 2-fold more chlorogenic acid than the control treatment, while the recovery following the treatment with the OS58 enzymatic pool was 2.9-fold higher. It is worth noticing that, for this compound, the difference between the OS58 strain and the WT achieved a 95 % statistical significance ( $p = 0.019$ ).

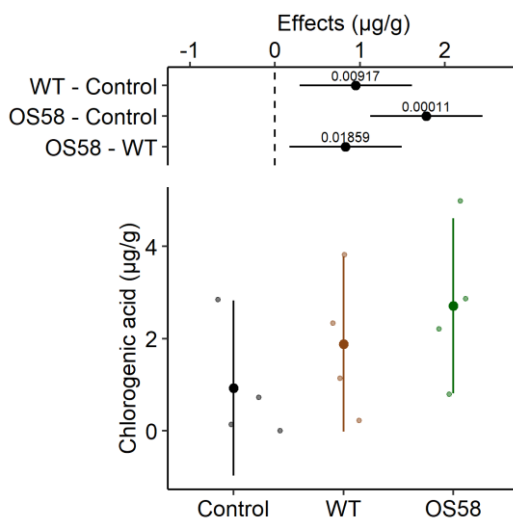


**Figure 32.** Chlorogenic acid content (calculated as  $\mu\text{g}$  per gram of fresh cauliflowers) is reported for the Control, WT, and PB1OPT groups. A detailed description of these types of plots is provided in Figure 30.

#### Recovery of sulfur-containing plant secondary metabolites

##### 4.4.6 Isothiocyanates

For this class of compounds, a very modest increase in the recovery (1.3-fold) was observed only within the OS58-treated group (Figure 33 and Table 5), which, however, did not reach statistical significance ( $p = 0.08$ ). The reasons for these results are discussed below.

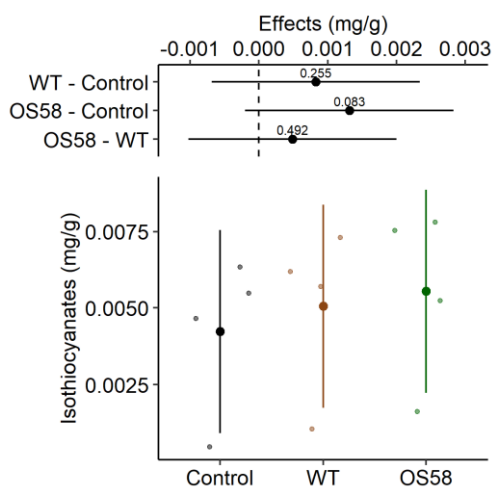


**Figure 33.** Isothiocyanates content (calculated as mg per gram of fresh cauliflowers) is reported for the Control, WT, and OS58 groups. A detailed description of these types of plots is provided in Figure 30.

## 4.5 Discussion

This work was part of the Phyver (PHYtochemicals from VEgetables Recycling) project, carried out in collaboration with the Nutrition and Nutraceuticals laboratory of the Dept. of Biology and Biotechnology. The project was focused on the valorization of agro-industrial wastes as source of phytochemicals endowed with a large variety of biological activities. In particular, it aimed at the identification of an efficient and sustainable method for the extraction of phytochemicals from discarded cauliflowers with the support of crude enzymatic mixture derived from *Bacillus subtilis* cultures.

The *Bacillus subtilis* strain OS58 hyper-produced cellulase and xylanase because the two selected enzymes are supposedly playing a pivotal role in vegetable matrix breakdown, although a plethora of additional enzymes, such as proteases and amylases, which *B. subtilis* is known to secrete, might contribute to the final effect on the substrate (Tjalsma et al., 2004).

The first part of the project was concentrated on the standardization of the enzymatic yields of the two *B. subtilis* strains, grown on a chemically defined medium, resulting in standard bacterial growth and enzymatic production protocols. The results confirmed that the enzymatic production from the optimized strain exceeded the one from the WT strain.

The single EAE treatment allowed to extract a higher quantity of compounds with the optimized strain compared to the WT strain. The largest differences between the two strains were observed for epicatechin gallate and epicatechin, belonging to the catechin subgroup and to which a powerful antioxidant activity is ascribed. Compared to the sole application of the Naviglio extractor®, an increased recovery of some compounds was obtained by combining it with the EAE pre-treatment. Among them, chlorogenic acid, which is a phenolic compound exhibiting several biological properties as anti-inflammatory and brain antioxidant, neurodegenerative protector among others (Zuo et al., 2015), and epicatechin gallate.

In the final assessment of the combined extraction procedure, the efficiency of the recovery of polyphenols, in particular chlorogenic acid, epigallo catechin gallate, and epicatechin, was correlated with the amount of enzymes administered. These results support a direct link between the extraction efficiency and the amount of secreted enzymes.

Contrarily, preliminary experiments indicated that isothiocyanates, relevant anticancer compounds abundantly present in Brassicaceae and giving the pungent aroma characteristic of the species, as well as vitexin and iso-orientin (data not shown) were hardly extractable by this procedure. It is worth reminding that these compounds are usually extracted from fresh material using organic solvents, and even in those cases, with extremely variable returns (Tang et al., 2013; Rodríguez De Luna et al., 2020; Karanikolopoulou et al., 2021). Indeed, only methanol and ethanol allowed to extract them from the different parts of the vegetable. Such solvents guarantee much higher yields with respect to those herein reported (Naczek & Shahidi 2006).

However, in this work, a precise choice was made not to use organic solvents, to avoid the generation of toxic or polluting waste and to preserve the green character of the process.

The sustainability of the extraction procedure was further enhanced by the fact that the vegetable material used was a real waste generated from a real agri-food supply chain because it did not meet the aesthetic quality standard requirements for large-scale retail channels. Cauliflowers from this source originated from farms located in different geographical areas in Italy were collected in three different seasons (spring, summer, and early autumn 2021). The uncontrolled origin of the experimental material granted it an intrinsic heterogeneity, since the content of secondary metabolites in fruits and vegetables is known to strongly depend on several parameters such as specific cultivar, seasonal harvesting time, cultivation site, endogenous circadian rhythms, and soil and pest-control strategies (Heimler et al., 2007; Soengas et al., 2018). Moreover, during the wheeled transport to the processing warehouse, the harvested material reached different maturation stages, also related to seasonal conditions.

These variables might have heavily impacted on the composition and overall content of the bioactive compounds of vegetables, thereby affecting the extraction yield among the replicates performed on different stocks of cauliflowers, and are partly responsible for the low statistical significance of some of the data. For this reason, the correlation among replicates was estimated by including the variable “replicate” as a random effect in the statistical model (see Materials and Methods).

Nevertheless, the extraction procedure might require further adjustments for some classes of compounds. For instance, the prolonged defrosting process (48 h) carried out at RT, might compromise the recovery of highly volatile and intrinsically unstable bioactive molecules. The extraction protocols should be adjusted based on the vegetable material and on the bioactives to be extracted. It is important to highlight that, as opposed to most of the literature data, this work was carried out on a pilot scale, using 5 kg of raw material for each sample and for each of the four experimental replicates, which make this work pioneering.

The entire process might be conceived as part of a complex biorefinery which includes: i) the recovery of natural bioactive compounds directly from vegetable waste produced by the biorefinery; ii) the use of part of this waste as substrate for microbial fermentation; iii) application of the post-extraction biomass on agricultural fields to enhance productivity, or alternatively, its use for clean energy generation. Indeed, the entire process would be in compliance with the principles of circular economy.

One of the initial aims of the project was the re-use of the post-extraction biomass for *B. subtilis* growth. Preliminary experiments demonstrated the ability of *B. subtilis* to grow on un-pretreated waste substrates, such as orange, banana and apple peels, or beet. However, cauliflower was not applicable as *B. subtilis* growth substrate, possibly because of its high concentration in sulfur-containing compounds with antimicrobial activities that inhibited bacterial growth.

The possibility of using other types of substrates that allow both the recovery of a wide range of bioactives and at the same time, the production of bacterial enzymatic extracts via fermentation is still an open challenge.

## References

- Abdel-Aal E. M., Young J. C.** 2009. Chapter 8 - CAROTENOIDS. Editor(s): Peter R. Shewry, Jane L. Ward. In American Associate of Cereal Chemists International, HEALTHGRAIN Methods, AACC International Press 69-94. DOI: 10.1016/B978-1-891127-70-0.50011-X . DOI: 10.3389/fnut.2020.00060.
- Ferreira J.F.S., Luthria D.L., Sasaki T., Heyerick A.** 2010. Flavonoids from *Artemisia annua* L. as Antioxidants and Their Potential Synergism with Artemisinin against Malaria and Cancer. *Molecules* 15, 3135-3170. DOI:10.3390/molecules15053135.
- Fraga C. G., Croft K. D., Kennedye D. O., Tomás-Barberán F. A.** 2019. The effects of polyphenols and other bioactives on human health. *Food Funct.* 10, 514-528. DOI:10.1039/C8FO01997E.
- Galanakis C.M.** 2015. *Food Waste Recovery: Processing Technologies and Industrial Techniques*; Elsevier: New York, NY, USA 381-392. DOI: 10.1016/C2013-0-16046-1.
- Garcia R.G., Martínez-Ávila G.C.G., Aguilar C.N.** 2012. Enzyme-assisted extraction of antioxidative phenolics from grape (*Vitis vinifera* L.) residues. *3 Biotech.* 2, 297-300. DOI: 10.1007/s13205-012-0055-7.
- Gligor O., Mocan A., Moldovan C., Locatelli M., Crisan G., Ferreira I.C.** 2019. Enzyme-assisted extractions of polyphenols—A comprehensive review. *Trends Food Sci. Technol.* 88, 302-315. DOI: 10.1016/j.tifs.2019.03.029.
- Gonzales G.B., Smaghe G., Raes K., Van Camp J.** 2014. Combined alkaline hydrolysis and ultrasound-assisted extraction for the release of nonextractable phenolics from cauliflower (*Brassica oleracea* var. botrytis) waste. *J. Agric. Food Chem.* 62, 3371-6. DOI: 10.1021/jf500835q.
- Han Z. P., Liu R. L., Cui H. Y., Zhang Z. Q.** 2013. MICROWAVE-ASSISTED EXTRACTION AND LC/MS ANALYSIS OF PHENOLIC ANTIOXIDANTS IN SWEET APRICOT (*PRUNUS ARMENIACA* L.) KERNEL SKINS, *J. Liq. Chromatogr. Relat.* 36, 2182-2195. DOI: 10.1080/10826076.2012.717057.
- Heimler D., Isolani L., Vignolini P., Tombelli S., Romani A.** 2007. Polyphenol Content and Antioxidative Activity in Some Species of Freshly Consumed Salads. *J. Agric. Food Chem.* 55, 1724-1729. DOI:10.1021/jf0628983.
- Huo S., Wang Z., Cui F., Zou B., Zhao P., Yuan Z.** 2015. Enzyme-assisted extraction of oil from wet microalgae *Scenedesmus* sp. G4. *Energies* 8, 8165-8174. DOI:10.3390/en8088165.
- Karanikolopoulou S., Revelou P.-K., Xagoraris M., Kokotou M.G., Constantinou-Kokotou V.** 2021. Current Methods for the Extraction and Analysis of Isothiocyanates and Indoles in Cruciferous Vegetables. *Analyt.* 2, 93-120. DOI:10.3390/analytica2040011.
- Kumar K., Yadav A.N., Kumar V., Vyas P., Dhaliwal H.S.** 2017. Food waste: A potential bioresource for extraction of nutraceuticals and bioactive compounds. *Bioresour. Bioprocess.* 4, 18. DOI:10.1186/s40643-017-0148-6.

**Lafarga T., Viñas I., Bobo G., Simó J., Aguiló-Aguayo I.** 2018. Effect of steaming and sous vide processing on the total phenolic content, vitamin C and antioxidant potential of the genus Brassica. *Innov. Food Sci. Emerg. Technol.* 47, 412-420. DOI:10.1016/j.ifset.2018.04.008.

**Lawson A.P., et al.** 2015. Naturally Occurring Isothiocyanates Exert Anticancer Effects by Inhibiting Deubiquitinating Enzymes. *Cancer Res.* 75, 5130-5142. DOI: 10.1158/0008-5472.CAN-15-1544.

**Lenucci M.S., et al.** 2015. Enzyme-aided extraction of lycopene from high-pigment tomato cultivars by supercritical carbon dioxide. *Food Chem.* 170, 193-202. DOI: 10.1016/j.foodchem.2014.08.081.

**Li Z., Lee H.W., Liang X., Liang D., Wang Q., Huang D., Ong C.N.** 2018. Profiling of Phenolic Compounds and Antioxidant Activity of 12 Cruciferous Vegetables. *Molecules.* 23, 1139. DOI: 10.3390/molecules23051139.

**Lola-Luz T., Hennequart F., Gaffney M.** 2014. Effect on yield, total phenolic, total flavonoid and total isothiocyanate content of two broccoli cultivars (*Brassica oleraceae* var *italica*) following the application of a commercial brown seaweed extract (*Ascophyllum nodosum*). *Agric. Food Sci.*, 23, 28-37. DOI: 10.23986/afsci.8832.

**Mamari H. H. A.** 2021, 'Phenolic Compounds: Classification, Chemistry, and Updated Techniques of Analysis and Synthesis', in F. A. Badria (ed.), *Phenolic Compounds - Chemistry, Synthesis, Diversity, Non-Conventional Industrial, Pharmaceutical and Therapeutic Applications*, IntechOpen, London. DOI: 10.5772/intechopen.98958.

**Marathe S.J., Jadhav S.B., Bankar S.B., Singhal R.S.** Enzyme-Assisted Extraction of Bioactives. In *Food Bioactives*; Puri, M., Ed.; Springer: Cham, Switzerland 171-201. DOI:10.1007/978-3-319-51639-4\_8.

**Muhamad I. I., Hassan N. D., Mamat S. N.H., Nawi N. M., Rashid W. A., Tan N. A.** 2017. Chapter 14 - Extraction Technologies and Solvents of Phytochemicals From Plant Materials: Physicochemical Characterization and Identification of Ingredients and Bioactive Compounds From Plant Extract Using Various Instrumentations. Editor(s): Alexandru Mihai Grumezescu, Alina Maria Holban. In *Handbook of Food Bioengineering, Ingredients Extraction by Physicochemical Methods in Food*, Academic Press 523-560. DOI: 10.1016/B978-0-12-811521-3.00014-4.

**Naczki M., Shahidi F.** 2006. Phenolics in cereals, fruits and vegetables: occurrence, extraction and analysis. *J. Pharm. Biomed. Anal.* 41, 1523-1542. DOI: 10.1016/j.jpba.2006.04.002.

**Nadar S., Rao P., Rathod V.K.** 2018. Enzyme assisted extraction of biomolecules as an approach to novel extraction technology: A review. *Food Res. Int.* 108, 309-330. DOI:10.1016/j.foodres.2018.03.006.

**Naviglio D., Formato A., Gallo M.** 2014. Comparison between 2 Methods of Solid-Liquid Extraction for the Production of *Cinchona calisaya* Elixir: An Experimental Kinetics and Numerical Modeling Approach. *J. Food Sci.* 79. DOI: 10.1111/1750-3841.12563.

**Pandita D.** 2021. Chapter 14 - Saffron (*Crocus sativus* L.): phytochemistry, therapeutic significance and omics-based biology. Editor(s):



Tariq Aftab, Khalid Rehman Hakeem. Open Access J. Med. Aromat. Plants 325-396. DOI: 10.1016/B978-0-12-819590-1.00014-8.

**Panzella L., Moccia F., Nasti R., Marzorati S., Verotta L., Napolitano A.** 2020. Bioactive Phenolic Compounds From Agri-Food Wastes: An Update on Green and Sustainable Extraction Methodologies. REVIEW, *Front. Nutr.* 7.

**Patel A., Shah A.R.** 2021. Integrated lignocellulosic biorefinery: Gateway for production of second-generation ethanol and value-added products. *J. Bioresour. Bioprod.* 6, 108-128. DOI:10.1016/j.jobab.2021.02.001.

**Pattnaik M., Pandey P., Martin G.J.O., Mishra H.N., Ashokkumar M.** 2021. Innovative Technologies for Extraction and Microencapsulation of Bioactives from Plant-Based Food Waste and Their Applications in Functional Food Development. *Foods* 10, 279. DOI:10.3390/foods10020279.

**Plazzotta S., Manzocco L.** 2018. Effect of ultrasounds and high-pressure homogenization on the extraction of antioxidant polyphenols from lettuce waste. *Innov. Food Sci. Emerg. Technol.* 50, 11-19. DOI: 10.1016/j.ifset.2018.10.004.

**Posadino A.M., et al.** 2018. Protective effect of cyclically pressurized solid-liquid extraction polyphenols from Cagnulari grape pomace on oxidative endothelial cell death. *Mol.* 23, 1-12. DOI: 10.3390/molecules23092105.

**Puri M., Sharma D., Barrow C.J.** 2012. Enzyme-assisted extraction of bioactives from plants. *Trends Biotechnol.* 30, 37-44. DOI: 10.1016/j.tibtech.2011.06.014.

**R Core Team.** 2021. R: A language and environment for statistical computing. R Foundation for Statistical Computing, Vienna, (Austria).

**Rodríguez De Luna S.L., Ramírez-Garza R.E., Serna Saldívar S.O.** 2020. Environmentally Friendly Methods for Flavonoid Extraction from Plant Material: Impact of Their Operating Conditions on Yield and Antioxidant Properties. *Sci. World J.* 2020. DOI: 10.1155/2020/6792069.

**Soengas P., Cartea M.E., Velasco P., Francisco M.** 2018. Endogenous Circadian Rhythms in Polyphenolic Composition Induce Changes in Antioxidant Properties in Brassica Cultivars. *J. Agric. Food Chem.* 66, 5984-5991. DOI: 10.1021/acs.jafc.8b01732.

**Starska-Kowarska K.** 2022. Dietary Carotenoids in Head and Neck Cancer—Molecular and Clinical Implications. *Nutrients.* 14, 531. DOI: 10.3390/nu14030531

**Su D., Wang Z., Dong L., Huang F., Zhang R., Jia X., Zhang M.** 2019. Impact of thermal processing and storage temperature on the phenolic profile and antioxidant activity of different varieties of lychee juice. *LWT Food Sci. Technol.* 116. DOI:10.1016/j.lwt.2019.108578.

**Tang L., Paonessa J.D., Zhang Y., Ambrosone C.B., McCann S.E.** 2013. Total isothiocyanate yield from raw cruciferous vegetables commonly consumed in the United States. *J. Funct. Foods* 5, 1996-2001. DOI: 10.1016/j.jff.2013.07.011.

**The R Project for Statistical Computing.** Available online: <https://www.R-project.org/> (accessed on 7 February 2022).

**Tjalsma H., et al.** 2004. Proteomics of protein secretion by *Bacillus subtilis*: Separating the “secrets” of the secretome. *Microbiol. Mol. Biol. Rev.* 68, 207-233. DOI: 10.1128/MMBR.68.2.207-233.2004.

**Wadhwa M., Bakshi M.P.S.** 2013. Utilization of Fruit and Vegetable Wastes as Livestock Feed and as Substrates for Generation of Other Value-Added Products; RAP Publication, FAO: Rome, Italy, 1-59. DOI:3/i3273e/i3273e.pdf

**Yuan L., Wang J., Wu W., Liu Q., Liu X.** 2016. Effect of isoorientin on intracellular antioxidant defence mechanisms in hepatoma and liver cell lines. *Biomed. Pharmacother.* 81, 356-362. DOI: 10.1016/j.biopha.2016.04.025.

**Zhang Y.** 2012. The 1,2-Benzenedithiole-Based Cyclocondensation Assay: A Valuable Tool for the Measurement of Chemopreventive Isothiocyanates. *Crit. Rev. Food Sci. Nutr.* 52, 525-532. DOI:10.1080/10408398.2010.503288.

**Zuo J., Tang W., Xu Y.** 2015. Chapter 68 - Anti-Hepatitis B Virus Activity of Chlorogenic Acid and Its Related Compounds, Editor(s): Victor R. Preedy, Coffee in Health and Disease Prevention, Academic Press 607-613. DOI: 10.1016/B978-0-12-409517-5.00068-1.

## 5 Conclusions

*Bacillus subtilis* is a versatile microorganism that can be employed for many different processes, ranging from the production of enzymes to the conversion of waste biomass into useful biocommodities. This work intends to provide a comprehensive study of the potential biotechnological applications of the soil bacterium *B. subtilis*, focusing on the bioconversion of lignocellulosic biomass.

The propensity of this bacterium to secrete high amounts of carbohydrate-active enzymes was improved with a view on its biotechnological applicability. Optimized strains of *B. subtilis* outperformed the wild-type strain in industrially relevant carbohydrate-active enzymes production. In future, the creation of a single hyper-producing strain can be easily obtained by merging up all the genetic optimization herein analyzed.

The usefulness of two of those *B. subtilis* strains was validated in two bioeconomy-relevant applications.

A positive correlation was identified between the level of cellulose hyper degrading enzymes production and the quality of dairy forages treated with the bacterium, thus providing a possible scientific basis to the positive effect of *B. subtilis* administration to lactating cows described by several authors. In an effort to ensure the economic viability of the process, the bacterial treatment could be conveniently performed using unpurified cultures grown on a waste-derived medium.

Additional experiments, both *in vitro* and *in vivo*, are required to validate the procedure on a broader range of forages, and assess animal acceptance of the treated fodders. Experiments are currently underway to determine whether rice straw, a huge non-valorized biomass, can be converted into a high-quality and nutrient-dense feedstock.

Furthermore, *Bacillus subtilis*-derived enzymes, used for Enzyme Assisted Extraction (EAE) of phytochemicals from biomass waste, were shown to improve the recovery of nutraceuticals when combined with a mechanical extraction procedure in aqueous environment. The application of the culture supernatants conferred a relevant economic advantage and guaranteed the environmental safety of the entire extraction process.

Additional research is ongoing to fine-tune the biotechnological procedure and explore its applicability to different food wastes, with different phytochemical compositions.

The above examples pave the way to the implementation of genetically improved *Bacillus subtilis* in a variety of applications in the expanding field of circular economy; besides, it can constitute a biotechnological model for the construction of new and more efficient organisms of industrial relevance.

The strains developed in this work can be considered the forefront for the creation of CBP microorganisms able to autonomously saccharify lignocellulosic material to transform it in biocommodities, thus bypassing time-consuming and expensive biomass pre-treatments, the current critical step in the valorization of recalcitrant biomass.

### List of original manuscripts

Doria E., Buonocore D., Marra A., Bontà V., Gazzola A., Dossena M., Verri M., Calvio C. 2022. Bacterial-Assisted Extraction of Bioactive Compounds from Cauliflower. *Plants*, 11, 816. DOI:10.3390/plants11060816.

Ermoli F., Bontà V., Vitali G., Calvio C. 2021. SwrA as global modulator of the two-component system DegSU in *Bacillus subtilis*. *Res. Microbiol.*, 172. DOI: 10.1016/j.resmic.2021.103877.

During the three years of my PhD, I worked on another project related to a small uncharacterized protein of *Bacillus subtilis*, SwrA, whose role is still not completely known. I studied the role of the protein in the secretion of degradative enzymes, cellulase and xylanase. A summary of the work is below.

#### **SwrA as global modulator of the two-component system DegSU in *Bacillus subtilis***

The two-component system (TCS) DegSU of *Bacillus subtilis* controls more than one hundred genes involved in several cellular behaviors. Over the last four decades, the degU32<sup>Hy</sup> allele, supposedly encoding a constitutively active mutant of the response regulator DegU, was exploited to define the impact of this system on cell physiology. SwrA is a small protein encoded only by wild strains whose role is not thoroughly understood.

In this work, we analyzed a range of phenotypes regulated by DegSU, highlighting the wide role of SwrA as a key regulator. Our results demonstrate that the role of SwrA in *B. subtilis* physiology is wider than expected and affects many other DegSU targets. SwrA reduces subtilisin, cellulases and xylanases production, while it positively modulates motility and competence for DNA uptake.

I wrote the chapter of the book called “Modern Approaches in Waste Bioremediation” which will be published by Springer Nature. The chapter title is “Poly-γ-Glutamic Acid and its application in bioremediation: a critical review”. I have summarized the most important characteristics of the biopolymer Poly-γ-Glutamic Acid (γ-PGA) and of its production, highlighting the advantages, but also the limits, in its application in bioremediation.

The data of the third chapter of this thesis will be described in an article under preparation; therefore, I will not include it in the List of the Manuscript.



Contents lists available at ScienceDirect

Research in Microbiology

journal homepage: [www.elsevier.com/locate/resmic](http://www.elsevier.com/locate/resmic)

Original Article

## SwrA as global modulator of the two-component system DegSU in *Bacillus subtilis*

Francesca Ermoli, Valeria Bontà, Giulia Vitali, Cinzia Calvio\*

Dept. of Biology and Biotechnology, Laboratories of Genetics and Microbiology, University of Pavia, Via Ferrata 9, 27100 Pavia (I), Italy



## ARTICLE INFO

## Article history:

Received 11 June 2021

Accepted 11 August 2021

Available online 4 September 2021

## Keywords:

degS200<sup>Hy</sup>

Competence

Subtilisin

Cellulases

Xylanases

γ-PGA

## ABSTRACT

The two-component system DegSU of *Bacillus subtilis* controls more than one hundred genes involved in several different cellular behaviours. Over the last four decades, the *degU32<sup>Hy</sup>* allele, supposedly encoding a constitutively active mutant of the response regulator DegU, was exploited to define the impact of this system on cell physiology. Those studies concluded that phosphorylated DegU (DegU-P) induced degradative enzyme expression while repressing flagellar motility and competence.

Recent experiments, however, demonstrated that flagella expression is enhanced by DegU-P if SwrA, a protein only encoded by wild strains, is present. Yet, to promote motility, SwrA must interact with DegU-P produced by a wild-type *degU* allele, as it cannot correctly cooperate with the mutant DegU32<sup>Hy</sup> protein.

In this work, the impact of DegSU was reanalysed in the presence or absence of SwrA employing a DegS kinase mutant, *degS200<sup>Hy</sup>*, to force the activation of the TCS. Our results demonstrate that the role of SwrA in *B. subtilis* physiology is wider than expected and affects several other DegSU targets. SwrA reduces subtilisin, cellulases and xylanases production while, besides motility, it also positively modulates competence for DNA uptake, remarkably relieving the inhibition caused by DegU-P alone and restoring transformability in *degS200<sup>Hy</sup>* strains.

© 2021 The Authors. Published by Elsevier Masson SAS on behalf of Institut Pasteur. This is an open access article under the CC BY license (<http://creativecommons.org/licenses/by/4.0/>).

## 1. Introduction

Two-component systems (TCS) are signal transduction modules common in bacteria and archaea, composed of a sensor histidine kinase (HK) and a cognate response regulator (RR). In response to specific environmental signals, sensor kinases autophosphorylate on a histidine residue and then transfer the phosphate group to an aspartic acid residue of their cognate RR, inducing a structural rearrangement that enables the RR to regulate gene expression. Moreover, HK can often quench spurious signals by dephosphorylating the RR [1]. The DegSU TCS of *Bacillus subtilis*, composed of the cytoplasmic HK DegS and the RR DegU, is involved in the regulation of several important physiological pathways, among which flagella-mediated motility, degradative enzyme synthesis, genetic competence, and sporulation [2]. Unfortunately, the DNA consensus sequence recognized by DegU has not been clearly identified, preventing a systematic identification of DegSU target

genes. For this reason, the extremely wide impact of this TCS has been evidenced through several transcriptional profiling experiments [3–5] or by using a particular class of mutations that lead to the activation of the TCS [6]. These mutations, collectively called Hy because of the hyperproduction of several degradative enzymes, cause a pleiotropic phenotype. In fact, besides promoting the synthesis of levansucrase, the *aprE*-encoded protease subtilisin, glucanases and xylanases among others, Hy mutations cause loss of genetic competence, absence of flagella, sporulation in the presence of glucose and elongated cell morphology [2,6–9]. They are missense mutations localized in either *degS* or *degU* genes or in the promoter of the *degQ*, a gene involved in the modulation of the DegSU TCS [10,11]. The DegS200<sup>Hy</sup> mutant protein carries a Gly to Glu substitution at position 218, which impairs the phosphatase activity of the HK, thus leading to the accumulation of DegU-P [2,12]. The *degU32<sup>Hy</sup>* mutant allele has an A-to-T transversion at nucleotide 35 of the open reading frame (ORF) that leads to a His to Leu amino acid change at position 12 [11]. The impact of this amino acid substitution on the structure of the RR has not been evaluated yet, however, as DegS<sup>Hy</sup> and DegU<sup>Hy</sup> mutants showed perfectly overlapping phenotypes in domestic strains [6]. DegU32<sup>Hy</sup> has since been considered as a constitutively active proxy of DegU-P,

\* Corresponding author.

E-mail addresses: [francesca.ermoli01@universitadipavia.it](mailto:francesca.ermoli01@universitadipavia.it) (F. Ermoli), [valeria.bonta01@universitadipavia.it](mailto:valeria.bonta01@universitadipavia.it) (V. Bontà), [giulia.vitali02@universitadipavia.it](mailto:giulia.vitali02@universitadipavia.it) (G. Vitali), [cinzia.calvio@unipv.it](mailto:cinzia.calvio@unipv.it) (C. Calvio).

<https://doi.org/10.1016/j.resmic.2021.103877>

0923-2508/© 2021 The Authors. Published by Elsevier Masson SAS on behalf of Institut Pasteur. This is an open access article under the CC BY license (<http://creativecommons.org/licenses/by/4.0/>).

without any further structural characterization. The third mutation causing the Hy phenotype, *degQ36<sup>Hy</sup>*, is localized in the promoter of DegQ. Identified in domestic strains, the *degQ36<sup>Hy</sup>* mutation consists of a nucleotide change in the -10 box of *degQ* promoter that leads to 10-fold increase in transcription, thereby increasing the intracellular concentration of DegQ [10]. This polypeptide (46 amino acids) intervenes in the DegSU signalling pathway by stimulating the transfer of the phosphate moiety from DegS to DegU [5]. The overexpressed *degQ36<sup>Hy</sup>* allele is naturally present in wild *B. subtilis* strains [13].

Besides the Up-promoter mutation in *degQ*, wild strains differ from domestic ones also for the presence of *SwrA*, a 117-amino acid protein identified thanks to its fundamental role in swarming motility [14]. In laboratory strains, an extra adenine is inserted in a poly-A tract present in the *swrA* ORF leading to a truncated, non-functional polypeptide (herein indicated as *swrA'*) [14–16]. These types of mutations can easily flip back to the wild-type form (wt) (herein indicated as *swrA*) and vice versa with the frequency of a phase-variation event ( $10^{-4}$ ) [14]. It is thus common to obtain mixed populations *swrA*<sup>+/−</sup> upon prolonged incubations of *swrA'* laboratory strains. When functional, *SwrA* supports DegU-P in stimulating the flagellar *P<sub>fla/che</sub>* promoter, thereby boosting *sigD* transcription which, in turn, warrants efficient cell separation by activating autolysin genes [17–20]. Although initially confined to motility regulation, *SwrA* was also shown to be essential for the expression of the otherwise-silent *pgs* operon, encoding the enzymes required for the synthesis of the biopolymer poly- $\gamma$ -glutamic acid ( $\gamma$ -PGA) [21,22]. Interestingly, also  $\gamma$ -PGA production depends on the presence of *SwrA* plus a Hy mutation in either *degQ* [22] or *degSU* [23].

Most of the studies on the DegSU TCS have relied on *degU32<sup>Hy</sup>* and were carried out in domestic strains (i.e., *swrA*). In these strains all phenotypes caused by DegU32<sup>Hy</sup> matched those obtained with DegS200<sup>Hy</sup>; in the absence of *SwrA* both Hy mutants completely suppress *P<sub>fla/che</sub>* expression, leading to the classically non-flagellated Hy-phenotype [9]. However, the restoration of a functional *swrA* allele in domestic strains led to hyperflagellation both in the normal *degSU* backgrounds as well as in *degS200<sup>Hy</sup>* mutants, while the same did not happen in *degU32<sup>Hy</sup>* mutants [20]. The interaction between *SwrA* and DegU-P, but not DegU32<sup>Hy</sup>, was also shown at the molecular level: a DNA fragment containing the *fla/che* promoter bound to DegU-P could be super-shifted by *SwrA*, while the same fragment bound to DegU32<sup>Hy</sup>, with or without phosphorylation, could not be super-shifted by *SwrA* [20], thus evidencing the profoundly different behaviour of the wt phosphorylated DegU and the DegU32<sup>Hy</sup> mutant protein. The physical interaction between DegU and *SwrA* was confirmed by other studies [24]. Ultimately, the impact of *SwrA* on motility is, remarkably, to turn *P<sub>fla/che</sub>* repression caused by DegU-P, produced by either wt DegS or DegS200<sup>Hy</sup>, into a transcriptional boost that enables swarming motility [18,20]. This dramatic overturn of the DegU-P impact on the motility operon cannot be appreciated in domestic strains, because of the absence of *SwrA*, or in wild strains if the *degU32<sup>Hy</sup>* allele is used as a proxy of DegU-P [25].

Although *SwrA* does not interact with DegU32<sup>Hy</sup> at the *P<sub>fla/che</sub>* promoter, it is not true that they never interact. Indeed,  $\gamma$ -PGA production is induced by *SwrA* in the presence of either *degU32<sup>Hy</sup>* or *degS200<sup>Hy</sup>* mutation [23]. However, a deep characterization of the differential impacts of the two Hy alleles on the promoter for  $\gamma$ -PGA biosynthesis, *P<sub>pgs</sub>*, has yet to be conducted.

Genetic competence is another tract controlled by DegSU. *degSU* null mutants are non-competent, suggesting the requirement of the activities of this TCS in the pathway. Yet, Hy mutants have been shown to repress competence, at least in laboratory strains [8]. According to the current view, unphosphorylated DegU is required,

possibly because it mediates the binding of ComK, the master regulator of competence genes, to its own promoter, while DegU-P has a negative impact on *comS*, an exchange factor necessary for ComK accumulation [26]. Recently, it was shown that the *degQ<sup>Hy</sup>* allele negatively affects *comK* and *comS* expression in both domestic (*swrA'*) and wild strains (*swrA*) [27].

In this work we analysed a range of phenotypes regulated by DegSU, highlighting the wide role of *SwrA* as key regulator. We demonstrated that, in addition to motility and  $\gamma$ -PGA production, *SwrA* positively modulates DegSU activity in competence for transformation and reduces DegU-P-dependent *aprE* transcription as well as the secretion of cellulases and xylanases. Moreover, we characterized the differential influence of *degU32<sup>Hy</sup>* and *degS200<sup>Hy</sup>* mutations on *pgs* operon expression, showing that the *degU32<sup>Hy</sup>* allele encodes a constitutively active mutant protein whose activity drastically differs from the phosphorylated wt DegU-P protein. Our results indicate that, as previously shown for motility, the use of the *degS200<sup>Hy</sup>* mutant may provide new insights into the real role of DegSU TCS in *B. subtilis* biology.

## 2. Materials and methods

### 2.1. Strain construction

All strains used in this study are listed in Table 1. PB5630, corresponding to strain DK1042 obtained by D. Kearns and co-workers [28] by introducing the *com<sup>R22L</sup>* mutation in the resident plasmid of the undomesticated NCIB3610, was transformed with the non-replicative plasmids pLoxSpec/degSU(Hy) or pLoxSpec/degS200 [23]. PB5814 and PB5815, respectively, were obtained after selection for spectinomycin resistance (60  $\mu$ g/ml). The mutant alleles were integrated at the *degSU* locus by allelic replacement, as verified by PCR.

The clean deletion of the *swrA* gene was obtained by transforming PB5249 with pCC $\Delta$ *swrA*, a non-replicative plasmid that, completely removing the *swrA* ORF, inserts a kanamycin resistance gene upstream of the *swrA* promoter, which controls the expression of the downstream *minJ* gene. pCC $\Delta$ *swrA* plasmid was obtained through the following steps: a PCR fragment comprising the region upstream the *swrA* gene, containing all the regulatory elements, was amplified from PB5249 genomic DNA with primers UPPromA/E (*EcoRI*)5'-ccgaaattcttggcttaagaagattggatc-3' and CC\_A\_rev (*XhoI*) 5'-aacgctcgagttgtaacccccatttctttatcacagataagcac-3'; the initial part of the following ORF, *minJ*, was amplified from the same source with primers CC\_B\_for (*XhoI*) 5'-accgctcgaggtctctgtcaatgggaatt-gaactgttaaaaaagc-3' and CC\_C\_rev (*SmaI*) 5'-tccccggggtttgcagctgctgctcgatg-3'. The two products were digested with *XhoI* (restriction sites underlined) and ligated. The resulting 934 bp product was inserted between the *EcoRI* and *SmaI* sites of the pJM114-derived pCC1 [18]. The plasmid pCC $\Delta$ *swrA* was verified by multiple restriction digestion and by sequencing of the relevant portions.

The plasmid pCC $\Delta$ *swrA* was used to transform PB5249. PB5606 was obtained by selecting for kanamycin (2  $\mu$ g/ml) resistance; deletion of the coding sequence of *swrA* and the integrity of its promoter and *minJ* were verified by PCR and DNA sequencing.

The *P<sub>aprE</sub>::gfp* strains were obtained by *in-locus* integration of the pGFP-*aprE* plasmid (a generous gift from Prof. J.W. Veening [29]) into the chromosome of *swrA*<sup>+</sup> and  $\Delta$ *swrA* isogenic strains producing, respectively, PB5392 [18] and PB5606 (described above), both carrying a kanamycin resistance gene upstream of the *swrA* promoter region. The resulting strains were named PB5717 and PB5719, respectively (Table 1). *degU32<sup>Hy</sup>* and *degS200<sup>Hy</sup>* alleles were introduced in PB5717 and PB5719 by transformation with pLox-Spec/degSU(Hy) and pLoxSpec/degS200 [23] as previously described. In the derived strains, PB5720, PB5722, PB5723 and



**Table 1**  
Strains used in this work.

Strain	Relevant genotype	Source or reference
PB5630	<i>comR</i> <sup>Δ21</sup>	BGSC # 3A38
PB 5814	<i>comR</i> <sup>Δ21</sup> <i>degU32</i> (Hy); Sp	This study
PB 5815	<i>comR</i> <sup>Δ21</sup> <i>degS200</i> (Hy); Sp	This study
PB5249	<i>trpC2 pheA1 swrA</i>	(Calvio et al., 2008)
PB5370	<i>trpC2 pheA1 swrA</i>	(Calvio et al., 2008)
PB5606	<i>trpC2 pheA1 ΔswrA</i> ; Km	This study
PB5383	<i>trpC2 pheA1 swrA degU32</i> (Hy); Sp	(Osera et al., 2009)
PB5384	<i>trpC2 pheA1 swrA degU32</i> (Hy); Sp	(Osera et al., 2009)
PB5390	<i>trpC2 pheA1 swrA degS200</i> (Hy); Sp	(Osera et al., 2009)
PB5391	<i>trpC2 pheA1 swrA degS200</i> (Hy); Sp	(Osera et al., 2009)
PB5717	<i>trpC2 pheA1 swrA P<sub>apre</sub>-gfp</i> ; Km, Cm	(This study)
PB5719	<i>trpC2 pheA1 ΔswrA P<sub>apre</sub>-gfp</i> ; Km, Cm	(This study)
PB5720	<i>trpC2 pheA1 swrA P<sub>apre</sub>-gfp degU32</i> (Hy); Km, Cm, Sp	(This study)
PB5722	<i>trpC2 pheA1 ΔswrA P<sub>apre</sub>-gfp degU32</i> (Hy); Km, Cm, Sp	(This study)
PB5723	<i>trpC2 pheA1 swrA P<sub>apre</sub>-gfp degS200</i> (Hy); Km, Cm, Sp	(This study)
PB5725	<i>trpC2 pheA1 swrA ywsc:RBSspoVG:sfGFP_Phyerspank:ywsc</i> ; Em	(This study)
PB5741	<i>trpC2 pheA1 swrA ywsc:RBSspoVG:sfGFP_Phyerspank:ywsc</i> ; Em	(This study)
PB5742	<i>trpC2 pheA1 swrA ywsc:RBSspoVG:sfGFP_Phyerspank:ywsc</i> ; Em	(This study)
PB5743	<i>trpC2 pheA1 swrA ywsc:RBSspoVG:sfGFP_Phyerspank:ywsc degU32</i> (Hy); Em, Sp	(This study)
PB5745	<i>trpC2 pheA1 swrA ywsc:RBSspoVG:sfGFP_Phyerspank:ywsc degS200</i> (Hy); Em, Sp	(This study)

PB5725, respectively (Table 1), the presence of the Hy mutation and the single copy insertion of each construct were assessed by PCR.

The  $P_{pgs}$ -*SfGfp* strains were obtained using a modified pMutin vector (pMATywsC). The construction of this plasmid occurred in multiple steps. First, in the pMutin-GFP vector (ECE149, obtained from the Bacillus genetic stock centre, <http://www.bgsc.org/>) the *gfp* gene was substituted by Gibson assembly with a super folder version of the GFP (*SfGfp*) amplified from pECE323 plasmid (Bacillus genetic stock centre) with primers RxeGFPda321- 5'-ggctcactagtctcgaattcattttataaagtctccaccctgg-3' and FxeGFPda321- 5'-tcggccggaaggagatacatatctgcaaaaggagaa-gaactttttacag-3' to give pMutinsfGFP. The 5' portion of *ywsc* together with the *Phyerspank* promoter were inserted in the resulting pMutinsfGFP through a tripartite Gibson assembly. The *Phyerspank* promoter was amplified from plasmid *Phyp.R0.sfGFP*(sp), *LacI\_operon* [30] using primers *PhypFor* 5'-agcttccaagaagatctcctggatcccttactctgttg-3' and

*PhypRev* 5'-ggctataatgagtaaccacattgttctctcttattagtaaac-3'; the 5' portion of *ywsc* (647 bp) was amplified from PB5249 chromosomal DNA using primers *ywscFor* 5'-taactaataaggagacaacacatgttgactcattatagccttg-3' and *ywscRev* 5'-gtaaaaagtctctcttctttacagagaagcgttatcagggaataac-3'. In the plasmid obtained, pPhyyswscsfGFP, the *spoVG* RBS was inserted in front of the *sfGFP* gene using two partially overlapping oligos designed upon the pJM116 vector [31], *oligoFORSpoVG* 5'-ccctgatacgtcttctggaattcccgatcccagctgttgatacactaactctttata-tagggaaaagtggtgactactatgTCAAAGGAG-3' and *oligoREVSpovG* 5'-CTCCTTTTTCATagatagctaccacctttccctataataaagcattagtgataca-caagctgggattccgggaattccagagaagcgttatcagg-3'. The final construct was verified by sequencing and saved as pMATywsC. This plasmid was used to transform PB5249 (*swrA*<sup>+</sup>) and PB5370 (*swrA*<sup>-</sup>), using erythromycin resistance (5 μg/ml) for selection and screening for integrants at the *pgs* locus, resulting in PB5741 and PB5742 strains, respectively. The *degU32*<sup>Hy</sup> and *degS200*<sup>Hy</sup> alleles were introduced in PB5741 by transformation with *pLoxSpec/degSU*(Hy) and *pLoxSpec/degS200* previously described, giving rise to PB5743 and PB5745, respectively. The presence of the Hy mutation and single copy insertion of each construct were assessed by PCR.

## 2.2. Competence evaluation

Cells were inoculated in LM (LB supplemented with MgSO<sub>4</sub>, 9 μM; tryptophan, 50 μg/ml; phenylalanine, 50 μg/ml) at optical

density at 600 nm (OD<sub>600</sub>) 0.2 and grown at 37 °C with shaking. At OD<sub>600</sub> 1, cells were diluted 1:20 in MD (K<sub>2</sub>HPO<sub>4</sub>, 9.8 mg/ml; KH<sub>2</sub>PO<sub>4</sub>, 5.52 mg/ml; Na<sub>2</sub>Citrate-5H<sub>2</sub>O, 0.92 mg/ml; glucose, 20 mg/ml; tryptophan, 50 μg/ml; phenylalanine, 50 μg/ml; ferric ammonium citrate, 11 μg/ml; K-aspartate, 2.5 mg/ml; MgSO<sub>4</sub>, 0.36 mg/ml) and grown at 37 °C until stationary phase (T<sub>0</sub>). About 200 ng of chloramphenicol (Cm)-selectable *B. subtilis* chromosomal DNA was added to 0.5 ml competent cells, which were further incubated 1.5 h at 37 °C with shaking before selection on 5 mg/ml-chloramphenicol plates. Resistant colonies were counted and related to cell density at T<sub>0</sub> to calculate the transformation efficiency, considering each dilution step before plating. Data shown represent the average of three independent experiments.

## 2.3. *aprE* and *pgs* expression evaluation by flow cytometry

For the analysis of  $P_{apre}$  activity, a *swrA* null mutant was used to avoid *swrA*<sup>+</sup> revertants, that often arise in the *swrA*<sup>-</sup> population upon long incubations, which might generate confusing results. Cells were inoculated in Shaeffer's sporulation medium [32] at OD<sub>600</sub> 0.2 and grown at 37 °C under continuous shaking for 20 h. Aliquots were collected every 60' for OD<sub>600</sub> readings; at the transition point (5 h), 5 and 15 h later, glycerol (final concentration 10%) was added to culture aliquots that were stored at -20 °C till cytofluorimetric analyses.

For the analysis of  $P_{pgs}$  activity, cells were inoculated in E-medium [33] at 0.1 OD<sub>600</sub> and grown at 37 °C under continuous shaking for 48 h. Aliquots were collected at 2-h intervals for OD<sub>600</sub> readings and cytofluorimetric analyses.

Before analyses, fresh and/or frozen samples were centrifuged for 5 min at 14,000 ×g; cell pellets were re-suspended in flow cytometry-grade D-PBS (Gibco, Thermo Fisher Scientific).

$P_{apre}$ -GFP and  $P_{pgs}$ -sfGFP samples were analysed with the Amnis® ImageStream®X Mk II Imaging Flow Cytometer using the INSPiRE software with the following set up: Channel 02 (GFP fluorescence), Channel 06 (Scattering channel); the Brightfield was visualized on Channel 01 or Channel 05, depending on the GFP expression level, to avoid interference from Channel 02. The 488 nm laser was used at either 50 mW or 100 mW power, according to the GFP expression level, in order to avoid sensor saturation. The flow rate was set to low speed/high sensitivity and images were taken at 60X magnification. For each sample at least 10,000 events were acquired.

All data were analysed using the IDEAS software (version 6.2). In-focus events were gated in a histogram displaying the Gradient RMS\_M01\_Ch01 on the x-axis. A plot of the Area versus Aspect Ratio Intensity in the Brightfield channel was used to exclude doublets from the analysis. A scatter plot of the Area in the Brightfield channel versus Intensity in the Scattering channel was used to exclude events characterized by high scatter such as beads. To avoid any bias in evaluating fluorescence intensity due to cell size, the GFP level of each cell was calculated through the Median Pixel feature on the fluorescence channel. The threshold value to distinguish the ON population was set at the maximum auto-fluorescence of a non-fluorescent population (i.e., PB5742) (20 arbitrary units) used as negative control (OFF). Data shown represent the average of three independent experiments.

#### 2.4. Cellulase and xylanase activity assays

PB5249, PB5370, PB5383, PB5384 PB5390 e PB5391 (Table 1) were inoculated at OD<sub>600</sub> 0.2 in a chemically-defined rich medium CDRM (Na<sub>3</sub> citrate tribasic·2H<sub>2</sub>O, 13.67 g/l; MgSO<sub>4</sub>·7H<sub>2</sub>O, 0.5 g/l; K<sub>2</sub>HPO<sub>4</sub>, 0.5 g/l; NH<sub>4</sub>Cl, 7 g/l; CaCl<sub>2</sub>, 0.15 g/l; MnSO<sub>4</sub>·H<sub>2</sub>O, 0.104 g/l; FeCl<sub>3</sub>·6H<sub>2</sub>O, 0.04 g/l; tryptophan, 50 µg/ml; phenylalanine, 50 µg/ml; glucose, 10 g/l) and grown at 37 °C under continuous shaking for 24 h. Aliquots were regularly collected for OD<sub>600</sub> readings to build growth curves; after the transition point (6 h, T<sub>0</sub>), aliquots corresponding to initial, middle and late the stationary phase, from T<sub>2</sub> to T<sub>18</sub>, were collected for measuring cellulases and endo-xylanases enzymatic activities. Cultures were centrifuged 10 min at 14,000×g and the supernatant was acidified by adding 0.1 volume of 1 M sodium acetate buffer (pH 4.5). Cellulase (endo-1,4-β-glucanase; EC 3.2.1.4) and xylanase (endo-1,4-β-xylanase; EC 3.2.1.8) enzymatic units were respectively obtained using the CelIG3 assay and the XylX6 assay kits (Megazyme Ltd, Bray, IE), following the protocols indicated by the manufacturer. Data shown represent the average of four independent experiments.

### 3. Results

#### 3.1. SwrA and motility in wild strains

Our previous work in *degSU*<sup>Hy</sup> domestic strain in which a functional *swrA* allele (*swrA*<sup>+</sup>) was reintroduced, showed that SwrA acts by subverting the impact of DegU-P on the *fla*/*che* promoter, transforming its action into a positive boost on flagellar gene expression. The functional interaction between SwrA-DegU-P only occurs with the wt phosphorylated form of the response regulator, while the DegU32<sup>Hy</sup> mutant protein does not effectively interface with SwrA at this promoter [20].

To verify this behaviour also in naturally *swrA*<sup>+</sup> wild strains, the *degU32*<sup>Hy</sup> or *degS200*<sup>Hy</sup> mutations were separately introduced in the transformable *comF*<sup>Q12L</sup> mutant of the undomesticated NCIB3610 *B. subtilis* strain [28]. The insertion of the DegU32<sup>Hy</sup> mutation caused a complete loss of motility, as previously shown by Stanley–Wall and collaborators [25]. Conversely, the *degS200*<sup>Hy</sup> derivative of the undomesticated strain proficiently swam and swarmed (Fig. S1), paralleling the results obtained in the domestic strain. The only difference with respect to the motility observed in domestic strains was the presence of a well-defined “lump” of γ-PGA that could be observed in the central part of the *degS200*<sup>Hy</sup> plates (Fig. S1). This characteristic is due to the abundant production of the polymer by the *degS200*<sup>Hy</sup> mutants, which is possibly linked to the presence of *degQ*<sup>Hy</sup> allele in wild strains. The γ-PGA lump was, however, not appreciable in the *degU32*<sup>Hy</sup> mutant strain. Interestingly, γ-PGA production was never visible in *degSU*<sup>+</sup>

undomesticated strains, although they naturally contain the *degQ*<sup>Hy</sup> allele.

We concluded that the powerful overturn of the DegU–P action on motility genes is a general phenomenon occurring not only in *swrA*<sup>+</sup>-revertant laboratory strains, but also in wild, undomesticated strains, even when the phosphorylation of DegU is maximal. Furthermore, also in wild strains, the positive effect of SwrA on motility cannot be appreciated if the *degU32*<sup>Hy</sup> allele is used.

#### 3.2. SwrA and competence for DNA uptake

The voluminous literature reporting the negative effect of Hy mutations on competence [2,6–8] refer to domestic *B. subtilis* strains which do not produce the SwrA protein. To establish whether SwrA has a general role as regulatory factor for DegSU activity in competence, genetic transformation was analysed in isogenic laboratory strains differing for the status of the *swrA* allele as well as for the source of DegU–P: either the intact phospho-protein obtained in the presence of *degS200*<sup>Hy</sup> or the mutant DegU32<sup>Hy</sup> protein.

Transformation efficiency was assessed in PB5370 and PB5249, respectively the *swrA*<sup>+</sup> and *swrA*<sup>−</sup> versions of the commonly used JH642 domestic strain [34], which do not contain any selectable marker. The introduction of a functional *swrA* allele in the domestic strain did not significantly increase the transformation efficiency compared to the *swrA*<sup>−</sup> strain, which was taken as reference for determining the efficiency of the other strains (Fig. 1). Both strains were transformed with the Hy mutation in either *degU* or *degS* and the resulting Hy mutants were transformed with a selectable genomic DNA. As shown in Fig. 1, consistent with the literature, in *swrA*<sup>−</sup> strains transformation efficiency was abolished by both *degU*<sup>Hy</sup> and *degS*<sup>Hy</sup> mutations (efficiency 1% and 4%, respectively). In the *degU*<sup>Hy</sup> strain competence did not substantially improve even in the presence of a functional *swrA* allele, i.e., the *swrA*<sup>+</sup>*degU32*<sup>Hy</sup> strain remained non-transformable (1% efficiency). However, the presence of SwrA in the *degS*<sup>Hy</sup> strain was sufficient to restore competence to 51% efficiency (Fig. 1).

Taken together, these data indicate that if SwrA is functional, competence is reduced but no longer abolished by phosphorylation of DegU. Thus, SwrA is able to modulate the activity of DegU–P on the competence pathway, partially suppressing its negative effect. This positive action is only possible in the presence of a *degS*<sup>Hy</sup> mutation, i.e., in the presence of a phosphorylated wt DegU protein.

#### 3.3. SwrA and subtilisin expression

The restoration of competence in a *degS*<sup>Hy</sup> strain prompted us to extend our investigation to *aprE* expression, which is known to be induced by the presence of a Hy mutation in either *degS* or *degU* [35]. To verify whether SwrA has a role also in subtilisin production, the P<sub>aprE</sub>-GFP reporter, developed by Veening et al. [29], was inserted in *swrA*<sup>+</sup> and Δ*swrA* laboratory strains. Analyses were carried out by imaging flow cytometry, which not only permits the quantification of average single cell fluorescence, but also to dissect the *aprE*-ON and -OFF populations due to heterogeneity in *aprE* expression [29]. The *degU32*<sup>Hy</sup> and *degS200*<sup>Hy</sup> alleles were separately introduced in each strain, as the expression of the reporter was not detected in their absence (data not shown). The analyses of the P<sub>aprE</sub>-GFP *degS*<sup>Hy</sup> or *degU*<sup>Hy</sup> in both *swrA*<sup>+</sup> and Δ*swrA* strains were focused on the transition phase (T<sub>0</sub>), and 5 and 15 h later (T<sub>5</sub> and T<sub>15</sub>). As shown in Fig. 2A, in DegU<sup>Hy</sup> strains, the percentage of *aprE*-ON cells did not substantially vary in the presence or absence of SwrA both at T<sub>0</sub> and at later time points. Conversely, in DegS<sup>Hy</sup> strains the percentage of *aprE*-ON cells was highly affected by the status of the *swrA* allele (Fig. 2B). The presence of SwrA led to a



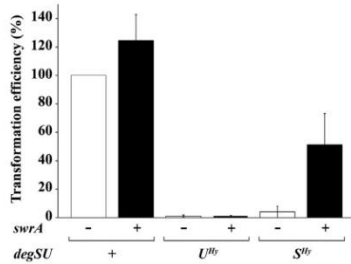


**Fig. 1. Transformation efficiency.** Competence was evaluated in strains differing for the status of the *degSU* and *swrA* alleles, which are indicated on the x-axis [PB5370 (*swrA<sup>+</sup> degSU<sup>-</sup>*), PB5249 (*swrA<sup>-</sup> degSU<sup>-</sup>*), PB5384 (*swrA<sup>-</sup> degSU<sup>hy</sup>*), PB5383 (*swrA<sup>+</sup> degSU<sup>hy</sup>*), PB5391 (*swrA<sup>-</sup> degS<sup>hy</sup>*) and PB5390 (*swrA<sup>+</sup> degS<sup>hy</sup>*)] (Table 1), by counting resistant colonies obtained by transformation with selectable genomic DNA. 100% efficiency was assumed for the *swrA<sup>+</sup>* strain (PB5370). Each experiment is the average of at least three independent replicates; error bars represent the standard error of the mean.

substantial decrease in the number of ON cells, particularly at T<sub>0</sub> (~70%). Remarkably, the percentage of ON cells was similar between *degU32<sup>hy</sup>* or *degS200<sup>hy</sup>* mutants in  $\Delta$ *swrA* strains.

Similarly, the level of activation of the P<sub>aprE</sub> promoter, i.e., the single cell fluorescence intensity, did not vary in the presence or absence of SwrA in *DegU<sup>hy</sup>* strains (Fig. 2C); however, in *DegS<sup>hy</sup>* mutants the presence of SwrA considerably decreased fluorescence

intensity (Fig. 2D). Also in this case, there are no appreciable differences in GFP levels among the two Hy strains in the  $\Delta$ *swrA* backgrounds. Representative images of *aprE* ON and OFF cells acquired during flow cytometry are provided in Fig. S2.

These data allowed to conclude that SwrA modulates the activity of DegU-P also at the *aprE* promoter. In fact, SwrA decreases the effectiveness of DegU-P on subtilisin expression, by reducing both the proportion of *aprE*-ON cells and the level of expression attained in the *aprE*-ON subpopulation. Analogously to what was observed for competence, the SwrA-mediated effect only occurs in a *degS<sup>hy</sup>* background, i.e., in the presence of a wt phosphorylated DegU protein.

#### 3.4. SwrA in cellulases and xylanases production

Besides subtilisin, cellulases and xylanases are additional degradative enzymes secreted by *B. subtilis*, which likely play a significant role in the physiology of this soil bacterium [36]. Transcriptome analyses revealed that several plant-wall degrading enzymes belong to the DegU regulon [3–5]. In those analyses, *bglC* and *bglS* glucosidases genes as well as *xynA*, *xynC* and *xynD* xylanase genes were identified as DegU up-regulated targets in both laboratory and undomesticated strains. To verify whether SwrA had an impact on the production of these types of enzymes, supernatants were collected after the exponential phase of growth from isogenic strains differing for the status of the *degSU* and *swrA* genes (Fig. S3). On these samples, highly specific assays for the enzymatic activities predicted for *bglC*, encoding an endo-1,4- $\beta$ -glucanase (EC 3.2.1.4), and *xynA*, encoding an endo-1,4- $\beta$ -xylanase (EC 3.2.1.8) were performed. As shown in Fig. 3A, endo-1,4- $\beta$ -glucanase activity

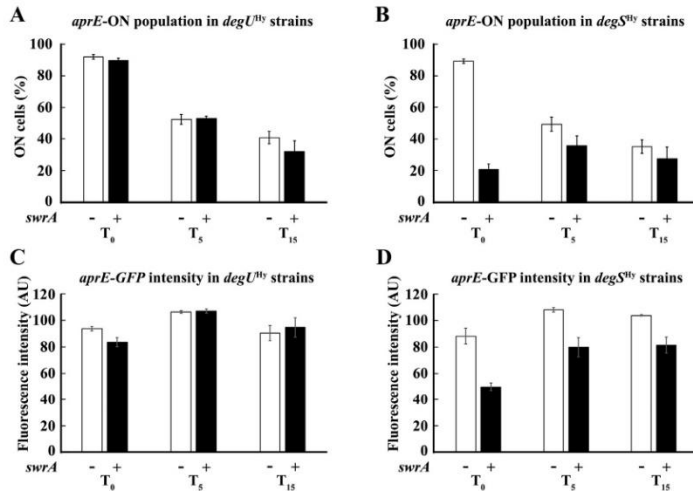


**Fig. 2. Expression of P<sub>aprE</sub>-GFP.** Strains PB5722 ( $\Delta$ *swrA* *degU<sup>hy</sup>*), PB5720 (*swrA<sup>+</sup> degU<sup>hy</sup>*) (in panels A and C), PB5725 ( $\Delta$ *swrA* *degS<sup>hy</sup>*) and PB5723 (*swrA<sup>+</sup> degS<sup>hy</sup>*) (in panels B and D), carrying an *aprE*-GFP reporter construct, were analysed by imaging flow cytometry to evaluate the percentage of GFP-ON/OFF cells and the peak of fluorescence intensity. Cultures were sampled at the transition point (T<sub>0</sub>), 5 and 15 h later (T<sub>5</sub> and T<sub>15</sub>), as indicated below each graph. A and C: *degU<sup>hy</sup>* strains; B and D: *degS<sup>hy</sup>* strains. The presence or absence of a functional *swrA* gene is indicated below each bar with a + and - symbol, respectively. Empty bars:  $\Delta$ *swrA* strains; black bars: *swrA<sup>+</sup>* strains. A and B: percentage of cells expressing the reporter gene (ON-population). C and D: fluorescence intensity peak of the ON-population. Values represent the average of at least three independent replicates; error bars represent the standard error of the mean.

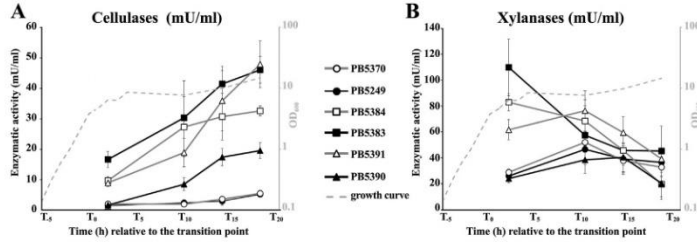


**Fig. 3.** Cellulases and xylanases enzymatic activities. Cellulase (A) and xylanase (B) enzymatic activities were recorded in strains differing for the status of the *swrA* and *degSU* alleles. Empty and full circles: PB5370 (*swrA*<sup>+</sup>*degSU*<sup>-</sup>) and PB5249 (*swrA*<sup>+</sup>*degSU*<sup>-</sup>), respectively. Empty and full squares: PB5384 (*swrA*<sup>+</sup>*degU*<sup>Hy</sup>) and PB5383 (*swrA*<sup>+</sup>*degU*<sup>Hy</sup>), respectively. Empty and full triangles: PB5391 (*swrA*<sup>+</sup>*degS*<sup>Hy</sup>) and PB5390 (*swrA*<sup>+</sup>*degS*<sup>Hy</sup>), respectively. Cells were grown in a chemically defined medium and assayed after the transition point ( $T_0$ ), at the time points indicated on the x-axis. The dashed line represents a typical growth curve in this medium (Fig. S3) and its ordinate axis (in logarithmic scale) is provided on the right side of each graph, in light grey. Enzymatic activity (in mU/ml) are reported on the left y-axis. Values represent the average of at least 3 independent experiments. Error bars represent the standard error of the mean.

was steadily induced by both *degU*<sup>Hy</sup> and *degS*<sup>Hy</sup> mutations. However, *SwrA* differently contributed to its regulation; it had a mild positive effect in the *degU*<sup>Hy</sup> mutant strain, while it considerably reduced cellulases accumulation in the *degS*<sup>Hy</sup> background.

Xylanase activity in the Hy mutants peaked in the early-middle stationary phase and gradually decreased over time (Fig. 3B). The effect of *SwrA* in the *degU*<sup>Hy</sup> strain was to further enhance xylanase production, albeit to a limited extent. Conversely, in the *degS*<sup>Hy</sup> background, *SwrA* completely abolished the positive effect of the Hy mutation, leading to a level of xylanase activity similar to that recorded in *degSU*<sup>+</sup> backgrounds. Interestingly, in the absence of Hy mutations, the level of both enzymatic activities did not differ in *SwrA*<sup>-/-</sup> strains.

These data demonstrated that *SwrA* significantly reduces the effectiveness of DegU-P on the production of both enzymes, with a greater impact on the level of xylanases. The effect of DegSU appears not to be linked to a general variation in protein secretion, nor is a global effect on protein expression, as the two enzymatic activities herein tested show opposite accumulation trends over time [Fig. 3].

Unlike our previous observations, *SwrA* mildly enhanced cellulases activity also in the presence of the *degU*<sup>Hy</sup> mutation. This

suggests that, at least in some cases, *SwrA* can also interact with the DegU32<sup>Hy</sup> mutant protein as observed at the *pgs* promoter.

### 3.5. Differences among *degS*<sup>Hy</sup> and *degU*<sup>Hy</sup> mutants in *pgs* expression

The activation of the *pgs* operon expression is known to depend on the co-presence of either one of the *degSU*<sup>Hy</sup> alleles and *SwrA*, implying that both alleles do functionally interact with *SwrA* at this promoter. However, to date, most of the data have been collected using *degU*<sup>Hy</sup> mutants; scant information is given on  $\gamma$ -PGA production in *degS*<sup>Hy</sup> strains [23] and differences among the two Hy alleles have never been analysed. To fill this gap, a *P*<sub>pgs</sub>-sfGFP reporter construct, based on a pMutin vector, was devised and inserted *in locus* in the *swrA*<sup>+</sup> laboratory strain. Since no fluorescence could be detected in these conditions (data not shown), the strain was further transformed with either *degS*<sup>Hy</sup> or *degU*<sup>Hy</sup> alleles. The Hy strains were grown under vigorous shaking in a glutamate-rich medium that supports  $\gamma$ -PGA production [33], with periodic sampling over a 48-h prolonged incubation. At relevant time-points, *P*<sub>pgs</sub> expression was quantified by imaging flow cytometry. In the *degU*<sup>Hy</sup> mutant, *P*<sub>pgs</sub> appeared to be

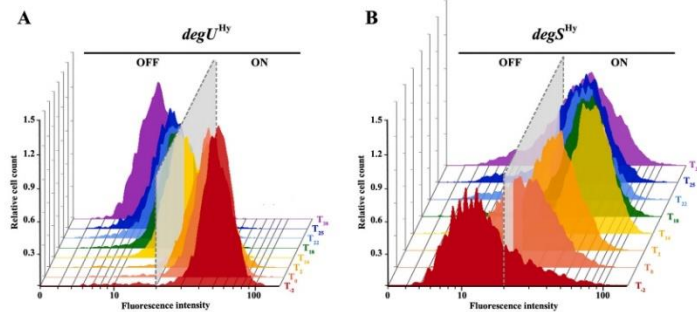


**Fig. 4.** Expression profile of *P*<sub>pgs</sub>-GFP. Strains PB5743 (*swrA*<sup>+</sup>*degU*<sup>Hy</sup>) (A) and PB5745 (*swrA*<sup>+</sup>*degS*<sup>Hy</sup>) (B), carrying a *pgsB*-GFP reporter construct, grown in E-medium, were analysed by imaging flow cytometry at different time points. The colour of the plots refers to the collection time (in h relative to the transition point  $T_0$ ) as specified on the right of each graph. A dashed line marks the ON threshold. The intensity values, represented in logarithmic scale on the x-axis, refer to the median pixel intensity of each single event.

homogeneously active from the beginning of the analysis (2 h post inoculum, data not shown), with intensity reaching a peak at T<sub>-2</sub> (8 h post inoculum) (Fig. 4A). This early peak of maximal intensity was followed by a monomodal decline over the next 40 h, with the majority of the population already OFF after T<sub>14</sub>. Conversely, in the DegS<sup>Hy</sup> strain, P<sub>pgs</sub> activation showed a 2-h delay: cells started displaying fluorescence at T<sub>0</sub> (10-h post inoculum), with a gradual increase over time (Fig. 4B). Intensity reached a peak at T<sub>14</sub> followed

by a slow decline of the GFP signal, which however remained appreciable, in most of the population, up to the end of the experiment (T<sub>38</sub>).

From these data it emerged that the impact of SwrA on *pgs* transcription is dramatic for both Hy mutants: no transcription is observed in *swrA* backgrounds ([21–23] and data not shown). However, there is a remarkable difference in the expression profile: upon interaction with SwrA, the constitutively active mutant

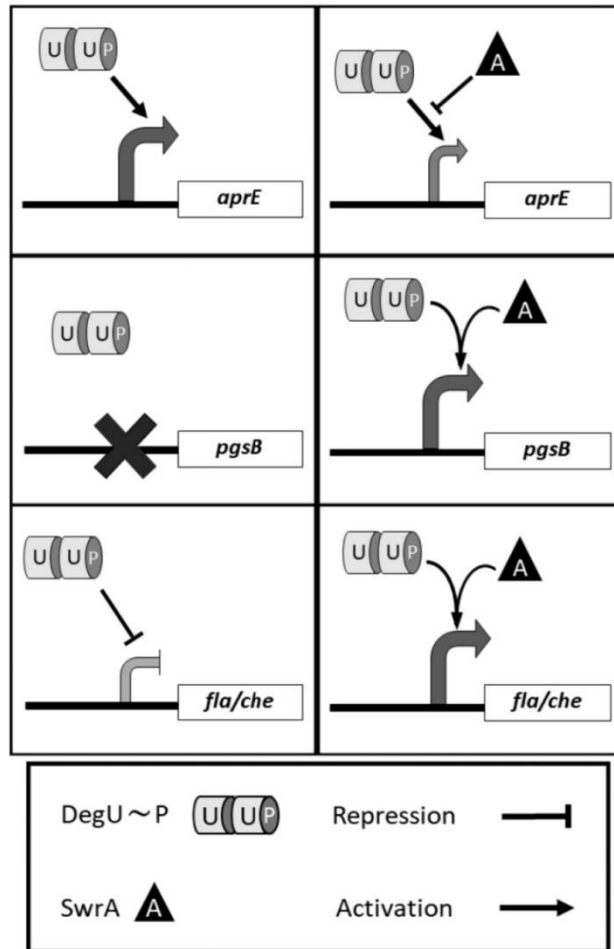


Fig. 5. SwrA effects on DegSU regulated promoters. The schematic representation summarises the global effects exerted by DegU~P with (right panels) and without (left panels) SwrA on *aprE*, *pgs* and *fla/che* transcription. The size of the curved arrows in front of each gene is indicative of the efficiency of transcription. Symbols are described in the box at the bottom.

**Table 2**  
DegSU-induced phenotypes in the presence or absence of SwrA.

Phenotype observed	Genetic background			Reference
	<i>degSU</i> <sup>+</sup> <i>swrA</i> <sup>-</sup>	<i>degS</i> <sup>Hy</sup> <i>swrA</i> <sup>-</sup>	<i>degS</i> <sup>Hy</sup> <i>swrA</i> <sup>+</sup>	
Swarming	Non-swarmer	Non-swarmer	Swarmer	Fig. S1/Ref. [20]
Subtilisin production	Non-producer	Hyperproducer <sup>b</sup>	Producer <sup>b</sup>	Fig. 2
γ-PGA production	Non-producer	Non-producer	Hyperproducer	Fig. 4
Competence	Competent	Non-competent	Competent (51% efficiency)	Fig. 1
Cellulase production	Low-producer	Hyperproducer <sup>c</sup> (10 X)	Producer <sup>c</sup> (-4 X)	Fig. 3
Xylanase production	Low-producer	Hyperproducer <sup>c</sup> (230 X)	Low-producer <sup>c</sup> (-0.8 X)	Fig. 3

<sup>a</sup> Basal phenotype of a *swrA*<sup>-</sup> laboratory strain, in the absence of Hy mutations. The phenotype of this strain is used as a standard against which the other two genetic backgrounds are compared.

<sup>b</sup> In *swrA*<sup>-</sup> background, 89.2 ± 1.4% of the cells expressed GFP at high level (fluorescence 88.3 ± 6.0 arbitrary units); in *swrA*<sup>+</sup> background, 20.6 ± 3.5% of the cells expressed GFP at low level (fluorescence 50.0 ± 2.9 arbitrary units).

<sup>c</sup> Fold-activation at the production peak, with respect to the production observed in the non-Hy strain.

protein DegU32<sup>Hy</sup> immediately exerts its positive pressure on the *pgs* promoter, but the effect is rapidly quenched. In the *degS*<sup>Hy</sup> strain, a delay in *pgs* activation is observed, most likely due to the requirement of the physiological trigger of the signalling pathway. However, once activated, the SwrA-DegU-P stimulus on *P*<sub>pgs</sub> is sustained up to 24 h (T<sub>14</sub>). These data are in line with our experimental evidence that DegS<sup>Hy</sup> strains produce a much higher amount of γ-PGA (data not shown) and indicate that, although an interaction between SwrA and DegU<sup>Hy</sup> occurs, the effect on *P*<sub>pgs</sub> transcription is considerably different from that obtained when SwrA interacts with the wt DegU-P protein.

#### 4. Discussion

This work extends the array of DegSU regulated phenotypes in which SwrA plays a pivotal role. Considering the targets thus far analysed, SwrA emerges as key modulator of DegSU on all the promoters tested so far, *P*<sub>aprE</sub>, *P*<sub>pgs</sub> (Figs. 2 and 4) and *P*<sub>Pla</sub>, [20] (Fig. 5), as well as on genetic competence (Fig. 1), and on plant-wall degrading enzymes production (Fig. 3). These results have been summarized in Table 2.

As for competence, the results obtained in *swrA*<sup>-</sup> backgrounds validate literature data collected in domestic *B. subtilis* strains (168, JH642, and others) [2,6–8], confirming the non-transformability of *degU*<sup>Hy</sup> and *degS*<sup>Hy</sup> strains. The novelty of this work concerns the restoration of competence in the presence of the *degS200*<sup>Hy</sup> mutation in the *swrA*<sup>-</sup> background (Fig. 1). Actually, our results might shed some light on a puzzling result obtained in the past. In 1991, Hahn and Dubnau, analysing the impact of *degU32*<sup>Hy</sup> and *degS200*<sup>Hy</sup> alleles on *P*<sub>stfA</sub> expression, could not interpret the fact that, differently from DegU<sup>Hy</sup>, DegS<sup>Hy</sup> did not repress *P*<sub>stfA</sub> transcription, the promoter from which *comS* is transcribed [37]. It is tempting to imagine that a high percentage of *swrA*<sup>+</sup> revertant cells arose in the DegS<sup>Hy</sup> strain used in the experiment, due to the high frequency of phase variation events (10<sup>-4</sup>) [14], and that in those revertants SwrA was able to mitigate –or suppress– the negative effect of DegU-P.

Presently, the main target of DegU-P in competence has not been clearly identified, due to the coexistence of at least two possible target promoters: *P*<sub>comK</sub> [8,26,27] and *P*<sub>stfA</sub>, from which *comS* is transcribed [37]. A negative effect of the *degQ*<sup>Hy</sup> allele has been evidenced on both promoters in domestic and undomesticated strains (*swrA*<sup>-</sup> and *swrA*<sup>+</sup>, respectively) [27]. Since the *degQ*<sup>Hy</sup> mutation increases DegU-P levels [5] without impacting the DegU structure, the interaction of DegU-P with SwrA is preserved. The

way in which the effects of SwrA and DegQ are balanced needs to be further analysed in well-defined genetic backgrounds.

A second fundamental result that emerges from this work is that the DegU32<sup>Hy</sup> mutant protein does not behave as the phosphorylated wt DegU protein. A bona fide proxy for DegU-P is rather represented by the *degS200*<sup>Hy</sup> mutation, which produces high levels of DegU-P without directly modifying the structure of the transcriptional activator DegU.

From *P*<sub>pgs</sub> analyses it can be hypothesized that DegU32<sup>Hy</sup> is able to bind directly to DNA, even before activation of the signalling pathway that would lead to its phosphorylation, i.e., in the non-phosphorylated form (see Fig. 4A). This notion is not novel: Stanely-Wall and collaborators showed that γ-PGA production in a *degU32*<sup>Hy</sup> background also occurs in a *degS* null mutant [38]. *In vitro*, Mordini et al. (2013) showed that DegU32<sup>Hy</sup> binds to DNA independently of the presence of its cognate kinase [20]. Moreover, the interaction of SwrA (physical and/or genetical) with the mutant DegU32<sup>Hy</sup> protein is compromised. Either it does not occur at all, or it markedly differs from the interaction with DegU-P naturally induced by *degS200*<sup>Hy</sup>. The lack of interaction is observed in competence (Fig. 1), *aprE* expression (Fig. 2), xylanase production (Fig. 3B) and motility (Fig. S1), while a non-physiological interaction is observed in γ-PGA (Fig. 4) and cellulases productions (Fig. 3A).

Our data demonstrate that the physiological role of DegU-P in *B. subtilis* should be approached using a DegS200<sup>Hy</sup> mutant. This also suggests that our current view of the impact of the DegSU TCS on *B. subtilis* physiology, mainly gained through the use of *degU32*<sup>Hy</sup> mutants and in *swrA*<sup>-</sup> strains, might need to be reconsidered, like in the case of motility.

The possibility of modulating the presence of SwrA through a phase variation mechanism [14] thus represents an additional strategy, besides bistable switches [39], through which natural populations of *B. subtilis* cells can diversify their metabolism to better cope with rapidly changing and challenging environments.

#### Declaration of competing interest

Authors declare that this work was conducted in the absence of any commercial or financial relationship that could constitute a potential conflict of interest.

#### Acknowledgements

This research was supported by the Italian Ministry of Education, University and Research (MIUR): Dipartimenti di Eccellenza



Program (2018–2022) - Dept. of Biology and Biotechnology "L. Spallanzani", University of Pavia and by Fondazione Cariplo, Bando Economia Circolare: ricerca per un futuro sostenibile; grant # 2018-1011. Authors are grateful to Prof. J. W. Veening for generously providing the  $P_{\text{PapE}}$  plasmid, and to A. Liguori and L. Gomulski for critically reading the manuscript. The contribution of Erlinda Rama, Matteo Cavaletti, Jessica Bollini, Laura Nucci is acknowledged. We also thank A. Azzalin, from the departmental imaging facility, and A. Serra, from Luminex Corporation, for support with the Amnis ImageStream data acquisition and analyses.

#### Appendix A. Supplementary data

Supplementary data to this article can be found online at <https://doi.org/10.1016/j.resmic.2021.103877>.

#### References

- Mitrophanov AY, Groisman EA. Signal integration in bacterial two-component regulatory systems. *Genes Dev* 2008;22:2601–11.
- Msadek T, Kunst F, Henner D, Klier A, Rapoport G, Dedonder R. Signal transduction pathway controlling synthesis of a class of degradative enzymes in *Bacillus subtilis*: expression of the regulatory genes and analysis of mutations in *degS* and *degJ*. *J Bacteriol* 1990;172:824–34.
- Ogura M, Yamaguchi H, Yoshida Ki, Fujita Y, Tanaka T. DNA microarray analysis of *Bacillus subtilis* DegU, ComA and PhoP regulons: an approach to comprehensive analysis of *B. subtilis* two-component regulatory systems. *Nucleic Acids Res* 2001;29:3804–13.
- Mäder U, Antelmann H, Buder T, Dahl M, Hecker M, Homuth G. *Bacillus subtilis* functional genomics: genome-wide analysis of the DegS-DegU regulon by transcriptomics and proteomics. *Mol Genet Genom* 2002;268:455–67.
- Kobayashi K. Gradual activation of the response regulator DegU controls serial expression of genes for flagellum formation and biofilm formation in *Bacillus subtilis*. *Mol Microbiol* 2007;66:395–409.
- Kunst F, Pascal M, Lepesant-Kejzarova J, Lepesant J, Billault A, Dedonder R. Pleiotropic mutations affecting sporulation conditions and the syntheses of extracellular enzymes in *Bacillus subtilis* 168. *Biochimie* 1974;56:1481–9.
- Dahl M, Msadek T, Kunst F, Rapoport G. The phosphorylation state of the DegU response regulator acts as a molecular switch allowing either degradative enzyme synthesis or expression of genetic competence in *Bacillus subtilis*. *J Biol Chem* 1992;267:14509–14.
- Van Sinderen D, Venema G. ComK acts as an autoregulatory control switch in the signal transduction route to competence in *Bacillus subtilis*. *J Bacteriol* 1994;176:5762–70.
- Amati G, Bisicchia P, Galizzi A. DegU-J represses expression of the motility *flaC* operon in *Bacillus subtilis*. *J Bacteriol* 2004;186:6003–14.
- Yang M, Ferrari E, Chen E, Henner D. Identification of the pleiotropic *sacQ* gene of *Bacillus subtilis*. *J Bacteriol* 1986;166:113–9.
- Henner DJ, Yang M, Ferrari E. Localization of *Bacillus subtilis* *sacU*(Hy) mutations to two linked genes with similarities to the conserved prokaryotic family of two-component signalling systems. *J Bacteriol* 1988;170:5102–9.
- Tanaka T, Kawata M, Mukai K. Altered phosphorylation of *Bacillus subtilis* DegU caused by single amino acid changes in DegS. *J Bacteriol* 1991;173:5507–15.
- McLoon AL, Guttenplan SB, Kearns DB, Kolter R, Losick R. Tracing the domestication of a biofilm-forming bacterium. *J Bacteriol* 2011;193:2027–34.
- Kearns DB, Chu F, Rudner R, Losick R. Genes governing swarming in *Bacillus subtilis* and evidence for a phase variation mechanism controlling surface motility. *Mol Microbiol* 2004;52:357–69.
- Calvio C, Celandroni F, Ghelardi E, Amati G, Salvetti S, Cecilian F, et al. Swarming differentiation and swimming motility in *Bacillus subtilis* are controlled by *swrA*, a newly identified dicistronic operon. *J Bacteriol* 2005;187:5356–66.
- Zeitler DR, Prágai Z, Rodriguez S, Chevreux B, Muffler A, Albert T, et al. The origins of 168, W23, and other *Bacillus subtilis* legacy strains. *J Bacteriol* 2008;190:6983–95.
- Kearns DB, Losick R. Cell population heterogeneity during growth of *Bacillus subtilis*. *Genes Dev* 2005;19:3083–94.
- Calvio C, Osera C, Amati G, Galizzi A. Autoregulation of *swrA* and motility in *Bacillus subtilis*. *J Bacteriol* 2008;190:5720–8.
- Chen R, Guttenplan SB, Blair KM, Kearns DB. Role of the  $\sigma^D$ -dependent autolysis in *Bacillus subtilis* population heterogeneity. *J Bacteriol* 2009;191:5775–84.
- Mordini S, Osera C, Marini S, Scavone F, Bellazzi R, Galizzi A, et al. The role of *SwrA*, *DegU* and *P(D3)* in *flaC* expression in *B. subtilis*. *PLoS One* 2013;8:e85065.
- Urushibata Y, Tokuyama S, Tahara Y. Difference in transcription levels of cap genes for gamma-polyglutamic acid production between *Bacillus subtilis* IFO 16449 and Marburg 168. *J Biosci Bioeng* 2002;93:252–4.
- Stanley N, Lazazzera B. Defining the genetic differences between wild and domestic strains of *Bacillus subtilis* that affect poly-gamma-dl-glutamic acid production and biofilm formation. *Mol Microbiol* 2005;57:1143–58.
- Osera C, Amati G, Calvio C, Galizzi A. *SwrA* activates poly-gamma-glutamate synthesis in addition to swarming in *Bacillus subtilis*. *Microbiol-Sgm* 2009;155:2282–7.
- Ogura M, Tsukahara K. *SwrA* regulates assembly of *Bacillus subtilis* DegU via its interaction with N-terminal domain of DegU. *J Biochem* 2012;151:643–55.
- Verhamme D, Kiley T, Stanley-Wall N. DegU co-ordinates multicellular behaviour exhibited by *Bacillus subtilis*. *Mol Microbiol* 2007;65:554–68.
- Hamoen LW, Van Werkhoven AF, Venema G, Dubnau D. The pleiotropic response regulator DegU functions as a priming protein in competence development in *Bacillus subtilis*. *Proc Natl Acad Sci U S A* 2000;97:9246–51.
- Miras M, Dubnau D. A DegU-P and DegQ-dependent regulatory pathway for the K-state in *Bacillus subtilis*. *Front Microbiol* 2016;7.
- Konkol MA, Blair KM, Kearns DB. Plasmid-encoded ComI inhibits competence in the ancestral 3610 strain of *Bacillus subtilis*. *J Bacteriol* 2013;195:4085–93.
- Veening J, Igoshin O, Eijlander R, Nijland R, Hamoen L, Kuipers O. Transient heterogeneity in extracellular protease production by *Bacillus subtilis*. *Mol Syst Biol* 2008;4:184.
- Guizani S, Sauveplane V, Chang HJ, Clerc C, Declerck N, Jules M, et al. A part toolbox to tune genetic expression in *Bacillus subtilis*. *Nucleic Acids Res* 2016;44:7495–508.
- Perego M. Integrational vectors for genetic manipulation in *Bacillus subtilis*. In: Sonenshein A, Hoch JA, Losick R, editors. *Bacillus subtilis* and other gram-positive bacteria. Washington, D.C: ASM Press; 1993. p. 615–24.
- Harwood CR, Cutting SM. Molecular biological methods for *Bacillus*. Chichester: John Wiley and Sons; 1990.
- Scoffone V, Dondi D, Biino G, Borghese G, Pasini D, Galizzi A, et al. Knockout of *pgdS* and *ggt* genes improves gamma-PGA yield in *B. subtilis*. *Biotechnol Bioeng* 2013;110:2006–12.
- Srivatsan A, Han Y, Peng J, Tehrani AK, Gibbs R, Wang JD, et al. High-precision, whole-genome sequencing of laboratory strains facilitates genetic studies. *PLoS Genet* 2008;4:e1000139.
- Henner DJ, Ferrari E, Perego M, Hoch JA. Location of the targets of the *hpr-97*, *sacU2*(Hy), and *sacQ36*(Hy) mutations in upstream regions of the *subtilisin* promoter. *J Bacteriol* 1988;170:296–300.
- Van Dijl JM, Hecker M. *Bacillus subtilis*: from soil bacterium to super-secreting cell factory. *Microb Cell Factories* 2013;12:3.
- Hahn J, Dubnau D. Growth stage signal transduction and the requirements for *srfA* induction in development of competence. *J Bacteriol* 1991;173:7275–82.
- Cairns LS, Marlow VL, Bissett E, Ostrowski A, Stanley-Wall NR. A mechanical signal transmitted by the flagellum controls signalling in *Bacillus subtilis*. *Mol Microbiol* 2013;90:6–21.
- Dubnau D, Losick R. Bistability in bacteria. *Mol Microbiol* 2006;61:564–72.

Article

## Bacterial-Assisted Extraction of Bioactive Compounds from Cauliflower

Enrico Doria <sup>1,\*</sup>, Daniela Buonocore <sup>1</sup>, Antonio Marra <sup>1</sup>, Valeria Bontà <sup>1</sup>, Andrea Gazzola <sup>2</sup>, Maurizia Dossena <sup>1</sup>, Manuela Verri <sup>1</sup> and Cinzia Calvio <sup>1</sup>

<sup>1</sup> Department of Biology and Biotechnology L. Spallanzani, University of Pavia, 27100 Pavia, Italy; daniela.buonocore@unipv.it (D.B.); antonio.marra03@universitadipavia.it (A.M.); valeria.bonta01@universitadipavia.it (V.B.); maurizia.dossena@unipv.it (M.D.); manuela.verri@unipv.it (M.V.); cinzia.calvio@unipv.it (C.C.)

<sup>2</sup> Department of Earth and Environmental Sciences, University of Pavia, 27100 Pavia, Italy; andrea.gazzola@unipv.it

\* Correspondence: enrico.doria@unipv.it

**Abstract:** The market for nutraceutical molecules is growing at an impressive pace in all Western countries. A convenient source of bioactive compounds is found in vegetable waste products, and their re-use for the recovery of healthy biomolecules would increase the sustainability of the food production system. However, safe, cheap, and sustainable technologies should be applied for the recovery of these beneficial molecules, avoiding the use of toxic organic solvents or expensive equipment. The soil bacterium *Bacillus subtilis* is naturally endowed with several enzymes targeting complex vegetable polymers. In this work, a raw bacterial culture supernatant was used to assist in the extraction of bioactives using isothermal pressurization cycles. Besides a wild-type *Bacillus subtilis* strain, a new strain showing increased secretion of cellulases and xylanases, pivotal enzymes for the digestion of the plant cell wall, was also used. Results indicate that the recovery of compounds correlates with the amount of cellulolytic enzymes applied, demonstrating that the pretreatment with non-purified culture broth effectively promotes the release of bioactives from the vegetable matrix. Therefore, this approach is a valid and sustainable procedure for the recovery of bioactive compounds from food waste.

**Keywords:** *Bacillus subtilis*; cellulases; xylanases; bioactives; extraction; nutraceuticals; phytochemicals; sustainability; vegetable by-products



**Citation:** Doria, E.; Buonocore, D.; Marra, A.; Bontà, V.; Gazzola, A.; Dossena, M.; Verri, M.; Calvio, C. Bacterial-Assisted Extraction of Bioactive Compounds from Cauliflower. *Plants* **2022**, *11*, 816. <https://doi.org/10.3390/plants11060816>

Academic Editors: Kwang-Hyun Baek and Petko Denev

Received: 11 February 2022  
Accepted: 17 March 2022  
Published: 18 March 2022

**Publisher's Note:** MDPI stays neutral with regard to jurisdictional claims in published maps and institutional affiliations.



**Copyright:** © 2022 by the authors. Licensee MDPI, Basel, Switzerland. This article is an open access article distributed under the terms and conditions of the Creative Commons Attribution (CC BY) license (<https://creativecommons.org/licenses/by/4.0/>).

### 1. Introduction

The agri-food sector generates massive amount of waste that not only causes the loss of market profit but, more importantly, represents a waste of precious environmental resources, such as land, water, fertilizers, chemicals, and energy expended in the production phase [1]. Moreover, organic waste might pose potentially severe pollution problems as it decomposes in landfills, releasing nitrogen and phosphorus in aquatic and terrestrial ecosystems and emitting harmful greenhouse gases [2].

In line with the circular economy concept, fruit and vegetable waste might be turned into a valuable resource as a natural and unlimited supply of biologically active compounds, including vitamins, polyphenols, dietary fibers, glucosinolates, essential oils, and organic acids, among the others, with an enormous economic potential as nutraceutical, pharmaceutical, cosmetic, and agro-pharmaceutical ingredients [3,4]. However, to maintain the green connotation, the recovery of natural bioactive compounds from discarded agro-food materials must rely on methods which (i) do not generate more polluting waste than the disposal of the raw biomass itself, (ii) are safe for the final product, and (iii) guarantee high revenues for the entire value chain [5].

Among the new emerging techniques, Enzyme Assisted Extraction (EAE) of biomolecules represents one of the most environmentally friendly and safe methodologies which can be used either as a stand-alone technique, or as a pretreatment that increases the efficiency of a coupled extraction system [6–8]. EAE is based on the fact that enzymes help to weaken or deconstruct the plant cell wall in which most bioactives are entrapped, making encased compounds more accessible for extraction. The most used enzymes for this purpose are hydrolytic enzymes such as cellulases, (endoglucanases, cellobiohydrolases,  $\beta$ -glucosidases), hemicellulases (endoxylanases and  $\beta$ -xylosidases), and pectinases (polygalacturonases, and pectinesterases). Other hydrolysing enzymes (proteases, amylases, pullulanases, pectate lyases, etc.) might further support the release of precious and low-abundant secondary metabolites from cellular components [6–8]. However, the use of expensive commercial enzymes would take a prohibitive toll on the entire process, mining the economic viability of the extraction [6,7].

One of the most formidable enzyme-producers is the Gram-positive soil bacterium *Bacillus subtilis*. *B. subtilis* is already heavily exploited for the industrial production of several biocommodities, such as degradative enzymes, heterologous proteins, bio insecticides, and antibiotics, and its products are considered as Generally Recognized as Safe (GRAS) [9–11]. Its reputation as an industrial pillar is due to its simple nutritional requirements, its excellent fermentation properties over a wide range of conditions, its genetic plasticity, enabling the optimization of its biotechnological performances, and its efficient secretory system, allowing for the recovery of massive amounts of bio-products directly from the growth medium [9–11].

*B. subtilis* lives predominantly in the soil, and this type of habitat has evolutionarily shaped its genome, leading to the accumulation of a large array of genes associated with the ability to degrade complex carbohydrates from decaying vegetable biomass. According to the Carbohydrate-Active Enzymes database [12], the bacterium is endowed with several genes encoding secreted enzymes involved in complex carbohydrates and lignocellulose degradation [13]. Moreover, it also encodes several proteases and many other hydrolytic enzymes [11,14]. Thanks to the above-mentioned characteristics, *B. subtilis* spent growth medium represents an inexpensive, rich, and wide-range collection of GRAS enzymatic activities, ideally suited to break down the plant matrix and improve the release of bioactives.

The aim of this work was to evaluate the efficacy of a method for the sustainable extraction of bioactive compounds from vegetable waste based on a low-cost EAE pretreatment. The economic viability of the procedure relied on the use of crude *B. subtilis* culture supernatants, obtained from a wild-type (WT) strain and from a new *B. subtilis* strain, overproducing cellulases and xylanases (OS58). The sustainability of the process was maintained by carrying out the extraction process in an aqueous environment, avoiding the use of any polluting solvent. The substrate, cauliflower (*Brassica oleracea* L. *conv. botrytis* (L.) Alef. *var. botrytis* L.), rich in phytochemicals endowed with a large range of beneficial biological activities, derived from the quota of raw products that did not meet the qualitative standards for commercialization and were discarded by an industrial agro-food processing plant.

## 2. Results

### 2.1. *Bacillus subtilis* Enzymes and Pretreatment

To evaluate the effectiveness of the low-cost enzymatic pretreatment, two *B. subtilis* strains were used. The WT strain corresponded to the commonly used lab strain JH642 [15] in which the tryptophan and phenylalanine auxotrophies were cured and prototrophy restored. The second strain, namely OS58, was obtained by improving the intrinsic cellulolytic and hemicellulolytic propensity of *B. subtilis* through genetic engineering of the WT strain. The cellulases and xylanases activities released in the growth medium by the two strains were determined after 24 h incubation. The optimization process led to a drastic enhancement in enzyme secretion. As shown in Figure 1, the enzymatic units found in OS58



culture broth increased by over 30-fold for cellulases and 3-fold for xylanases compared to those released by the WT strain. These enzymes are supposedly playing a pivotal role in vegetable matrix breakdown, although a plethora of additional enzymes, which *B. subtilis* is known to secrete, might contribute to the final effect on the substrate [16].

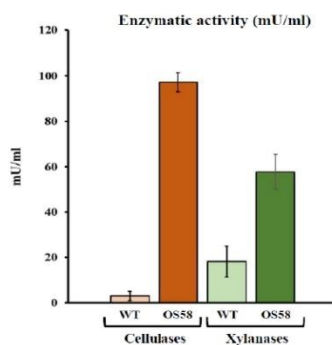


**Figure 1.** The enzymatic activity of cellulases (in orange) and xylanases (in green) in the WT and OS58 strains (as indicated on the x-axis). Cells were grown in a chemically defined medium for 24 h and assayed with a commercial kit. Enzymatic activity (in mU/mL of spent medium) is reported on the y-axis. Values represent the average of at least five independent experiments. Error bars represent the standard error of the mean (SEM).

## 2.2. Recovery of Phenolic Compounds

In order to verify whether the crude enzymatic mixture released by the bacterial strains represented an effective pretreatment for improving the extraction of bioactive compounds, cauliflowers discarded from the food supply chain were collected from an industrial processing plant during different seasonal periods. The biomass, originated from different regions across Italy, was treated according to a standardized protocol. The processing began with the grinding of thawed cauliflowers into 0.2–0.5 cm<sup>3</sup> pieces. The fragmented material was incubated at 50 °C with culture supernatants from either the WT strain, OS58, or the sterile growth medium, which was used as a negative control for the treatment. Subsequently, each mash was subjected to 60 cycles of pressurization at room temperature (20°–23 °C) for the extraction of bioactive compounds. Part of the liquid flow, collected from the apparatus after each extraction, was dried and resuspended in 50% methanol for the analyses of the nutraceutical compounds.

Important differences in the content of bioactives were observed among the four replicates, which were performed on different stocks of cauliflowers; such differences are presumably linked to seasonal effects and the geographical origins of the vegetable material. For this reason, the correlation among replicates was estimated by including the variable “replicate” as a random effect in the statistical model (see Materials and Methods).

The total polyphenols recovered under the three conditions demonstrated that the enzymatic treatment improved the extraction efficiency (Figure 2 and Table 1). In particular, the polyphenols recovered upon treatment with the WT strain increased by 1.3-fold with respect to the control ( $p < 0.1$ , weak significance); however, the recovery further increased (by 1.4-fold with respect to the control,  $p < 0.05$ ) when the treatment was performed with the optimized strain OS58, which is a better enzyme producer (Figure 2). The progressive increase in the recovery of polyphenols, observed by comparing the control, the WT, and the OS58 treatment, respectively (Table 1), suggests that the beneficial effect of the bacterial supernatants might be linked to the progressively higher amount of enzymes produced by the two strains.



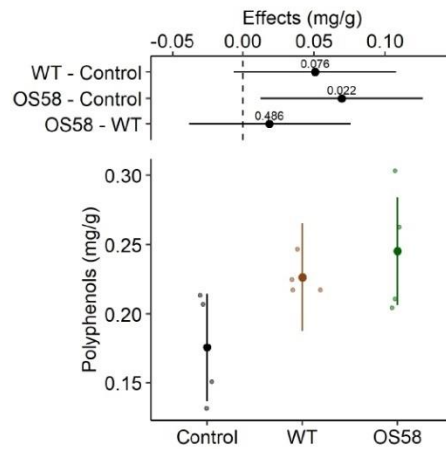


**Figure 2.** The total polyphenols content (calculated as mg per gram of fresh cauliflowers, before freezing) is reported for Control, WT, and OS58 groups as estimated means and 95% confidence intervals (larger dots and colored lines, respectively) by the linear mixed model (LMM). On the upper side of the plot, treatment effects are reported in mg/g as the estimated means and 95% confidence intervals for each comparison, as indicated on the left (degrees of freedom-df = 10.7). The level of significance (*p*-value) is reported above each horizontal line; the dashed line corresponds to the “no effect” hypothesis. The values reported were obtained from the model using the emmeans package (*n* = 4, for each group) [17].

**Table 1.** The concentration of secondary metabolite extracted (mg or µg per gram of fresh cauliflower) for each pretreatment group [control = sterile medium; WT = spent medium from the WT strain; OS58 = spent medium from the optimized strain].

	Control	WT	OS58
Polyphenols (mg/g)	0.176 ± 0.020	0.227 ± 0.007	0.245 ± 0.023 *
Epigallocatechin gallate (g/g)	1.094 ± 0.185	2.170 ± 0.829	3.071 ± 0.740 **
Epicatechin (g/g)	4.685 ± 0.778	8.670 ± 1.346 *	11.30 ± 2.769 **
Epicatechin gallate (g/g)	3.293 ± 0.573	4.411 ± 0.590 **	4.108 ± 0.469 *
Chlorogenic acid (g/g)	0.928 ± 0.658	1.880 ± 0.776 **	2.711 ± 0.871 **
Isothiocyanates (g/g)	0.004 ± 0.001	0.005 ± 0.001	0.006 ± 0.001

A descriptive analysis of the data—mean values ± standard error of the mean (SEM)—was conducted to describe the difference of the treated groups vs. control. The asterisks (\*) indicate the significant differences, obtained by the Linear Mixed Models (*p* < 0.05 \*; *p* < 0.01 \*\*; *p* < 0.001 \*\*\*).

### 2.2.1. Catechins

The analysis of polyphenols was further deepened for the group of catechins. The HPLC profile for these compounds was evaluated in the treatment and control groups, revealing a significant improvement in their recovery, even with the WT strain (Figure 3). With respect to the control, the WT enzymes allowed the extraction of 2-fold more epigallocatechin gallate, 1.8-fold more epicatechin, and 1.3-fold more epicatechin gallate (Table 1). As observed for polyphenols in general, in all but the last case, the effect of the bacterial pretreatment appeared stronger with the optimized OS58 strain, where the yield with respect to the control raised by 2.8-fold for epigallocatechin gallate and by 2.4-fold for epicatechin, reinforcing the hypothesized link between the effect on the extraction efficiency and the amount of secreted enzymes. Conversely, the recovery of epicatechin gallate upon

OS58 treatment (1.2-fold increase) was slightly lower than that obtained with the WT strain (1.3-fold higher than the control).

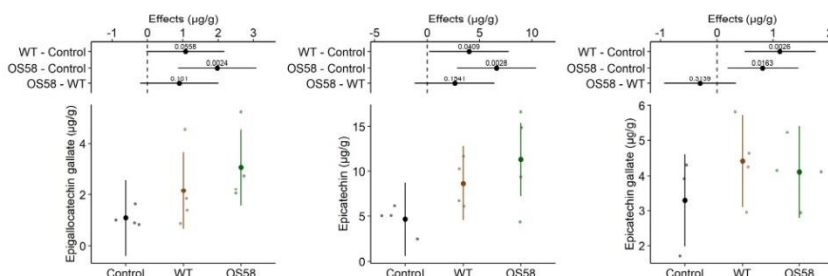


**Figure 3.** The catechins content (calculated as µg per gram of fresh cauliflowers) is reported for the Control, WT, and OS58 groups. A detailed description of these types of plots is provided in Figure 2.

### 2.2.2. Chlorogenic Acid

For the phenolic acids class of polyphenols, the recovery of chlorogenic acid was examined in detail in the three different extracts. As shown in Figure 4 and Table 1, the enzymatic treatment appeared to be extremely efficient in releasing the compound from the matrix. The enzymes produced by the WT strain were able to release 2-fold more chlorogenic acid than the control treatment, while following the treatment with the OS58 enzymatic pool, the recovery of chlorogenic acid was 2.9-fold higher with respect to the untreated control, validating the effectiveness of the enzymatic treatment. It is worth noticing that, for this compound, the difference between the OS58 strain and the WT achieved a 95% statistical significance ( $p = 0.019$ ), corroborating the hypothesis that the effect is indeed due to higher amount of enzymes released by the optimized strain.

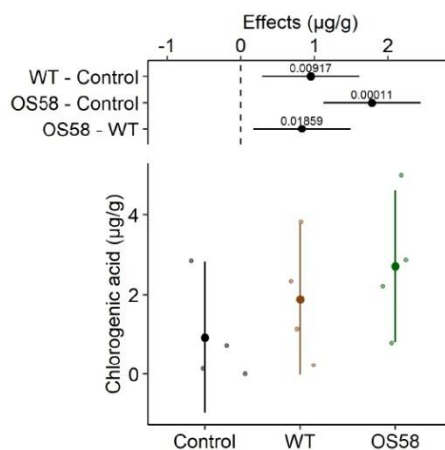


**Figure 4.** The chlorogenic acid content (calculated as µg per gram of fresh cauliflowers) is reported for the Control, WT, and OS58 groups. A detailed description of these types of plots is provided in Figure 2.

### 2.3. Recovery of Sulphur-Containing Plant Secondary Metabolites Isothiocyanates

For this class of compounds, the yields were below our expectations. Only within the OS58-treated group, a very modest increase in the recovery (1.3-fold) was observed (Figure 5 and Table 1), which, however, did not reach high statistical significance ( $p = 0.082$ ). The reasons for these results are discussed below.

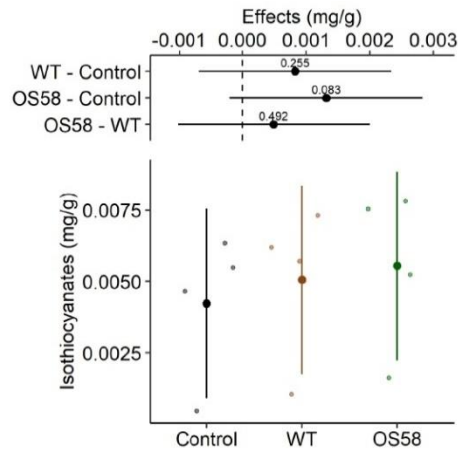


**Figure 5.** The isothiocyanates content (calculated as mg per gram of fresh cauliflowers) is reported for the Control, WT, and OS58 groups. A detailed description of these types of plots is provided in Figure 2.

### 3. Discussion and Conclusions

Enzymatic pretreatments have been shown to favorably impact the extraction of valuable compounds from different vegetable sources in a green and sustainable manner [6–8,18]. The extraction of lycopene from tomato waste resulted 3-fold higher in enzyme-treated matrices with respect to untreated controls [19], while the phenolic content released from grape waste increased by more than 25%, with respect to the control [20]. In this work, a new *Bacillus subtilis* strain (OS58), with optimized production of at least two enzymes relevant for EAE (cellulases and xylanases), was developed and applied as a pretreatment before cyclic pressurization extraction for the recovery of valuable secondary metabolites from cauliflower. The performance of OS58 was compared to that of a WT *B. subtilis* strain and a control containing the sterile bacterial growth medium.

The recovery of polyphenols, and in particular, of chlorogenic acid and catechins (epigallo catechin gallate, epicatechin, and epicatechin gallate), was enhanced by the pretreatment procedure using the enzymatic mixture derived from the WT strain, and in all cases but one, it further improved with the enzymatic mixture derived from the optimized OS58 strain, demonstrating that the efficiency of the extraction was proportional to the enzymatic activity applied (Table 1). It is worth recalling that no organic solvents were used, avoiding the generation of toxic or polluting waste and preserving the green character of the extraction. Concurrently, the choice of applying a raw culture supernatant of a cellulolytic bacterium such as *B. subtilis*, avoiding expensive commercial enzymes, is a cost-effective strategy that guarantees the economic viability of the process. Moreover, being a soil microorganism, *B. subtilis* grows efficiently over a wide range of conditions and media and can even be fed with agro-industrial waste [21]. *Bacillus subtilis* is ideally suited to industrial

applications for the above-mentioned characteristics, and because it secretes many different enzymes directly in the medium, simplifying their recovery [9,10,13,16]; it is also considered a Plant Growth-Promoting Bacterium (PGPB), shown to exert several beneficial effects both on plants and on soil quality [11,22]. For the above reasons, the entire process might be conceived as part of a complex biorefinery which includes: (i) agricultural production of vegetables and their processing before commercialization, (ii) recovery of natural bioactive compounds from vegetable waste, (iii) the use of part of this waste as feedstock for bacterial enzyme production, supporting the compounds' extraction procedure, (iv-a) application of the post-extraction biomass on agricultural fields to enhance productivity, and (iv-b) alternatively, the post-extraction biomass waste can be used for clean energy production. Indeed, with the introduction of steps iv-a or iv-b, the entire process would be in compliance with the principles of circular economy.

The sustainability of the extraction procedure described here is further enhanced by the fact that the vegetable material used was a waste generated from a real agri-food supply chain because it simply did not meet the aesthetic quality standard requirements for large-scale retail channels. Cauliflowers from this source were collected over three different seasons (spring, summer, and early autumn 2021), and originated from farms located in different geographical areas in Italy. It is known that the content of several secondary metabolites in fruits and vegetables is strongly dependent on several parameters, such as specific cultivar, seasonal harvesting time, cultivation site, endogenous circadian rhythms, and soil and pest-control strategies [23–26]. Moreover, during the wheeled transport to the processing warehouse, the produce reached different maturation stages, also related to seasonal conditions. The uncontrolled origin of the experimental material granted it an intrinsic heterogeneity that could not be overcome. These variables heavily impact the composition and overall content of the bioactive compounds of vegetables and are partly responsible for the low statistical significance of some of the data.

Moreover, the solubilisation, and thus, the extraction efficiency, of some compounds occurs in polar organic solvents, which were not used in this work. For example, isothiocyanates, relevant anticancer compounds abundantly present in Brassicaceae [27], are usually extracted from fresh material using organic solvents, and even in those cases, with extremely variable returns, as reported in the literature [28–30]. In general, however, organic solvents guarantee much higher yields with respect to those reported in this work (Table 1). Only Wang et al. [31] reported a low content of isothiocyanates (0.023  $\mu\text{mol/g}$ ) in raw cauliflowers extracted using the cooking water. This value is slightly lower than the result obtained in this work, corresponding to 0.027  $\mu\text{mol/g}$  (considering the Mw of 1,3-Benzodithiole-2-thione as 1843 g/mol). Indeed, in our laboratory, by using methanol, isothiocyanates could be recovered from the frozen material 5-fold more efficiently than through the sustainable procedure herein described, with or without the enzymatic pretreatment (Doria E., unpublished data). Nevertheless, the extraction procedure might require further adjustments for some classes of compounds. For instance, the prolonged defrosting process (48 h) carried out at room temperature (20 °C–23 °C), might compromise the recovery of highly volatile and intrinsically unstable bioactive molecules.

It is important to highlight that, as opposed to most of the literature data, this work was carried out on a pilot scale, using 5 kg of raw material for each sample and for each of the four experimental replicates. To our knowledge there are no previous reports on such large-scale extractions.

In conclusion, the OS58-based sustainable extraction procedure was demonstrated to be more effective than the WT strain-based extraction in the recovery of bioactives from *Brassica oleracea* L. *conv. botrytis* (L.) Alef. *var. botrytis* L.; the unpurified bacterial enzymes notably improved the retrieval of valuable phytochemicals from the matrix in a concentration-dependent manner. The applicability of the promising sustainable enzymatic pretreatment, coupled with solid-liquid extraction at high pressure, is currently being tested on raw vegetable materials with different structural characteristics and bioactives



composition, to validate the applicability of raw enzymatic mixtures for nutraceuticals recovery.

#### 4. Materials and Methods

##### 4.1. Bacterial Strains

*Bacillus subtilis* strains used in this study are a WT strain and its derivative, OS58. The WT derives from PB5249, a *swrA*<sup>+</sup> spontaneous derivative [32] of the auxotrophic *trpC2 pheA1* strain JH642 (GenBank accession no. CM000489.1) [15], which was sequentially transformed with the PCR products of the *trpC* and *pheA* genes, obtained from the genomic DNA of the wild NCIB 3610 strain (GenBank accession no. CP020102.1). Amplifications of the *trpC* and *pheA* genes were performed using the primer pairs *trpC*\_Up 5'-AGTGAAAACACTGGTCTGCGG-3' and *trpC*\_Dw 5'-GATGGATTGCTTTACGCTGAGAAG-3' followed by *pheA*\_Up 5'-AACAGCCTTTGCCAATCGTGGG-3' and *pheA*\_Dw 5'-GTATACATGGATGCAGCCGCTCAG-3', respectively. For the first transformation, the selection of the *trpC*<sup>+</sup> prototroph occurred on minimal medium containing 1.5% agar, 1 mg/mL glucose and phenylalanine (50 µg/mL). Subsequently, *pheA*<sup>+</sup> transformants were selected on minimal medium without amino acids.

OS58 was obtained from the WT strain by genetic engineering. A patent application is under preparation for this strain; for this reason, the details of the engineering design are undisclosed herein.

##### 4.2. Bacterial Growth

For cellulase and xylanase production, *B. subtilis* WT and OS89 spores were revitalized on LB (Difco Laboratories, New York, NY, USA) 1.5% agar plates and incubated overnight at 37 °C. Isolated colonies were inoculated in Antibiotic Medium 3 (Difco Laboratories) containing 5 mg/mL glucose and grown 16 h at 37 °C with shaking. In the same medium, a second pre-inoculum was set at optical density of 600 nm (OD<sub>600</sub>) 0.2 and grown for 6 h at 37 °C with shaking. The synthetic medium CMD (containing, per liter: 13.67 g Na citrate; 10 g glucose; 7 g NH<sub>4</sub>Cl; 0.5 g MgSO<sub>4</sub>·7H<sub>2</sub>O; 0.5 g K<sub>2</sub>HPO<sub>4</sub>; 0.15 g CaCl<sub>2</sub>·2H<sub>2</sub>O; 0.104 g MnSO<sub>4</sub>·H<sub>2</sub>O; 0.04 g FeCl<sub>2</sub>·6H<sub>2</sub>O; pH6.5) was inoculated at OD<sub>600</sub> 0.2 and grown for 24 h at 37 °C with 150 rpm orbital shaking. Bacterial growth was followed by OD<sub>600</sub> readings. Culture supernatant was collected after 40' centrifugation at room temperature at 2268 × g. The spent medium (500 mL) was immediately used for the maceration of 5 kg-smashed cauliflowers.

##### 4.3. Cellulase and Xylanase Activity Assays

Cellulase (endo-1,4-β-glucanase; EC 3.2.1.4) and endo-xylanase (endo-1,4-β-xylanase; EC 3.2.1.8) activities were assayed in an aliquot of the culture supernatants after acidification, as previously described [33], using CellG3 and XylX6 Assay Kits (Megazyme®), following the protocol provided by the manufacturer.

##### 4.4. Plant Material

Fresh cauliflowers (*Brassica oleracea* L. *conv. botrytis* (L.) Alef. *var. botrytis* L.) were obtained, during spring, summer, and autumn 2021, from a food processing plant that collects vegetables from farms located in southern and northern Italy. The fresh material was weighted, aliquoted, and stored at -45 °C ± 1 °C (monitored by a datalogger, Testo 184 T4, Liebherr) for over one month. For each treatment (including controls) and for each of the four experimental replicate, aliquots of 5 kg each (fresh weight before freezing) were thawed at room temperature for 2 days. After draining the residual water, each whole cauliflower, including flowers, leaves and stems, was cut into four parts and ground using an industrial mill (M100, Enoitalia s.r.l., Florence, Italy); the material was completely shattered into small pieces (0.5–1.0 cm in diameter) for subsequent processing. The set of extraction experiments (conducted with the supernatant of the WT strain, the OS58

supernatant, or the sterile medium as a control) was independently carried out four times, on four different lots of cauliflowers.

#### 4.5. EAE Pretreatment Procedure of the Cauliflower Waste Material

To 5 kg of fresh material, ground as previously described, 500 mL of bacterial culture supernatant was added, and the final volume was brought to 5 L with water. The suspension was acidified with 85% phosphoric acid to pH 5.0 and was incubated for 16 h at 50 °C with 40 rpm orbital shaking (LOM-7450 Incubator, MRC, London, UK). For each of the four replicates, the material was incubated with 500 mL of sterile CMD instead of the spent medium, as a negative control.

#### 4.6. Extraction Process

An isothermal cyclically pressurized extraction process (rapid solid–liquid dynamic extraction) was applied to pretreated cauliflowers using the Naviglio mechanical extractor (Nuova Estrazione, Naples, Italy). The principle is based on cyclic compression and decompression phases that exert a suction effect on extractable compounds present in the vegetable matrix [34]. The solid material was placed into a 50 µm-filtering membrane bag, inserted together with the maceration liquid, into the pressure gradient cylinder that was then filled with deionized water, up to a total volume of 35 L. Each extraction cycle consisted of a 3 min static phase, followed by a 2 min dynamic phase; the number of cycles was 60, for a total time of 5 h. At the end of the extraction, the bag with the solid residue was removed and squeezed, and the aqueous liquid was recovered in a tank. One liter of the collected extract was dried using a rotary evaporator (Rotavapor System R-300, Büchi Labortechnik AG, Flawil, Switzerland); the solid residue was suspended in 50% methanol and filtered using 0.22 µm nylon filter before analyses.

#### 4.7. Total Polyphenol Content

The total content of polyphenols was measured using the Total Polyphenols Colorimetric Assay Kit (Steroglass, Perugia, Italy) according to the manufacturer's instructions. Absorbance was measured at 725 nm and results were expressed in gallic acid equivalents using a gallic acid standard curve.

#### 4.8. Catechins and Chlorogenic Acid HPLC Analyses

A 20-µL aliquot of the filtered sample was injected into the HPLC pump (Kontron 420; Kontron Instruments, Munich, Germany) equipped with a C18 column (ZORBAX ODS 250 × 4.6 mm column, 5 µm particle size, Sepachrom, Milan, Italy). For catechins and chlorogenic acid, HPLC analyses were performed with a 0.8 mL/min flow rate and setting the detector at 280 nm; the mobile phases consisted in 5% acetic acid (A) and pure methanol (B), and the chromatographic gradient conditions are summarized in Table 2:

**Table 2.** The mobile phase gradient.

Time (Min)	A (%)	B (%)
1	90	10
5	90	10
7	80	20
8	80	20
10	75	25
15	70	30
20	20	80
25	50	50
28	70	30
30	90	10

#### 4.9. Isothiocyanates HPLC Analyses

Isothiocyanates were analyzed by HPLC after cyclocondensation, according to the protocol described by Tang et al. [28], with modification. For each sample, an aliquot of 250  $\mu$ L of extract was mixed with 250  $\mu$ L of 100 mM potassium phosphate buffer (pH 8.5) and 500  $\mu$ L of 10 mM 1,2-benzenedithiol in methanol. The reaction mixture was incubated for 2 h at 65 °C and then cooled at room temperature. The mixture was centrifuged at low speed and finally filtered with a 0.22  $\mu$ m nylon filter before being injected into the HPLC. In this process, 1,2-benzenedithiol reacts with the carbon atom of the  $-N=C=S$  group of isothiocyanates to form a five-membered 1,3-benzodithiole-2-thione and the corresponding amine. Using RP-HPLC with an isocratic mobile phase of 80% methanol, a flow rate of 1 mL/min, at 40 °C and UV 365 nm, 1,3-benzodithiole-2-thione can be eluted, providing an analytical measure of the total isothiocyanates present [35]. Different concentrations of allyl-isothiocyanate were used as standards for the calibration curve.

#### 4.10. Statistical Analysis

The variation in the amount of the compound extracted among the three experimental conditions, considered as response variable, was explored by using a series of linear mixed models (LMMS). Each model had a common fixed effect, represented by the experimental treatment adopted (factor with three levels: control, WT, OS58), and a common random effect (random intercept) represented by the different samples of organic matter (i.e., replicates). The estimated means, related confidence intervals, and planned comparison among treatments were computed using the emmeans and contrast functions of the emmeans package (version 1.7.2) [17]. All model assumptions were explored by checking residuals distribution against fitted values (Tukey–Anscombe plot) and residual normality against theoretical normal distribution (quantile–quantile plot). Percentual changes with respect to the control were obtained from the raw data.

All statistical analyses were performed in R (R Core Team, 2021. R: A language and environment for statistical computing. R Foundation for Statistical Computing, Vienna, Austria) [36].

**Author Contributions:** Conceptualization, E.D., D.B. and C.C.; methodology, E.D., C.C., A.M. and V.B.; software, A.G. and D.B.; validation, E.D., D.B. and C.C.; formal analysis, A.M. and V.B.; investigation, A.M. and V.B.; data curation, A.G., C.C. and D.B.; original draft preparation, E.D. and C.C.; review and editing, C.C. and D.B.; visualization, M.V. and M.D.; supervision, E.D. and C.C.; project administration, D.B.; funding acquisition, D.B. All authors have read and agreed to the published version of the manuscript.

**Funding:** This study was supported and funded by Fondazione Cariplo, grant n. 2018-1011, Circular Economy 2018, grant n. 2015-0400, Biotechnology 2015, and by the Italian Ministry of Education, University and Research (MIUR): Dipartimenti di Eccellenza Program (2018–2022), Department of Biology and Biotechnology “L. Spallanzani,” University of Pavia.

**Data Availability Statement:** The data presented in this study are available on request from the corresponding author. The data are not publicly available due to the privacy statement in the original project.

**Acknowledgments:** The authors would like to thank AOP UNOLOMBARDIA sac a rl, Italy, and Ambrogio De Ponti, for providing the raw materials.

**Conflicts of Interest:** The authors declare no conflict of interest.

## References

1. Springmann, M.; Clark, M.; Mason-D’Croz, D.; Wiebe, K.; Bodirsky, B.L.; Lassaletta, L.; De Vries, W.; Vermeulen, S.J.; Herrero, M.; Carlson, K.M.; et al. Options for keeping the food system within environmental limits. *Nature* **2018**, *562*, 519–525. [CrossRef] [PubMed]
2. Vilarinho, M.V.; Franco, C.; Quarrington, C. Food loss and Waste Reduction as an Integral Part of a Circular Economy. *Front. Environ. Sci.* **2017**, *5*, 21. [CrossRef]

3. Wadhwa, M.; Bakshi, M.P.S. *Utilization of Fruit and Vegetable Wastes as Livestock Feed and as Substrates for Generation of Other Value-Added Products*; RAP Publication, FAO: Rome, Italy, 2013; pp. 1–59. Available online: <https://www.fao.org/3/i3273e/i3273e.pdf> (accessed on 7 February 2022).
4. Kumar, K.; Yadav, A.N.; Kumar, V.; Vyas, P.; Dhaliwal, H.S. Food waste: A potential bioresource for extraction of nutraceuticals and bioactive compounds. *Bioresour. Bioprocess.* **2017**, *4*, 18. [CrossRef]
5. Galanakis, C.M. *Food Waste Recovery: Processing Technologies and Industrial Techniques*; Elsevier: New York, NY, USA, 2015; pp. 381–392.
6. Puri, M.; Sharma, D.; Barrow, C.J. Enzyme-assisted extraction of bioactives from plants. *Trends Biotechnol.* **2012**, *30*, 37–44. [CrossRef] [PubMed]
7. Marathe, S.J.; Jadhav, S.B.; Bankar, S.B.; Singhal, R.S. Enzyme-Assisted Extraction of Bioactives. In *Food Bioactives*; Puri, M., Ed.; Springer: Cham, Switzerland, 2017; pp. 171–201. [CrossRef]
8. Nadar, S.; Rao, P.; Rathod, V.K. Enzyme assisted extraction of biomolecules as an approach to novel extraction technology: A review. *Food Res. Int.* **2018**, *108*, 309–330. [CrossRef]
9. Schallmeyer, M.; Singh, A.; Ward, O.P. Developments in the use of *Bacillus* species for industrial production. *Can. J. Microbiol.* **2004**, *50*, 1–17. [CrossRef]
10. Cui, W.; Han, L.; Suo, F.; Liu, Z.; Zhou, L.; Zhou, Z. Exploitation of *Bacillus subtilis* as a robust workhorse for production of heterologous proteins and beyond. *World J. Microbiol. Biotechnol.* **2018**, *34*, 145. [CrossRef]
11. Su, Y.; Liu, C.; Fang, H.; Zhang, D. *Bacillus subtilis*: A universal cell factory for industry, agriculture, biomaterials and medicine. *Microb. Cell Factories* **2020**, *19*, 173. [CrossRef]
12. CAZY Carbohydrate Active enZymes. Available online: <http://www.cazy.org/b67.html> (accessed on 7 February 2022).
13. Van Dijk, J.M.; Hecker, M. *Bacillus subtilis*: From soil bacterium to super-secreting cell factory. *Microb. Cell Factories* **2013**, *12*, 3. [CrossRef]
14. Danilova, I.; Sharipova, M. The Practical Potential of Bacilli and Their Enzymes for Industrial Production. *Front. Microbiol.* **2020**, *11*, 1782. [CrossRef]
15. Srivatsan, A.; Han, Y.; Peng, J.; Tehrani, A.K.; Gibbs, R.; Wang, J.D.; Chen, R. High-Precision, Whole-Genome Sequencing of Laboratory Strains Facilitates Genetic Studies. *PLoS Genet.* **2008**, *4*, e1000139. [CrossRef] [PubMed]
16. Tjalsma, H.; Antelmann, H.; Jongbloed, J.D.; Braun, P.G.; Darmon, E.; Dorenbos, R.; Dubois, J.Y.F.; Westers, H.; Zanen, G.; Quax, W.J.; et al. Proteomics of protein secretion by *Bacillus subtilis*: Separating the “secrets” of the secretome. *Microbiol. Mol. Biol. Rev.* **2004**, *68*, 207–233. [CrossRef] [PubMed]
17. The Comprehensive R Archive Network-Emmeans: Estimated Marginal Means, Aka Least-Squares Means. R Package Version 1.7.2. Available online: <https://cran.r-project.org/web/packages/emmeans/emmeans.pdf> (accessed on 7 February 2022).
18. Gligor, O.; Mocan, A.; Moldovan, C.; Locatelli, M.; Crisan, G.; Ferreira, I.C. Enzyme-assisted extractions of polyphenols—A comprehensive review. *Trends Food Sci. Technol.* **2019**, *88*, 302–315. [CrossRef]
19. Lenucci, M.S.; De Caroli, M.; Marrese, P.P.; Iurlaro, A.; Rescio, L.; Böhm, V.; Dalessandro, G.; Piro, G. Enzyme-aided extraction of lycopene from high-pigment tomato cultivars by supercritical carbon dioxide. *Food Chem.* **2015**, *170*, 193–202. [CrossRef] [PubMed]
20. Garcia, R.G.; Martínez-Ávila, G.C.G.; Aguilar, C.N. Enzyme-assisted extraction of antioxidative phenolics from grape (*Vitis vinifera* L.) residues. *3 Biotech* **2012**, *2*, 297–300. [CrossRef]
21. Rane, A.N.; Baiker, V.V.; Ravi Kumar, V.; Deopurkar, R.L. Agro-Industrial Wastes for Production of Biosurfactant by *Bacillus subtilis* ANR 88 and Its Application in Synthesis of Silver and Gold Nanoparticles. *Front. Microbiol.* **2017**, *8*, 492. [CrossRef]
22. Radhakrishnan, R.; Abeer, H.; Abd Allah, E.F. *Bacillus*: A Biological Tool for Crop Improvement through Bio-Molecular Changes in Adverse Environments. *Front. Physiol.* **2017**, *8*, 667. [CrossRef]
23. Heimler, D.; Isolani, L.; Vignolini, P.; Tombelli, S.; Romani, A. Polyphenol Content and Antioxidative Activity in Some Species of Freshly Consumed Salads. *J. Agric. Food Chem.* **2007**, *55*, 1724–1729. [CrossRef]
24. Koh, E.; Wimalasiri, K.; Chassy, A.; Mitchell, A. Content of ascorbic acid, quercetin, kaempferol and total phenolics in commercial broccoli. *J. Food Compos. Anal.* **2009**, *22*, 637–643. [CrossRef]
25. Valverde, J.; Reilly, K.; Villacreses, S.; Gaffney, M.; Grant, J.; Brunton, N. Variation in bioactive content in broccoli (*Brassica oleracea* var. *italica*) grown under conventional and organic production systems. *J. Sci. Food Agric.* **2015**, *95*, 1163–1171. [CrossRef]
26. Soengas, P.; Cartea, M.E.; Velasco, P.; Francisco, M. Endogenous Circadian Rhythms in Polyphenolic Composition Induce Changes in Antioxidant Properties in Brassica Cultivars. *J. Agric. Food Chem.* **2018**, *66*, 5984–5991. [CrossRef] [PubMed]
27. Lawson, A.P.; Long, M.; Coffey, R.T.; Qian, Y.; Weerapana, E.; El Oualid, F.; Hedstrom, L. Naturally Occurring Isothiocyanates Exert Anticancer Effects by Inhibiting Deubiquitinating Enzymes. *Cancer Res.* **2015**, *75*, 5130–5142. [CrossRef] [PubMed]
28. Tang, L.; Paonessa, J.D.; Zhang, Y.; Ambrosone, C.B.; McCann, S.E. Total isothiocyanate yield from raw cruciferous vegetables commonly consumed in the United States. *J. Funct. Foods* **2013**, *5*, 1996–2001. [CrossRef]
29. ToTšek, J.; Trška, J.; LeFneroVá, D.; STrohaLm, J.; Vrchoťová, N.; Zendlulka, O.; Průchová, J.; Chaloupková, J.; Novotná, P.; Houška, M. Contents of sulfuraphane and total isothiocyanates, antimutagenic activity, and inhibition of clastogenicity in pulp. *Czech J. Food Sci.* **2011**, *29*, 548–556. [CrossRef]
30. Karanikolopoulou, S.; Revelou, P.-K.; Xagoraris, M.; Kokotou, M.G.; Constantinou-Kokotou, V. Current Methods for the Extraction and Analysis of Isothiocyanates and Indoles in Cruciferous Vegetables. *Analytica* **2021**, *2*, 93–120. [CrossRef]



31. Wang, Z.; Kwan, M.L.; Pratt, R.; Roh, J.M.; Kushi, L.H.; Danforth, K.N.; Zhang, Y.; Ambrosone, C.B.; Tang, L. Effects of cooking methods on total isothiocyanate yield from cruciferous vegetables. *Food Sci. Nutr.* **2020**, *8*, 5673–5682. [[CrossRef](#)]
32. Mordini, S.; Osera, C.; Marini, S.; Scavone, F.; Bellazzi, R.; Galizzi, A.; Calvio, C. The role of SwrA, DegU and P<sub>D3</sub> in *fla/che* expression in *B. subtilis*. *PLoS ONE* **2013**, *8*, e85065. [[CrossRef](#)]
33. Ermoli, F.; Bontà, V.; Vitali, G.; Calvio, C. SwrA as global modulator of the two-component system DegSU in *Bacillus subtilis*. *Res. Microbiol.* **2021**, *172*, 103877. [[CrossRef](#)]
34. Naviglio, D.; Formato, A.; Gallo, M. Comparison between 2 Methods of Solid-Liquid Extraction for the Production of Cinchona calisaya Elixir: An Experimental Kinetics and Numerical Modeling Approach. *J. Food Sci.* **2014**, *79*, E1704–E1712. [[CrossRef](#)]
35. Zhang, Y. The 1,2-Benzenedithiole-Based Cyclocondensation Assay: A Valuable Tool for the Measurement of Chemopreventive Isothiocyanates. *Crit. Rev. Food Sci. Nutr.* **2012**, *52*, 525–532. [[CrossRef](#)]
36. The R Project for Statistical Computing. Available online: <https://www.R-project.org/> (accessed on 7 February 2022).

## Query Details

[Back to Main Page](#)

1. The citation 'Shah (2021)' has been changed to 'Shah (2021a, b)' to match the author name/date in the reference list. Please check here and in subsequent occurrences, and correct if necessary.

## Poly- $\gamma$ -Glutamic Acid and Its Application in Bioremediation: A Critical Review

Valeria Bontà [Affiliationids : Aff1](#)

Cinzia Calvio [✉](#)

Email : cinzia.calvio@unipv.it

[Affiliationids : Aff1](#), [Correspondingaffiliationid : Aff1](#)

[Aff1](#) Department of Biology and Biotechnology, Pavia University, Pavia, Italy

### Abstract

Poly-gamma glutamic acid ( $\gamma$ -PGA) is an anionic bacterial polymer constituted by glutamic acid residues only. It has the intrinsic ability to strongly interact with positively charged ions and flocculate them. For this reason, a large body of literature has accumulated on its application in bioremediation, particularly targeted to positively charged heavy metals. In this work, the most important characteristics of  $\gamma$ -PGA and of its production are summarized, highlighting the advantages, but also the limits, in its application in bioremediation.

### Keywords

PGA  
Bacteria  
Bioremediation  
Polymer

## 1. $\gamma$ -PGA Biosynthesis

Poly-gamma glutamic acid ( $\gamma$ -PGA) is a natural anionic, high molecular weight (Mw), homo-polyamide, made up of repeating units of L- and/or D-glutamic acid residues connected by amide linkages between  $\alpha$ -amino and  $\gamma$ -carboxyl groups; these pseudopeptide bonds are resistant to classical proteases. The ribosome-independent synthesis, that can lead to molecules most often above  $10^6$  Da, occurs via a transmembrane ATP-dependent  $\gamma$ -PGA synthase complex, which also secretes the polymer outside the cell (Sung et al. 2005). The synthase is constituted by the products of four genes, which are known as *pgsB*, *pgsC* and *pgsA* in species releasing the polymer in the environment. A fourth small gene, *pgsE*, completes the *pgs* operon in *B. subtilis*, *B. amyloliquefaciens*, *B. pumilus* and *B. licheniformis* (Fujita et al. 2021). In *B. anthracis* and other capsule forming bacteria, the *pgs* homologues are known as *cap* genes (*capBCA*). In this latter group, the three biosynthetic genes are followed by *capD*, which encodes a product that bears resemblance to  $\gamma$ -glutamyl transferases, responsible for anchoring the polymer to the cell wall (Candela and Fouet 2005).

Microbial fermentation is the only viable way to obtain  $\gamma$ -PGA in significant amount, as the chemical synthesis of  $\gamma$ -PGA molecules longer than few residues is troublesome, inefficient, expensive and non-sustainable, requiring the constant protection of the  $\alpha$ -carboxylic group.

Significative amounts of  $\gamma$ -PGA are produced by Gram-positive bacteria, mainly *B. subtilis*, *B. licheniformis* and *B. amyloliquefaciens* species. Aerobic, spore-forming, ubiquitous in soil and plants, *Bacilli* are ideal workhorses for  $\gamma$ -PGA production for many different reasons: they are generally non-pathogenic, fast growing, amenable to genetic manipulation, have simple nutritional requirements, and their products possess a long track record of safe use in human food products (Tamang et al. 2016). *B. subtilis* is indeed the model organism for Gram-positive bacteria and a large number of scholars, all over the world, have focused their studies on this organism. In fact, scientific investigations on *B. subtilis* date back to 1835, although *B. subtilis* got its present name only in 1872 by Ferdinand Cohn (Harwood 1989). These has led to the accumulation of endless and thorough knowledge on its genetics and physiology in general, and on  $\gamma$ -PGA production, in particular.

The polymer characteristics greatly vary among different producer strains, different growth media and fermentation conditions. Neither the enantiomeric composition nor the Mw are fixed. Analyses of purified  $\gamma$ -PGA showed that it can be made of D-glutamic acid, L-





$\gamma$ -PGA producer strains come in two flavours: those requiring an external supply of L-glutamic acid and those that can produce it even in the absence of an external source of the amino acid. Productivity is much higher for L-glutamic acid-dependent strains, but polymer yield is directly correlated to the amount of L-glutamic acid added, which impacts on the production costs. Despite many efforts have been devoted to the isolation of new glutamic acid-independent strains, their productivity is scant in the absence of exogenous glutamate or its metabolic precursors (Zhang et al. 2012).

To reconcile needs and costs, several efforts were dedicated to the development of genetically engineered strains characterized by high  $\gamma$ -PGA productivity or simply to improve the intracellular glutamate synthesis, which is the limiting factor for  $\gamma$ -PGA synthesis (Cai et al. 2018). The genetic and metabolic optimization of all processes responsible for  $\gamma$ -PGA production is relatively easy in *Bacilli*'s genome thanks to the existence of well-established techniques and molecular biology tools (Appelbaum and Schweder 2021), supporting the improvement in production yields and reduction in fermentation costs. Over the past years, a number of genes that are involved in  $\gamma$ -PGA production have been characterized, and much has been published on how different parameters affect productivity and costs.

As one of the main costs for commercial-scale  $\gamma$ -PGA production is the requirement of large amount of L-glutamate in the fermentation media (Nair et al. 2021), huge efforts were posed on strategies designed to reduce or replace this expensive component. These approaches generally aimed at rewiring the central carbon metabolism to enhance the carbon flux toward the tricarboxylic acid (TCA) cycle, as  $\alpha$ -ketoglutarate is a direct precursor of  $\gamma$ -PGA. Metabolic models now available can predict genes to be targeted to enhance  $\gamma$ -PGA synthesis (Massaiu et al. 2019). Another successful approach was taken by Feng and collaborators' group, who took inspiration from a well-known glutamate producer microorganism: a 9.1% improvement in  $\gamma$ -PGA production was obtained by introducing the NADPH-dependent GDH pathway from *Corynebacterium glutamicum* into a glutamate-independent *B. amyloliquefaciens* strain; the yield further improved by 66.2% by manipulating the enzymes of the TCA cycle (Feng et al. 2017). Also, the deletion of two  $\gamma$ -PGA hydrolases, GGT and PgdS, was effective in doubling productivity in the presence of glutamate (Scoffone et al. 2013). However, the simple over-expression of the *pgsBCA* operon was shown to lead to a reduction in polymer yield, possibly because the excess of the synthase complex imbalanced other membrane-associated metabolic processes (Feng et al. 2015). In more systemic approaches, several of the previously explored genome engineering strategies were joined in modular way in the same strains, leading to a substantial increase in productivity (Feng et al. 2015; Cai et al. 2018).

*Bacilli* are considered as "strictly aerobic" and grow poorly in oxygen-limiting conditions (Nakano and Zuber 1998). For this reason,  $\gamma$ -PGA is mainly produced by aerobic fermentation in liquid media. However, during growth, oxygen transfer from the gas phase to the liquid phase is progressively reduced due to the high viscosity of the polymer that accumulates in the growth medium. This phenomenon limits cell growth and leads to a decrease in  $\gamma$ -PGA yield at later stages of cultivation. To overcome this problem a successful strategy was the introduction of the gene encoding the *Vitreoscilla* hemoglobin in *B. subtilis* chromosome, enhancing cell growth and increasing  $\gamma$ -PGA yield (Su et al. 2010). Although, the efforts dedicated to genetic improvement, the polymer is still too expensive; alternative routes have been parallelly explored to decrease  $\gamma$ -PGA market price.

## 5. Strategies to Reduce Fermentation Costs

Besides improving strains productivity, reduction of  $\gamma$ -PGA production costs is sought through the replacement of expensive components of the fermentation media with low-cost substrates. The dominant carbon sources used in the  $\gamma$ -PGA biosynthesis are glucose and citric acid, that are mainly derived from sources that are in competition with human nutrition, inevitably raising social dilemmas and raising the production costs imposed to the process. Recently, the urge to valorise agro-industrial waste as feedstock for bacterial fermentations has encouraged investigations on solid-state fermentation also for  $\gamma$ -PGA production. Indeed, as an alternative, a wide range of abundant and renewable lignocellulosic biomasses or agro-industrial wastes, such as rice straw, cane molasses, rapeseed meal, soybean residue, corncob fibres, crude glycerol from biodiesel plants, macroalgae, goose feathers and paper waste have been proposed as cost-attractive and environmentally sustainable carbon sources (Fang et al. 2020). Such biomasses not only represent cheap substrates for microbial growth, but their valorisation through fermentation mitigates the impact they would have on eutrophication; moreover, the solid-state fermented substrate can be directly used as agricultural fertilizer, exploiting the beneficial effects of both *Bacillus* species and  $\gamma$ -PGA on plant performance (Zhang et al. 2017). Among the industrial wastes, untreated cane molasses and monosodium glutamate waste liquor, by-products of refining sugarcane and from the glutamic acid fermentation process, respectively, or powdered fulvic acid, recovered from the wastewater of molasses fermentation by yeast, were successfully exploited in cost-effective biosynthesis of  $\gamma$ -PGA (Zhang et al. 2012; Li et al. 2020). However, most often, direct and efficient fermentation of lignocellulosic feedstock is unfeasible; pretreatments are generally required for the utilization of the sugars therein contained. For this reason, bacterial feedstocks based on biomass hydrolysates are preferentially used. Hydrolysates of rice straw or corncob fibers have been tested for the convenient fermentation of  $\gamma$ -PGA (Hassan et al. 2014; Tang et al. 2015; Zhu et al. 2013). Unfortunately, lignocellulosic biomass hydrolysis often implies the use of polluting agents to break the recalcitrant matrix. An environmentally sustainable alternative for hydrolysing biomasses is the application of microbial degradative enzymes for the pretreatment of feedstock biomasses. Altun (2019) employed goose feathers from poultry processing plants as source of protein hydrolysates; however, feathers were first used as the sole carbon and nitrogen source to produce keratinolytic enzymes by *Streptomyces pactum*. The lyophilized crude enzymatic extract was applied to obtain feather hydrolysates, which was finally used as a cheap and renewable medium for  $\gamma$ -PGA production (Altun 2019).

Also, short fibres produced from paper linerboard recycling could be enzymatically turned into fermentable sugars and later used as carbon source for the biosynthesis of  $\gamma$ -PGA with yields compared to the one obtained by using glucose (Scheel et al. 2019).

Many additional industrial wastes have been suggested for production of  $\gamma$ -PGA, as well as of other biocommodities. All these approaches combine the valorisation of industrial wastes for the creation of value-added products, thus introducing circularity in the economic process.

## 6. The Applications of $\gamma$ -PGA

$\gamma$ -PGA is basically a long chain of glutamic acid residues joined by pseudopeptide bonds; the composition in glutamic acid mainly in the D-form makes it biocompatible, non-immunogenic and even edible; in fact, it is one of the main components of *natto* and *chungkookjang*, traditional Japanese and Korean foods, respectively, made from soybeans fermented with *Bacillus subtilis* species. The slow degradation profile prevents inflammatory responses. Furthermore, the microbial production is sustainable and safe also for the environment, as the polymer is bioproduced and easily biodegradable.

The configuration of the  $\gamma$ -amide bond confers to the polymer particular chemical-physical characteristics that make it a valid anionic biomaterial in various application fields (Ogunleye et al. 2014). However, the extreme viscosity of the high Mw chains makes the polymer not easily manageable. The problem can be alleviated by random reduction of the Mw by alkaline hydrolysis, sonication, or enzymatic degradation; on the other hand, excessive size reduction limits some properties of the polymer, which are dependent on the length of the chains (Shih and Van 2001).

The presence of several pending and negatively charged carboxyl groups in position  $\alpha$  profoundly affects the solubility of the polymer: in basic conditions the  $-\text{COOH}$  groups are deprotonated, making the polymer hydrophilic, hygroscopic and superabsorbent, and favouring the formation of  $\gamma$ -PGA salts in the presence of metal ions; conversely, in acidic environments, the carboxylic groups are protonated, making the molecule water-insoluble. Besides, these pending groups represent ideal reactive centres for conjugation and crosslinking of any type of molecules. Thanks to the above properties, high Mw  $\gamma$ -PGA represents a versatile candidate for various industrial applications, as attested by the massive literature accumulated over the last few years. Biocompatibility has prompted several potential applications in the biomedical and food sectors. The long hydrophilic moiety of  $\gamma$ -PGA, which is metabolized at a slow pace in mammals, represents a perfect drug carrier to improve the administration of poorly soluble drugs. It can also be transformed in various  $\gamma$ -PGA-based composites, including hydrogels, nanofibers, and nanoparticles for medical applications, such as biological adhesives or scaffolding materials for tissue engineering; in these composites, the conjugated materials provide adhesion or mechanical strength (Park et al. 2021).  $\gamma$ -PGA-nanoparticles have been explored as substitute of adenoviral vectors for the delivery of anticancer agents (Khalil et al. 2018). In addition, the ability to chelate metal ions (e.g., magnesium or calcium), and release them slowly in the digestive tract, has been exploited to create highly effective controlled-release mineral supplements for human and farm animals use.

Another well-developed field in which  $\gamma$ -PGA has already found wide application is processed food production; it is used as an additive to improve the rheological properties of wheat gluten by increasing the water-holding capacity (Xie et al. 2020), as viscosity enhancer for beverages, as cryoprotectant for frozen food, aging inhibitor, texture enhancer or bitterness relieving agent. It also acts as preservative for probiotic bacteria during freeze drying (Bhat et al. 2015).

$\gamma$ -PGA can absorb water at an amount that is several hundred times higher than its original weight without dissolving. The high-water absorbability can be further increased by combining the polymer with other materials or by intramolecular crosslinking, leading to the formation of hydrogels. The super-absorbent capacity is the key property in cosmetics and personal care products, such as  $\gamma$ -PGA-based moisturizer, exfoliating and anti-wrinkle creams.  $\gamma$ -PGA has been shown to enhance skin elasticity more than collagen and hyaluronic acid (Lee et al. 2014); moreover, it has been explored also in products as diapers and napkins, as substitute of more toxic acrylates (Castrillon et al. 2019).

Another class of  $\gamma$ -PGA-based products which are already on the market are fertilizers and other agricultural adjuvants. In these types of applications,  $\gamma$ -PGA is considered an environmental-friendly fertilizer synergist for improving plant uptake of nitrogen, phosphorus, and potassium; it is often provided together with the producing organisms, as raw fermentation broth, thanks to the numerous positive effects that *Bacillus* species have on vegetable growth, making it a perfect Plant Growth Promoting bacterium (PGPB) (Zhang et al. 2017).

Moreover,  $\gamma$ -PGA can also positively impact on soil quality indirectly, by promoting water retention (Guo et al. 2021) and by sustaining the flourishing of the soil microflora (Xu et al. 2013).

## 7. $\gamma$ -PGA in Bioremediation

Bioremediation of contaminated matrices exploiting  $\gamma$ -PGA has been extensively investigated by several authors. At the basis of its application in this field lays the ability to efficiently chelate and flocculate polluting metal ions such as nickel, copper, cadmium, cobalt, chromium, aluminium, uranium, arsenic or lead, as well as various organic compounds. In turn, those are supported by the presence of multiple negatively charged carboxyl groups in the polymer structure that readily bind to several environmental cations, forming both intra- and inter-molecular hydrogen bonds favouring the formation of flocks (McLean et al. 1990; Inbaraj et al. 2009).

### 7.1. Wastewater Treatment

Detection and removal of heavy metal ions in water is of paramount threats for the planet and for human and animal health; however, decontamination solution should not impose an additional threat to already endangered sites. Aluminium- or polyacrylamide-based coagulants, often used in water treatment plants, have indeed been linked to the development of neurodegenerative diseases (Bondy 2010; Pennisi et al. 2013). Being safe and biodegradable,  $\gamma$ -PGA represents instead the ideal solution for the removal of pollutants



from wastewater, in particular of heavy metals, as it promotes the formation of small flocs entrapping the metal ions, that readily agglomerate into larger and sedimentable particles, without leaving toxic traces behind. The dynamics of complexes formation with bivalent lead ions at various concentrations of both adsorber and ligands and the characteristics of the flocs at different pH values were deeply characterized (Bodnár et al. 2008). One of the requirements for the activity of  $\gamma$ -PGA as adsorber and flocculant is the maintenance of a pH that allows the ionization of the  $-\text{COOH}$  groups, which must be neither below the  $\text{p}K_a$  of  $\gamma$ -PGA (4.09 according to Inbaraj et al. 2009), nor too basic, so that cation exchange reactions can occur rapidly and efficiently. In fact, purified acidic  $\gamma$ -PGA, which is insoluble in water, was shown to adsorb cesium from radioactive wastewater more efficiently than the corresponding sodium salt, even if cesium is preferentially bound with respect to sodium and calcium. Moreover, the adsorption equilibrium is attained in very short time (Sakamoto and Kawase 2016). Indeed, commercial bio-adsorbers containing  $\gamma$ -PGA, among other components, are already on the market (<http://www.poly-glusb.jp/basic.html>) and their efficacy was experimentally tested, for example on wastewater from ethanol distillation, characterized by high levels of organic and inorganic matter. Results showed that the use of  $\gamma$ -PGA combined with sodium hypochlorite and sand filters removed about 70% of the turbidity and reduced chemical oxygen demand by 79.5% (Carvajal-Zarrabal et al. 2012).

The flocculation properties of  $\gamma$ -PGA can also be improved by coupling with other materials. As an example, the sequential addition of chitosan and  $\gamma$ -PGA was shown to substantially reduce the chemical oxygen demand from the wastewater of a potato starch plant, subtracting nitrogen and phosphorus and improving turbidity. The synergistic effect is thought to be linked to the ability of chitosan to neutralize negative charges, thereby reducing electrostatic repulsion, while  $\gamma$ -PGA provides a bridging function that promotes flocculation. By using biodegradable components, the sediments, rich in organic matter, could be classified as potential soil fertilizers (Li et al. 2020). A super  $\text{Cu}^{2+}$  adsorber was developed by cross-linking  $\gamma$ -PGA onto *Pseudomonas putida* cells displaying two recombinant metal-binding proteins on its surface. The biocomposite biosorbent allowed the quantitative recovery of copper from liquid matrices over a sufficiently varied range of pH and temperatures (Hu et al. 2017).

However, there are completely different approaches in which the multiple properties of  $\gamma$ -PGA can be highly valuable in wastewater treatment, e.g., as biostimulant for other microorganisms or plants directly involved in the bioremediation processes (Wojtowicz et al. 2022).

For the bioremediation of trichloroethylene-contaminated groundwater sites, reductive dechlorination can be carried out by anaerobic bacteria which use  $\text{H}_2$  as electron donor to replace chlorine atoms with hydrogens. A mixture containing  $\gamma$ -PGA and emulsifiers, vitamins and a degreaser could be successfully injected in contaminated sites to speed up bioremediation by acting at multiple levels: (i) as physical adsorption agent for trichloroethylene; (ii) as slow-release carbon supplement for the maintenance of anaerobic dechlorinators (i.e. as biostimulant); (iii) as pH-stabilizer, thanks to the neutralizing effect of the amine groups released by the degrading polymer (Luo et al. 2021).

The complexation with  $\gamma$ -PGA was also shown to improve the performances of a catalytic dechlorination method based on the used palladium-doped zero-valent iron nanoparticles.  $\gamma$ -PGA complexation stabilized and provided electrostatic and steric repulsion to prevent particle aggregation due to attractive magnetic forces. The positive role of  $\gamma$ -PGA was demonstrated by comparing the dechlorination activity of naked and  $\gamma$ -PGA-complexed nanoparticles on chlorophenol as model pollutant (Zhang et al. 2018).

In marine sediments treatments, a new role for  $\gamma$ -PGA was devised as biological glue and protective agent to wrap oil-degrading bacteria adsorbed on solid zeolite particles, thus preventing dispersion of the microbial species directly responsible for the bioremediation of sediments contaminated by crude oil by marine currents (Zhao et al. 2018).

Moreover, due to its highly efficient cation-binding character, can also be used as biosensor of metal contamination,  $\gamma$ -PGA-stabilized gold nanoparticles have been synthesized and used to sense trivalent chromium levels in aqueous solution, which could be conveniently assessed via a colorimetric change occurring upon chromium binding. The reported sensitivity is very high (up to the 0.2 ppb) and the biosensor was successfully tested in different liquid matrices (Yuan et al. 2020).

## 7.2. Soil Bioremediation

The suitability of  $\gamma$ -PGA properties in soil washing simulations has been poorly explored. This is probably linked to the existence of several alternative soil remediation methods and to the technical problems in envisaging the scale up of soil-washing procedures based on an expensive bio-adsorber as  $\gamma$ -PGA. The only real advantage that the polymer offers with respect to similar conventional techniques relies on the fact that upon  $\gamma$ -PGA washing, soil characteristics do not change, and the soil microbiota appears unaffected (Peng et al. 2020), which is a fundamental asset for future restoration of degraded soil (Coban et al. 2022).

However, the metal-chelation properties of  $\gamma$ -PGA can be indirectly exploited in contaminated soils.  $\gamma$ -PGA, applied to soil spiked with Cd and Pb, reduced the growth inhibitory effects of those metal ions on cucumber seedlings by reducing their bioavailability, as demonstrated by the lower metal ions content in the plant tissue (Pang et al. 2018).

Moreover, in phytoremediation of hypersaline soil, the growth of two different halophytes was shown to increase upon addition of  $\gamma$ -PGA solutions to the soil (Mu et al. 2021). This effect is supposedly linked to the  $\gamma$ -PGA-mediated reduced bioavailability of  $\text{Ca}^{2+}$ ,  $\text{Mg}^{2+}$  and  $\text{NO}_3^-$ , the ions analysed in this study, which mitigates the salt stress and promotes plant growth. The increase in plant biomass is thereby turned into a larger amount of ions adsorbed by the plants and, ultimately, into a more efficient phytoremediation of the hypersaline site (Mu et al. 2021).

Analogously to what described for wastewater treatments,  $\gamma$ -PGA can also be used as biostimulant for the activity of microbial consortia able to degrade specific pollutants. This strategy has been applied for the bioremediation of soil samples contaminated by

petroleum hydrocarbons by Wojtowicz and collaborators (2022). An autochthonous degrading microbial consortium was introduced in soil derived from a contaminated site alone or together with  $\gamma$ -PGA, in a combined bioaugmentation and biostimulation approach. The rate of pollutants degradation over a 6-month period improved significantly in the presence of the polymer with respect to the non-biostimulated consortium (Wojtowicz et al. 2022). This approach has the advantage of being potentially applicable in situ even to urbanized polluted sites.

## 8. Open Challenges and Perspectives

A large body of literature explored the propensity of  $\gamma$ -PGA to flocculate several cationic compounds rapidly and efficiently, a feature that has prompted a wide array of research studies on its applicability in bioremediation. The efficiency of ion binding is pH dependent, and the selectivity mainly depends on compounds' relative concentration and charge. However, the field implementation of the lab-conceived applications is still far from being realized.  $\gamma$ -PGA, as a commercial product, is currently too expensive for massive use in large wastewater and soil treatment plants.

$\gamma$ -PGA appears more valuable as a slow-release carbon and nitrogen source for the biostimulation of microbes degrading organic compounds, (Luo et al. 2021; Zhang et al. 2018; Zhao et al. 2018). It has also shown to be applicable as metals-immobilization agent to support phytoremediation techniques. However, its biodegradability in this respect is a double-edged weapon: it makes it a perfectly biologically safe immobilization agent, able to preserve and even improve soil quality, but it does not guarantee the long-term stability of the immobilized metals, because of the ubiquitous presence of viral, bacterial, and eukaryotic hydrolases. Experimental proof of its actual survival in real natural environments is still missing, as most of the data have been collected in simulated natural conditions (Pang et al. 2018). The unstable nature of  $\gamma$ -PGA in an uncontrolled environment is also a major shortcoming when considering the option of recycling it after desorption of the payload through mild acidic conditions.

A still unexplored strategy to decrease  $\gamma$ -PGA-based bioremediation costs and, concurrently, overcome the degradation might be represented by the use of  $\gamma$ -PGA-producing bacteria grown in situ, alone or in combination with other suitable microbial species to ensure a constant  $\gamma$ -PGA-based bioremediating action. Alternatively, in order to stabilize PGA molecules in the natural environment, conjugated molecules can be explored, thus decreasing the degradation rate, and prolonging its survival.

The high production costs may be overcome by exploring novel fermentation strategies, for instance, biofilm fermentation. This technique has been applied by Moni and colleagues (2022) for the convenient production of proteases by *Bacillus subtilis* (Moni et al. 2022). However, the suitability of this technique largely depends on the specific nature of the substrate for bacterial growth, the aeration conditions and the stability of the external conditions, therefore further investigations should be done for its application in  $\gamma$ -PGA production.

In conclusion,  $\gamma$ -PGA is an attractive biopolymer with high potential in several application fields. However, first and foremost, the hopes placed in new overproducer engineered strains and ideal fermentation conditions of low-cost recycled organic wastes, must be fulfilled. Once these two conditions are met, solving the other issues, as the one correlated to the stability of the polymer, would be downhill.

## References

- Altun M (2019) Bioproduction of  $\gamma$ -Poly (glutamic acid) using feather hydrolysate as a fermentation substrate. *Trak Univ J Nat Sci* 20(1): 27–34. <https://doi.org/10.23902/trkjnat.448851>
- Appelbaum M, Schweder T (2021) Metabolic engineering of bacillus—new tools, strains, and concepts. In: Nielsen J, Stephanopoulos G, Lee SY (eds) *Metabolic engineering*. <https://doi.org/10.1002/9783527823468.ch13>
- Bhat AR et al (2015) Improving survival of probiotic bacteria using bacterial poly- $\gamma$ -glutamic acid. *Int J Food Microbiol* 196:24–31. <https://doi.org/10.1016/j.ijfoodmicro.2014.11.031>
- Birrer GA, Cromwick A, Gross RA (1994)  $\gamma$ -Poly (glutamic acid) formation by *Bacillus licheniformis* 9945a: physiological and biochemical studies. *Int J Biol Macromol* 16(5):265–275. [https://doi.org/10.1016/0141-8130\(94\)90032-9](https://doi.org/10.1016/0141-8130(94)90032-9)
- Bodnár M et al (2008) Nanoparticles formed by complexation of poly- $\gamma$ -glutamic acid with lead ions. *J Hazard Mater* 153(3):1185–1192. <https://doi.org/10.1016/j.jhazmat.2007.09.080>
- Bondy SC (2010) The neurotoxicity of environmental aluminium is still an issue. *Neurotoxicology* 31(5):575–581. <https://doi.org/10.1016/j.neuro.2010.05.009>
- Cai D et al (2018) Enhanced production of poly- $\gamma$ -glutamic acid by improving ATP supply in metabolically engineered *Bacillus licheniformis*. *Biotechnol Bioeng* 115(10):2541–2553. <https://doi.org/10.1002/bit.26774>
- Calvio C, Romagnuolo F, Vulcano F, Speranza G, Morelli CF (2018) Evidences on the role of the lid loop of  $\gamma$ -glutamyltransferases (GGT) in substrate selection. *Enzyme Microb Technol* 114:55–62. <https://doi.org/10.1016/j.enzmictec.2018.04.001>

- Candela T, Fouet A (2005) Bacillus anthracis CapD, belonging to the gamma-glutamyltranspeptidase family, is required for the covalent anchoring of capsule to peptidoglycan. *Mol Microbiol* 57(3):717–726. <https://doi.org/10.1111/j.1365-2958.2005.04718.x>
- Carvajal-Zarrabal O, Nolasco-Hipólito C, Barradas-Dermitz DM, Hayward-Jones PM, Aguilar-Uscanga MG, Bujang K (2012) Treatment of vinasse from tequila production using polyglutamic acid. *J Environ Manage* 95. <https://doi.org/10.1016/j.jenvman.2011.05.001>
- Castrillon N, Molina EM, Fu H, Roy A, Toombs J (2019) Super absorbent polymer replacement for disposable baby diapers. <https://doi.org/10.13140/RG.2.2.15095.98720>
- Coban O, De Deyn GB, Van der Ploeg M (2022) Soil microbiota as game-changers in restoration of degraded lands. *J Sci* 375:6584. <https://doi.org/10.1126/science.abe072>
- Ermoli F, Bontà V, Vitali G, Calvio C (2021) SwrA as global modulator of the two-component system DegSU in *Bacillus subtilis*. *Res Microbiol* 172(6):103877. <https://doi.org/10.1016/j.resmic.2021.103877>
- Fang J, Liu Y, Huan C, Xu L, Ji G, Yan Z (2020) Comparison of poly-γ-glutamic acid production between sterilized and non-sterilized solid-state fermentation using agricultural waste as substrates. *J Clean Prod* 255:120248. <https://doi.org/10.1016/j.jclepro.2020.120248>
- Feng J et al (2015) Improved poly-γ-glutamic acid production in *Bacillus amyloliquefaciens* by modular pathway engineering. *Metab Eng* 32:106–115. <https://doi.org/10.1016/j.ymben.2015.09.011>
- Feng J et al (2017) Enhancing poly-γ-glutamic acid production in *Bacillus amyloliquefaciens* by introducing the glutamate synthesis features from *Corynebacterium glutamicum*. *Microb Cell Fact* 16(1):88. <https://doi.org/10.1186/s12934-017-0704-y>
- Fujita KI et al (2021) Effect of pgsE expression on the molecular weight of poly (γ-glutamic acid) in fermentative production. *Polym J* 53:409–414. <https://doi.org/10.1038/s41428-020-00413-7>
- Guo J, Shi W, Li J, Zhai Z (2021) Effects of poly-γ-glutamic acid and poly-γ-glutamic acid super absorbent polymer on the sandy loam soil hydro-physical properties. *PLoS One* 16(1):e0245365. <https://doi.org/10.1371/journal.pone.0245365>
- Harwood CR (1989) Introduction to the Biotechnology of *Bacillus*. In: Harwood CR (eds) *Bacillus*. Biotechnology handbooks, vol 2. Springer, Boston, MA. [https://doi.org/10.1007/978-1-4899-3502-1\\_1](https://doi.org/10.1007/978-1-4899-3502-1_1)
- Hassan SHA et al (2014) Electricity generation from rice straw using a microbial fuel cell. *Int J Hydrog Energy* 39(17):9490–9496. <https://doi.org/10.1016/j.ijhydene.2014.03.259>
- Hsueh YH, Huang KY, Kunene SC, Lee TY (2017) Poly-γ-glutamic acid synthesis, gene regulation, phylogenetic relationships, and role in fermentation. *Int J Mol Sci* 18(12):2644. <https://doi.org/10.3390/ijms18122644>
- Hu P et al (2017) Poly-γ-glutamic acid coupled *Pseudomonas putida* cells surface-displaying metallothioneins: composited copper(II) biosorption and inducible flocculation in aqueous solution. *RSC Adv* 7(30):18578–18587. <https://doi.org/10.1039/C7RA01546A>
- Inbaraj BS, Wang JS, Lu JF, Siao FY, Chen BH (2009) Adsorption of toxic mercury (II) by an extracellular biopolymer poly (gamma-glutamic acid). *Bioresour Technol* 100(1):200–207. <https://doi.org/10.1016/j.biortech.2008.05.014>
- Jang J, Cho M, Chun JH et al (2011) The poly-γ-D-glutamic acid capsule of *Bacillus anthracis* enhances lethal toxin activity. *Infect Immun* 79(9):3846–3854. <https://doi.org/10.1128/IAI.01145-10>
- Khalil IR et al (2018) Poly-Gamma-Glutamic Acid (γ-PGA)-based encapsulation of adenovirus to evade neutralizing antibodies. *Molecules* 23(10):2565. <https://doi.org/10.3390/molecules23102565>
- Kocianova S et al (2005) Key role of poly-γ-dl-glutamic acid in immune evasion and virulence of *Staphylococcus epidermidis*. *J Clin Invest* 115(3):688–694. <https://doi.org/10.1172/JCI23523>
- Lee NR et al (2014) In vitro evaluation of new functional properties of poly-γ-glutamic acid produced by *Bacillus subtilis* D7. *Saudi J Biol Sci* 21(2):153–158. <https://doi.org/10.1016/j.sjbs.2013.09.004>



- Li M et al (2020) Treatment of potato starch wastewater by dual natural flocculants of chitosan and poly-glutamic acid. *J Clean Prod* 264. <https://doi.org/10.1016/j.jclepro.2020.121641>
- Luo Z, Guo Y, Liu J, Qiu H, Zhao M, Zou W, Li S (2016) Microbial synthesis of poly- $\gamma$ -glutamic acid: current progress, challenges, and future perspectives. *Biotechnol Biofuels* 9:134. <https://doi.org/10.1186/s13068-016-0537-7>
- Luo SG, Chien CC, Sheu YT, Verpoort F, Chen SC, Kao CM (2021) Enhanced bioremediation of trichloroethene-contaminated groundwater using modified  $\gamma$ -PGA for continuous substrate supplement and pH control: batch and pilot-scale studies. *J Clean Prod* 278. <https://doi.org/10.1016/j.jclepro.2020.123736>
- Mamberti S et al (2015)  $\gamma$ -PGA hydrolases of phage origin in bacillus subtilis and other microbial genomes. *PLoS One* 10(7):e0130810. <https://doi.org/10.1371/journal.pone.0130810>
- Massaiu I et al (2019) Integration of enzymatic data in Bacillus subtilis genome-scale metabolic model improves phenotype predictions and enables in silico design of poly- $\gamma$ -glutamic acid production strains. *Microb Cell Fact* 18:3. <https://doi.org/10.1186/s12934-018-1052-2>
- McLean RJ, Beauchemin D, Clapham L, Beveridge TJ (1990) Metal-binding characteristics of the gamma-glutamyl capsular polymer of bacillus licheniformis ATCC 9945. *Appl Environ Microbiol* 56(12):3671–3677. <https://doi.org/10.1128/aem.56.12.3671-3677.1990>
- Moni R, Khan AAN, Islam Z, Zohora US, Rahman MS (2022) Biofilm fermentation: a propitious method for the production of protease enzyme by bacillus subtilis RB14. *Ind Biotechnol* 18(1). <https://doi.org/10.1089/ind.2021.0016>
- Mu Y et al (2021) Phytoremediation of secondary saline soil by halophytes with the enhancement of  $\gamma$ -polyglutamic acid. *Chemosphere* 285. <https://doi.org/10.1016/j.chemosphere.2021.131450>
- Nair P, Navale GR, Dharne MS (2021) Poly-gamma-glutamic acid biopolymer: a sleeping giant with diverse applications and unique opportunities for commercialization. *Biomass Conv Bioref*. <https://doi.org/10.1007/s13399-021-01467-0>
- Nakano MM, Zuber P (1998) Anaerobic growth of a "strict aerobe" (Bacillus subtilis). *Ann Rev Microbiol* 52(1):165–190. <https://doi.org/10.1146/annurev.micro.52.1.165>
- Ogunleye A, Bhat A, Irorere VU, Hill D, Williams C, Radecka I (2014) Poly- $\gamma$ -glutamic acid—production, properties and applications. *Microbiology* 6. <https://doi.org/10.1099/mic.0.081448-0>
- Ohsawa T, Tsukahara K, Ogura M (2009) Bacillus subtilis response regulator DegU is a direct activator of pgsB transcription involved in gamma-poly-glutamic acid synthesis. *Biosci Biotechnol Biochem* 73(9):2096–2102. <https://doi.org/10.1271/bbb.90341>
- Osera C, Amati G, Calvio C, Galizzi A (2009) SwrAA activates poly-gamma-glutamate synthesis in addition to swarming in Bacillus subtilis. *Microbiology (reading)* 155(7):2282–2287. <https://doi.org/10.1099/mic.0.026435-0>
- Pang X, Lei P, Feng X, Xu Z, Xu H, Liu K (2018) Poly- $\gamma$ -glutamic acid, a bio-chelator, alleviates the toxicity of Cd and Pb in the soil and promotes the establishment of healthy Cucumis sativus L. seedling. *Environ. Sci. Pollut Res Int* 25(20):19975–19988. <https://doi.org/10.1007/s11356-018-1890-9>
- Park SB, Sung MH, Uyama H, Han DK (2021) Poly (glutamic acid): production, composites, and medical applications of the next-generation biopolymer. *Prog Polym Sci* 113:101341. <https://doi.org/10.1016/j.progpolymsci.2020.101341>
- Park C et al (2005) Synthesis of super-high-molecular-weight poly- $\gamma$ -glutamic acid by Bacillus subtilis subsp. chungkookjang. *J Mol Catal B Enzym* 35(4–6):128–133. <https://doi.org/10.1016/j.molcatb.2005.06.007>
- Peng YP, Chang YC, Chen KF, Wang CH (2020) A field pilot-scale study on heavy metal-contaminated soil washing by using an environmentally friendly agent-poly- $\gamma$ -glutamic acid ( $\gamma$ -PGA). *Environ Sci Pollut Res Int* 27(28):34760–34769. <https://doi.org/10.1007/s11356-019-07444-5>
- Pennisi M, Malaguamera G, Puglisi V, Vinciguerra L, Vacante M, Malaguamera M (2013) Neurotoxicity of acrylamide in exposed workers. *Int J Environ Res Public Health* 10(9):3843–3854. <https://doi.org/10.3390/ijerph10093843>

- Ramaswamy S, Rasheed M, Morelli CF, Calvio C, Sutton BJ, Pastore A (2018) The structure of PghL hydrolase bound to its substrate poly  $\gamma$ -glutamate. *FEBS J* 285:4575–4589. <https://doi.org/10.1111/febs.14688>
- Sakamoto S, Kawase Y (2016) Adsorption capacities of poly- $\gamma$ -glutamic acid and its sodium salt for cesium removal from radioactive wastewater. *J Environ Radioact* 165:151–158. <https://doi.org/10.1016/j.jenvrad.2016.10.004>
- Scheel RA, Fusi AD, Min BC, Thomas CM, Ramarao BV, Nomura CT (2019) Increased production of the value-added biopolymers poly(R-3-Hydroxyalkanoate) and poly ( $\gamma$ -Glutamic acid) from hydrolyzed paper recycling waste fines. *Front Bioeng Biotechnol* 7. <https://doi.org/10.3389/fbioe.2019.00409>
- Scoffone V, Dond D, Biino G, Borghese G, Pasini D, Galizzi A, Calvio C. Knockout of *pgdS* and *ggt* genes improves  $\gamma$ -PGA yield in *B. subtilis*. *Biotechnol. Bioeng.*, 110: 2006–2012. 2013. <https://doi.org/10.1002/bit.24846>.
- Scorpio A et al (2007) Poly- $\gamma$ -glutamate capsule-degrading enzyme treatment enhances phagocytosis and killing of encapsulated bacillus anthracis. *Antimicrob Agents Chemother* 51(1):215–222. <https://doi.org/10.1128/AAC.00706-06>
- Shah MP (2020) *Microbial Bioremediation & Biodegradation*. Springer
- Shah MP (2021a) Removal of refractory pollutants from wastewater treatment plants. CRC Press
- Shah MP (2021b) Removal of emerging contaminants through microbial processes. Springer
- Shih IL, Van YT (2001) The production of poly- ( $\gamma$ -glutamic acid) from microorganisms and its various applications. *Bioresour Technol* 79:207–225. [https://doi.org/10.1016/S0960-8524\(01\)00074-8](https://doi.org/10.1016/S0960-8524(01)00074-8)
- Srivatsan A et al (2008) High-precision, whole-genome sequencing of laboratory strains facilitates genetic studies. *PLoS Genet* 4(8):e1000139. <https://doi.org/10.1371/journal.pgen.1000139>
- Stanley NR, Lazizzera BA (2005) Defining the genetic differences between wild and domestic strains of *Bacillus subtilis* that affect poly- $\gamma$ -glutamic acid production and biofilm formation. *Mol Microbiol* 57:1143–1158. <https://doi.org/10.1111/j.1365-2958.2005.04746.x>
- Su Y et al (2010) Improved poly- $\gamma$ -glutamic acid production by chromosomal integration of the *Vitreoscilla* hemoglobin gene (*vhb*) in *Bacillus subtilis*. *Bioresour Technol* 101(12):4733–4736. <https://doi.org/10.1016/j.biortech.2010.01.128>
- Sung MH, Park C, Kim CJ, Poo H, Soda K, Ashiuchi M (2005) Natural and edible biopolymer poly- $\gamma$ -glutamic acid: synthesis, production, and applications. *Chem Rec* 5(6):352–366. <https://doi.org/10.1002/tcr.20061>. PMID: 16278834
- Tamang JP, Watanabe K, Holzapfel WH (2016) Review: diversity of microorganisms in global fermented foods and beverages. *Front Microbiol* 7. <https://doi.org/10.3389/fmicb.2016.00377>
- Tang B et al (2015) Highly efficient rice straw utilization for poly- ( $\gamma$ -glutamic acid) production by *Bacillus subtilis* NX-2. *Bioresour Technol* 193:370–376. <https://doi.org/10.1016/j.biortech.2015.05.110>
- Wojtowicz K, Steliga T, Kapusta P, Brzeszcz J, Skalski T (2022) Evaluation of the effectiveness of the biopreparation in combination with the polymer  $\gamma$ -PGA for the biodegradation of petroleum contaminants in soil. *Mater Lett* 15(2):400. <https://doi.org/10.3390/ma15020400>
- Wu Q, Xu H, Xu L, Ouyang P (2006) Biosynthesis of poly ( $\gamma$ -glutamic acid) in *Bacillus subtilis* NX-2: regulation of stereochemical composition of poly ( $\gamma$ -glutamic acid). *Process Biochem* 41:1650–1655. <https://doi.org/10.1016/j.procbio.2006.03.034>
- Xie X et al (2020) Effect of poly- $\gamma$ -glutamic acid on hydration and structure of wheat gluten. *J Food Sci* 85(10):3214–3219. <https://doi.org/10.1111/1750-3841.15400>
- Xu ZQ et al. Effect of poly ( $\gamma$ -glutamic acid) on microbial community and nitrogen pools of soil. *Acta Agric. Scand. B Soil Plant Sci.* 63:657–668. <https://doi.org/10.1080/09064710.2013.849752>
- Yuan X, Zhou B, Li M, Shen M, Shi X (2020) Colorimetric detection of  $\text{Cr}^{3+}$  ions in aqueous solution using poly ( $\gamma$ -glutamic acid)-stabilized gold nanoparticles. *Anal Methods* 12:3145–3150. <https://doi.org/10.1039/D0AY00842G>

### **Acknowledgements**

This research was supported by the Italian Ministry of Education, University and Research (MIUR): Dipartimenti di Eccellenza Program (2018e2022) - Dept. of Biology and Biotechnology "L. Spallanzani", University of Pavia and by Fondazione Cariplo, Bando Economia Circolare: ricerca per un futuro sostenibile; grant # 2018-1011.

A particular thank to Raffaella for her efficiency and kindness.

An acknowledgment goes to AOP UNOLOMBARDIA sac a rl, Italy, and Ambrogio De Ponti, for providing the raw materials for the Phyver Project.